Available online at www.sciencedirect.com
ScienceDirect
Geochimica et Cosmochimica Acta 75 (2011) 1308–1345
Geochimica et Cosmochimica Acta
www.elsevier.com/locate/gca

Growth rate of the preserved continental crust: II. Constraints from Hf and O isotopes in detrital zircons from Greater Russian Rivers

Christina Yan Wang [a,b], Ian H. Campbell [b,*], Aleksandr S. Stepanov [b], Charlotte M. Allen [b], Igor N. Burtsev [c]

[a] Guangzhou Institute of Geochemistry, Chinese Academy of Sciences, Guangzhou 510640, China
[b] Research School of Earth Sciences, The Australian National University, Canberra ACT 0200, Australia
[c] Institute of Geology, Komi Science Centre, Uralian Branch of Russian Academy of Science, Pervomayskaya 54, Syktyvkar 167982, Russia

Received 14 April 2010; accepted in revised form 12 December 2010; available online 21 December 2010

Abstract

Detrital zircons from the Ob, Yenisey, Lena, Amur, Volga, Dnieper, Don and Pechora rivers have been analyzed for U–Th–Pb, O and Lu–Hf isotopes to constrain the growth rate of the preserved continental crust in Greater Russia. Four major periods of zircon crystallization, 0.1–0.55, 0.95–1.3, 1.45–2.0 and 2.5–2.9 Ga, were resolved from a compilation of 1366 zircon U/Pb ages. The Archean zircons have $\delta^{18}O$ values lying between 4.53‰ and 7.33‰, whereas Proterozoic and Phanerozoic zircons have a larger range of $\delta^{18}O$ values in each of the recognized U/Pb time intervals with maximum $\delta^{18}O$ values up to 12‰. We interpret the zircons with $\delta^{18}O$ between 4.5‰ and 6.5‰ to have been derived from a magmatic precursor that contains little or no sedimentary component. The variable $\delta^{18}O$ values of the zircons were used to constrain the $^{176}Lu/^{177}Hf$ ratios of the crustal source region of the zircons, which, in turn, were used to calculate Hf model ages (T_{DM}^{V}). The crustal incubation time, the time difference between primitive crust formation (dated by T_{DM}^{V}) and crustal melting (dated by zircon U/Pb age), varies between 300 to 1000 Myr for the majority of analyzed zircon grains, but can be up to 2500 Myr. The average T_{DM}^{V} Hf model age weighted by the fraction of zircons in the river load is 2.12 Ga, which is in reasonable agreement with the area-weighted average of 2.25 Ga. The T_{DM}^{V} Hf model age crustal growth curve for zircons with mantle-like $\delta^{18}O$ values (4.5–6.5‰), weighted by area, shows that growth of the Great Russian continental crust started at 4.2 Ga, and that there are two principal periods of crustal growth, 3.6–3.3 Ga and 0.8–0.6 Ga, which are separated by an interval of low but more or less continuous growth. An alternative interpretation, in which the average $^{176}Lu/^{177}Hf$ ratio (0.0115) of the continental crust is used for the Paleoproterozoic zircons from the Lena River, lowers the average T_{DM}^{V} age of these grains by about 500 Myr and delays the onset of significant crustal growth to 3.5 Ga.

The two principal growth periods recognized in Greater Russia differ from those identified from the Gondwana and the Mississippi river basin, which show peaks at 1.7–1.9 and 2.9–3.1 Ga (Hawkesworth and Kemp, 2006a) and 1.6–2.2 and 2.9–3.4 Ga (Wang et al., 2009), respectively. The older 3.6–3.3 Ga or 3.5–3.3 Ga peak for Greater Russia is slightly older than the older Gondwana-Mississippi peaks, whereas the younger 0.8–0.6 Ga peak is distinctly younger than the youngest peak in either Gondwana or the Mississippi river basin. This suggests that the two major peaks of crustal growth identified in Gondwana and the Mississippi river basin may not be global periods of enhanced continental growth and that the major periods of crustal growth may differ from continent to continent.

* Corresponding author. Tel.: +61 2 6125 4366.
E-mail addresses: wang_yan@gig.ac.cn (C.Y. Wang), Ian.Campbell@anu.edu.au (I.H. Campbell), aleksandr.stepanov@anu.edu.au (A.S. Stepanov), Charlotte.Allen@anu.edu.au (C.M. Allen), Burtsev@geo.komisc.ru (I.N. Burtsev).

0016-7037/$ - see front matter © 2010 Elsevier Ltd. All rights reserved.
doi:10.1016/j.gca.2010.12.010

1. INTRODUCTION

The development of new analytical techniques that enable analyses of U–Th–Pb, Lu–Hf and O isotopes of a single zircon crystal (Hawkesworth and Kemp, 2006a; Kemp et al., 2006; Wang et al., 2009) is improving estimates of the growth rate of the continental crust so that it is now possible to identify individual periods of crustal extraction and the onset of crustal growth. U–Th–Pb, Lu–Hf and O isotopic analyses of detrital zircons collected from near mouth of the Earth's major rivers provide different and complementary information to Nd isotopic studies, and a new perspective on the growth rate of the continental crust of the basin drained by the sampled rivers (Wang et al., 2009). U–Th–Pb isotope system can be used to date the time of crystallization of a zircon, normally the age of a crustal melting event and the $^{176}Hf/^{177}Hf$ ratio of the zircon can be used to calculate a model age for the source region that melted to form the magma from which the zircon crystallized. This can be interpreted to be the average mantle separation age or crustal growth age of the magma source region. The oxygen isotope ratio of the zircon contains information about the fraction of sediment in the source region (Valley et al., 2005) and can be used to constrain the $^{176}Lu/^{177}Hf$ ratio of the crustal source region of the zircon, which is an essential component of the model age calculation (Wang et al., 2009).

Such an approach has been used to constrain the periods of crustal growth in Gondwana (Hawkesworth and Kemp, 2006a) and to constrain the rate of growth in the Mississippi river basin of the North America (Wang et al., 2009). Both studies resolved two remarkably similar peaks in the growth, 1.7–1.9 and 2.9–3.1 Ga for the Gondwana continent (Hawkesworth and Kemp, 2006a) and 1.6–2.2 and 2.9–3.4 Ga for the Mississippi river basin (Wang et al., 2009), suggesting that continental growth may be episodic and provide evidence for two important periods of global continental crustal growth. However, this hypothesis is based on a limited data set, with restricted geographical coverage, and the conclusions need to be confirmed by similar studies of other continents before it can be accepted with any degree of confidence.

This paper reports U–Th–Pb, Lu–Hf and O isotopic analyses for detrital zircons separated from samples collected mainly near the mouth of the major rivers in Greater Russia, applying a similar approach to that used in the study of the Mississippi river basin (Wang et al., 2009). The aims are to resolve the major periods of crustal growth for Greater Russia, to test whether these growth periods are similar or different to those identified from the Gondwana and Mississippi river basin, and to calculate a growth curve for the preserved continental crust of Greater Russia. It forms part of a larger study aimed at determining the growth rate of all of the continents except Antarctica.

2. GEOLOGICAL BACKGROUND

Fig. 1 is a sketched map showing the principal tectonic units of Greater Russia. Its principal components are two ancient cratons: the Eastern European and Siberian cratons, which are largely covered by sedimentary basins and rimmed by orogenic belts (Zonenshain et al., 1990; Metelkin and Vernikovsky, 2005).

2.1. Eastern European craton

Bogdanova et al. (2008) recognized three major segments, Fennoscandia, Sarmatia and Volgo-Uralia, in the Eastern European Craton (EEC). These segments consist of blocks of Archean crust surrounded by Proterozoic crust.

The formation of Archean crust in Fennoscandia started at 3.5–3.2 Ga and the major assembly occurred between 3.1–2.7 Ga with the formation of Fenno-Karelian protocraton (Bogdanova and Bibikova, 1993; Gorbatschev and Bogdanova, 1993; Bogdanova et al., 2008). Sarmatia contains several Archean blocks with ages of 3.7–2.8, 3.6–2.8, 3.2–3.0 and 2.7–2.6 Ga (Shchipansky and Bogdanova, 1996; Bogdanova et al., 2008). The Volgo-Uralia segment is entirely covered by sediments and, as a consequence, the presence of Archean crust in this block is debatable. A recent overview map by Condie et al. (2009) shows that the Archean blocks are confined to Baltica and Sarmatia in the EEC and the basement of the Volgo-Uralia segment is interpreted to be Proterozoic. However, we apply the interpretation of Archean basement by Bogdanova et al. (2008) in Fig. 1 because they confirmed the age of Archean basement in the region by dating samples from boreholes (Bogdanova et al., 2005; Bibikova et al., 2008).

Consolidation of the EEC crust occurred between 2.2 and 1.7 Ga and started with amalgamation of the Sarmatia and Archean blocks, followed by the attachment of Volgo-Uralia to Sarmatia at 2.05–2.02 Ga. The assembly of the ECC craton was completed by collision of Fennoscandia with Volgo-Sarmatia between 1.8–1.7 Ga (Bogdanova et al. 2008). During the collisional events large blocks of interpreted juvenile Proterozoic crust were incorporated into the structure of the basement of the EEC (Bogdanova et al., 2008).

Subsequently the eastern and western parts of EEC evolved differently. The eastern part stabilized and was only deformed by rifting. The western part of EEC was affected by several tectonic and magmatic events between 1.7 to 1.0 Ga. Juvenile crust was considered to be accreted to the western margin of Fennoscandia (Gothian orogeny) between 1.73 and 1.55 Ga (Bogdanova et al., 2008). The Gothian orogeny was accompanied by the intrusion of an anorthosite – mangerite – charnockite – granite suite stating at 1.65 Ga, but with the main event between 1.52 and 1.5 Ga.

The Sveconorwegian orogeny, in which several distinct phases (1.14–1.08 Ga, 1.05–0.98 Ga, 0.98–0.96 Ga and 0.96–0.90 Ga) are recognized, was synchronous with Grenvillean orogeny of the North America craton (Bogdanova et al., 2008). It is confined to the western margin of EEC and involved reworking of crust that formed between 1.73 and 1.44 Ga.

Intensive rifting occurred on both the eastern and western parts of EEC between 1.4 and 1.2 Ga. The largest rift structures that formed at this stage include the Pachelma, Volyn-Orsha and Mezen aulacogens and Moscow grabens, which were accompanied by bimodal magmatism. Two

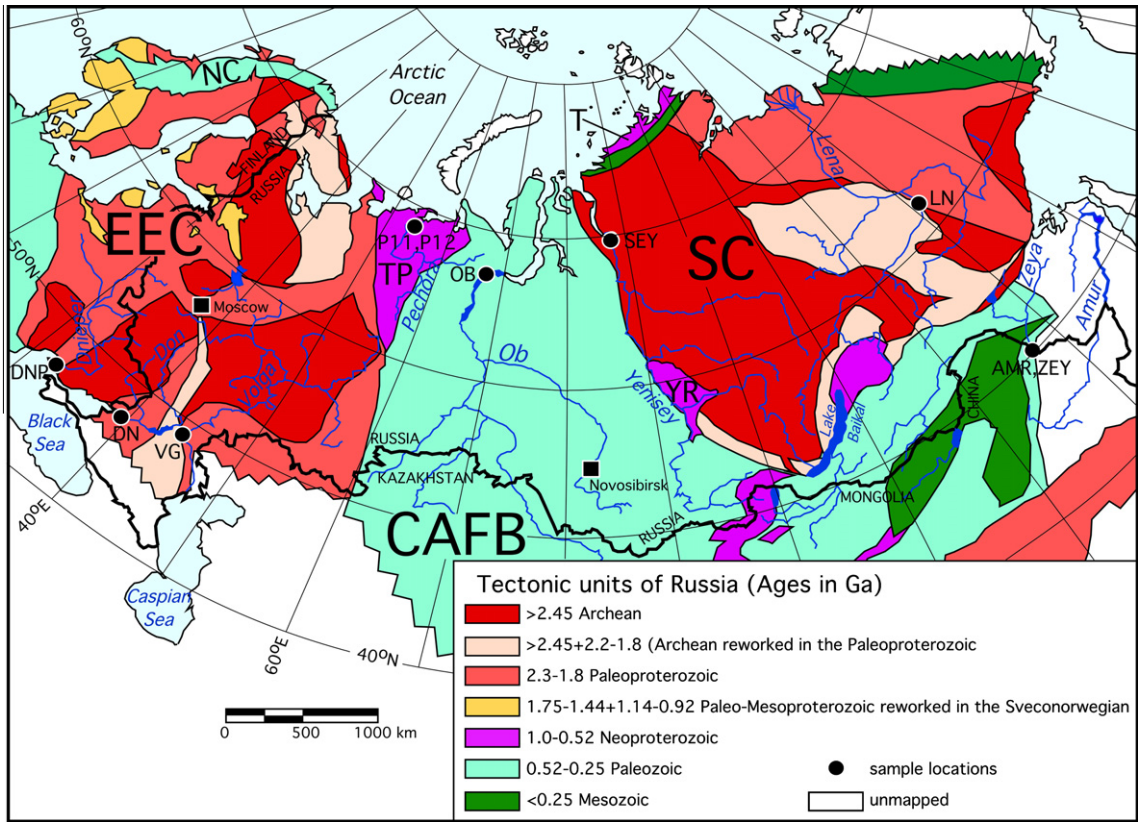

Fig. 1. Tectonic map of Greater Russia showing the major units of the continental crust. EEC–Eastern European craton, SC–Siberian craton, CAFB–Central Asia fold belt, T–Taymyr fold belt, TP–Timan-Pechora region, NC–Norwegian Caledonides, and YR–Yenisey Ridge. Compiled from maps by Zonenshain et al. (1990), Bogdanova et al. (2008), Smelov and Timofeev (2007), Kuzmichev et al. (2001) and Gordienko (2001).

further rifting events are recognized in EEC, one between 0.85–0.6 Ga and the other in Devonian. The latter was accompanied by alkaline magmatism.

2.2. Siberian craton

The Siberian craton is exposed in the Anabar and Aldan shields, and in the Olenek, Akitkan and Near-Sayan uplifts. Formation of the Siberian craton started in the Paleoarchaean (Turkina et al., 2009) but consolidation of the basement was delayed until the 2.0–1.8 Ga orogeny. Sediments, which are younger than 1.65 Ga, cover most of the Siberian craton. Finally, platform rifting occurred in the Neoproterozoic and Devonian.

The Anabar shield is composed of two Archean terranes: the Daldyn (3.1 Ga) and Magan (3.2–2.6 Ga) terranes and two Paleoproterozoic terranes: the Khapchan and Olenek (Berekta) terranes, which formed between 2.4 and 1.9 Ga (Rosen and Turkina, 2007; Smelov and Timofeev, 2007). There are also three Archean terranes: the Western Aldan (3.0–2.7 Ga) (Nutman et al., 1992), Central Aldan and Tynda (2.6–2.95 Ga) terranes, and two Proterozoic terranes: the Uchur and Batomga terranes (1.7–2.0 Ga) (Smelov and Timofeev, 2007) on Aldan shield. The Akitkan terrane, which is exposed along northern part of Lake Baikal, formed between 1.9 and 1.84 Ga from a combination of interpreted juvenile material and Archean protolith (Bibikova et al., 1992; Donskaya et al., 2009). In the Near-Sayan region the Sharyzhalgay block is Archean in age (Turkina et al., 2009; Turkina, 2010). The Archean Daldyn, Tynda and Sharyzhalgay terranes were intensively reworked during Paleoproterozoic (1.9–1.8 Ga) when metamorphism was associated with widespread crustal melting and granite formation (Rosen and Turkina, 2007; Smelov and Timofeev, 2007).

The cratonic basement, which underlies the sedimentary rocks, is divided into several terranes: the Tunguska, Tyung, Berekta, Tyryn and Lena-Aldan terranes (Smelov and Timofeev, 2007). The Tunguska terrane formed in Archean (Kovach et al., 2000; Smelov and Timofeev, 2007), whereas the Tyung terrane has Archean Nd model ages (Buzlukova et al., 2004; Shatsky et al., 2005), but zircons from crustal xenoliths give ages of 1.81–1.94 Ga (Koreshkova et al., 2009). Thus this terrane is considered to be an Archean crust that was reworked in Proterozoic (Shatsky et al., 2005). Smelov and Timofeev (2007) proposed that the eastern part of the craton is Mesoproterozoic in age. However, detrital zircons from Neoproterozoic sediments with ages of 1.5–1.05 Ga were interpreted to originate from the North America craton (Rainbird et al., 1998) and Mesoproterozoic zircons are absent in the Siberian rivers (Fig. 2). Thus we consider this terrane to be Paleoproterozoic.

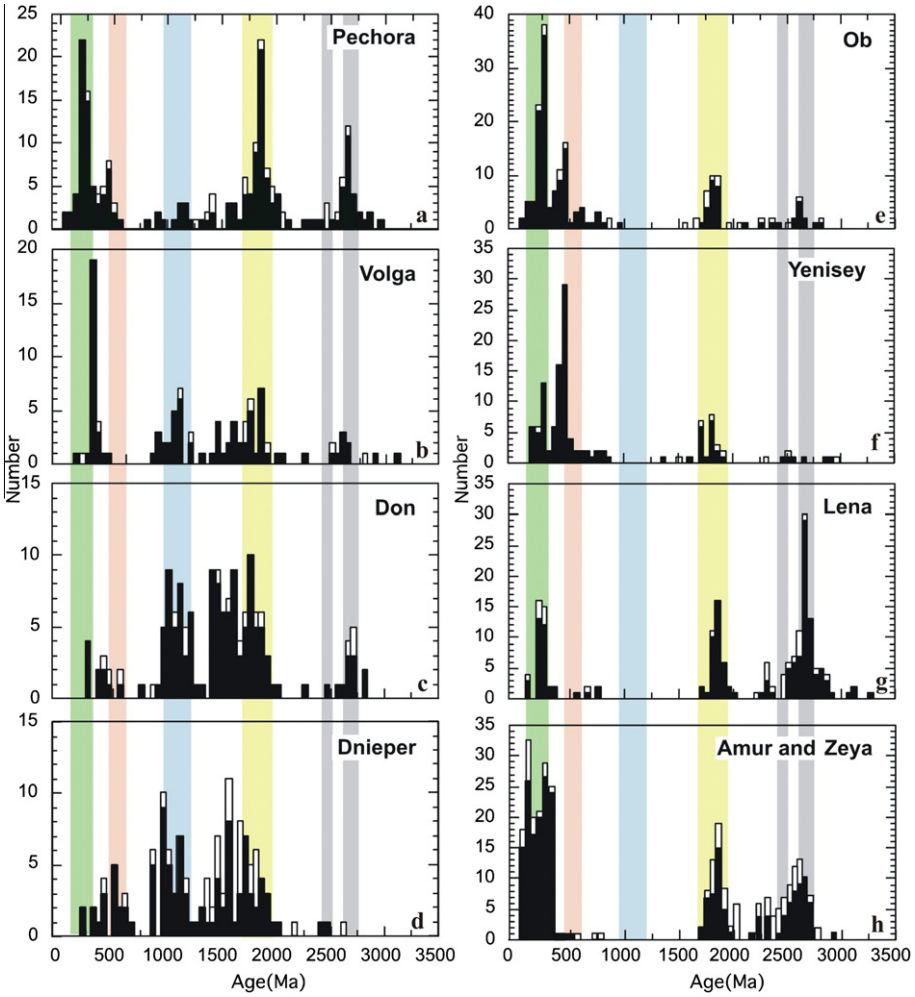

Fig. 2. Histograms of zircon U/Pb ages for the Greater Russia Rivers analyzed in this study. Those with concordant (as defined in the text) or selected ages are shown with filled bars, whereas those with less concordant (rejected) ages are shown with unfilled bars. (a–d) Show the rivers west to the Urals. Note the consistancy in the patterns including a significant 1.9 Ga peak, and the presence of all major orogenic ages except the Grenville (~1.0 Ga) and Pan-Gondwanan (~0.55 Ga, patchy or absent). (e–h) Show the rivers east of the Urals. Note the absence of a 1.0 Ga or "Grenville" peak and a general smearing of ages between 1.9 and 1.0 Ga. The vertical shading shows the major supercontinent forming orogenic events: Pangea (350–225 Ma), Gondwana (650–400 Ma), Rodinia (1.25–0.95 Ga), Nuna (1.95–1.6 Ga), and Superia/Sclavia (2.75–2.6 Ga).

2.3. Timanian and Baikalian orogenies

Complexes that formed between 1.0 and 0.5 Ga have traditionally been assigned to the Baikalian or Timanian orogeny. The largest blocks of this age are the Yenisey Ridge and Timan Block but several smaller blocks with the same age are also known from the Central Asia fold belt, especially south and southwest from the Siberia craton.

The Timan Block is located to the northeast of the Russian platform and west of the Urals. It formed between the Neoproterozoic and Middle Cambrian by accretion to the edge of European Craton (Metelkin and Vernikovsky, 2005; Kuznetsov et al., 2007). A thick layer of younger sedimentary rocks covers most of the basement, which is exposed only on the western slope of northern Ural Mountains (Kuznetsov et al., 2007). Basement is intruded by subduction-related I-type granites dated at 700–515 Ma and A-type granites with ages between 500 and 565 Ma (Kuznetsov et al., 2007). Detrital zircons from the Timanian terrane constrain the duration of magmatism in this terrane between 750 and 490 Ma (Pease and Scott, 2009).

The Yenisey Ridge, which is situated along the western margin of the Siberian craton, was intruded by granites at 860–880 Ma, 720–760 Ma and 630 Ma, respectively (Nozhkin et al., 1999; Vernikovsky et al., 2007).

Terranes of the Baikalian orogeny are abundant in the south and southwest from Lake Baikal in Sayan Mountains and Transbaikalia. They are mostly covered by sedimentary rocks and were intruded by granites during later orogenic events (Kuzmichev et al., 2001; Egorova et al., 2006). Another block of this age is the Tom' inlier (Mountainous Shoriya) located in the Central Asia fold belt. It consists of

interpreted juvenile crust that formed at ~700 Ma (Vladimirov et al., 1999).

2.4. Central Asia fold belt

The vast area among the Eastern European, Siberian, Tarim and North China cratons consists predominantly of Paleozoic, and to a lesser extent Mesozoic, fold belt (so called Central Asia fold belt, or Ural-Mongolia belt) (Khain et al., 2003; Jahn, 2004), which is also known as the Altaid tectonic collage (Sengör et al., 1993; Sengör and Natal'in, 1996). The belt is subdivided into several major structures: the Urals, Central Kazakhstan, Altai-Sayan, Transbaikalia, Sayan and Mongol-Ohotsk belts (c.f, Sengör and Natal'in, 1996). Sedimentary rocks cover a significant part of these fold belts and form two young platforms: Western Siberian and Turan platform. The fold belt was formed by the successive accretion of arcs and microcontinents to the Siberian and Eastern European cratons, followed by the collision of Siberia with the Eastern European, Tarim and North China cratons. Although significant portion of the fold belt was formed during the Baikalian and Caledonian orogenies, the major period of the crust growth is believed to have occurred during Hercynian orogeny (380–280 Ma) (Heinhorst et al., 2000).

Accretion of ancient microcontinents played a significant role in the evolution of the Central orogenic belt. The highest percentage of ancient crust is in Transbaikalia, which contains blocks of Baikalian crust (Kuzmichev et al., 2001). According to Aplonov (1995), the basement of the West Siberian platform consists of 1/6 microcontinents. Pre-existing Caledonian structures are estimated to constitute approximately 13% of the Central Kazakhstan area (Glukhan, 1996).

The Ural Mountains are located between Western Siberian platform and EEC. There were several major episodes of magmatic activities in the Urals: 460–420, 415–395, 365–355, 345–330, 320–315 and 290–250 Ma (Fershtater et al., 2007). The older igneous events of this orogeny were dominantly of mantle origin, but the geochemistry of the magmas evolved progressively from crust-mantle sources at the beginning to crustal sources by the end of orogeny (Fershtater et al., 2007).

Central, Eastern and Northern Kazakhstan is composed of Precambrian microcontinents (for example the Kokchetav continent) and Caledonian arcs, which were assembled during Hercynian orogeny (Glukhan, 1996; Dobretsov et al., 2006). The age distribution of granites shows that intensive granite production started at 500 Ma and reached its maximum between 300 and 250 Ma (Kostitsyn, 1996). Nd model ages of granitoids show that the overall role of ancient crust in this region was limited (Heinhorst et al., 2000; Jahn, 2004).

The Western Siberian platform is composed of folded basement rocks covered by Mesozoic and Cenozoic sedimentary rocks. Most studies conclude that the basement is composed dominantly of Hercynian fold belt material and that the eastern part is underlain by the Siberian craton (Yolkin et al., 2007). Alternatively oceanic crust may underlie the central and northern parts of the platform (Aplonov, 1995).

The Sayan Mountains, located to the west and southwest of Lake Baikal, consists of Baikalian and Riphean terranes with the Caledonian complexes lying between the older terranes and overprinting them (Kuzmichev et al., 2001; Turkina et al., 2007). The typical Sangilen terrane consists of Riphean basement that experienced high-grade metamorphism and granite production between 530 and 460 Ma (Egorova et al., 2006).

Another period of granite generation and granulite metamorphism occurred between 510 and 480 Ma along the southern margin of the Siberian craton and in the area adjacent to Lake Baikal (Gladkochub et al., 2008).

Transbaikalia region, to the south of Lake Baikal, is a region of intense and prolonged granitic magmatism (Kuzmichev et al., 2001; Tsygankov et al., 2007; Zorin et al., 2009). The oldest granites in the region are dated at 800 Ma (Kuzmichev et al., 2001). The largest granite complex is the Angara-Vitim batholith with an area of more than 150,000 km^2. The batholith formed in two stages, 340–320 Ma and 310–270 Ma, on a heterogeneous basement with a variable isotopic signature (Tsygankov et al., 2007).

2.5. Mesozoic and Cenozoic events

The Mesozoic era in Greater Russia started with eruption of giant Siberian Traps at 250 Ma, which covered large areas of the Siberian craton, and in the Ural-Mongolia fold belt, especially on the Western Siberian platform (Yolkin et al., 2007).

The Eastern European and Siberia cratons formed a single continent in the Permian and crust growth was confined to its margins (Stampfli and Borel, 2002). Crustal growth continued in Mesozoic on the eastern (Verkhoyansk-Kolyma region) and southern (Mongol-Okhotsk belt) edges of the Siberian craton. Closure of Tethys Ocean on the southern edge of EEC produced the magmatic complexes of Caucasus Mountains (Zonenshain et al 1990; Stampfli and Borel, 2002). A block of Neoproterozoic crust was accreted to the northern edge of the Siberian craton, forming the Taymyr fold belt (Zonenshain et al., 1990).

The western part of Verkhoyansk-Kolyma region is composed of the deformed passive margin of the Siberian craton. The central part consists mainly of granites with ages ranging from 165 to 80 Ma, whereas the eastern part consists of an ancient terrane mélange (Pushcharovskiy et al., 1983; Zonenshain et al., 1990; Akinin et al., 2009).

Mongol-Okhotsk fold belt formed between 310 and 120 Ma during the collision of the Siberia craton and North China craton. The collision terminated at 150 Ma in the western part of the fold belt and continued to 120 Ma in the eastern part (Zonenshain et al., 1990; Litvinovsky et al., 1999). The Sikhote-Alin Sakhalin fold belt along the Eastern edge of Eurasia formed between 130 and 65 Ma (Zonenshain et al., 1990; Faure et al., 1995; Bazhenov et al., 2001).

Alkaline granitic intrusions, which intruded between 125 and 200 Ma (Kovalenko et al., 1999), and postcollisional metamorphic core complexes that formed between 240 and 150 Ma, occur widely in the Transbaikalia region

(Zorin et al., 1997; Donskaya et al., 2008). These granites formed from remelting of Precambrian, Caledonian and Hercynian basement and inherited the isotopic characteristics of the protoliths (Kovalenko et al., 1999).

Crustal formation in the Cenozoic continued on the eastern edge of Eurasia on the Kamchatka peninsula and Kurils arc. Basalts that formed at Mesozoic-Cenozoic boundary occurred in the Tian Shan region (Southern Central Asia) (Simonov et al., 2008). Cenozoic intraplate mafic magmatism also occurred in regions adjacent to Lake Baikal and in Mongolia (Zorin et al., 2006).

3. ANALYTICAL METHODS

Six samples were collected from near the mouths of six major rivers in Greater Russia: the Ob, Yenisey, Volga, Dnieper, Don and Pechora rivers (Fig. 1). The remaining two samples, the Lena and Amur river samples, were collected near their confluence with large tributaries due to access difficulties that made it impossible to sample further down stream (Fig. 1). We make an assumption that each of the samples is representative of the average crust within the basin. Although this assumption is reasonable when calculating growth curves and average Hf model ages for the continent as a whole, it has some limitations when considering the provenance of individual zircons within a given river basin. As will be discussed in more detail below, some zircons have no obvious sources within a basin where they were sampled. They are probably recycled zircons from older sediments that sampled a different drainage system and were transported to the present one, or they could also sample unrecognized events within the current basin.

Zircons were separated using conventional magnetic and heavy liquid separation techniques. Analyses of U/Pb, O and Lu–Hf isotopic compositions were carried out at the Research School of Earth Sciences, The Australian National University.

3.1. U/Pb age dating

The Excimer Laser Ablation Inductively Coupled Plasma Mass Spectrometry (ELA-ICP-MS) method used to date zircons was described by Campbell et al. (2005). First, a suite of zircons was mounted in a conventional electron microprobe-style epoxy mount with normal precautions taken to avoid sampling bias during mounting and analyses as described by Wang et al. (2009). A total of 1366 grains were analyzed as follows: Dnieper, 129; Don, 149; Volga, 100; Pechora, 198; Ob, 181; Yenisey, 126; Lena, 183; Amur, 149 and Zeya, 151. The U/Pb age data of all the grains are available in the Electronic annex Table 1. The distribution of the U/Pb ages of the zircons from individual rivers is plotted in Fig. 2. When the data from all rivers are plotted in a histogram four distinct age ranges can be recognized: 0.1–0.55 Ga, 0.95–1.3 Ga, 1.45–2.0 Ga, and 2.5–2.9 Ga (Fig. 3a). The two age divisions that contain the most zircons, 0.1–0.55 Ga and 1.45–2.0 Ga, were arbitrarily subdivided into 0.1–0.4 and 0.4–0.55 Ga, and 1.45–1.7, 1.7–1.85 and 1.85–2.0 Ga, respectively, in order to obtain higher resolution (Fig. 3b).

A second suite of zircons was dated to select suitable grains from each of the seven age ranges identified in the conventional U/Pb dating for later analyses of O and Lu–Hf isotopes. These zircons were soaked over night in HF to remove matamict grains and then mounted on tape and dated by the rim-piercing method described by Campbell et al. (2005), in which a laser hole is ablated from the unprepared rim towards the centre of the grain. One hundred and seventy-nine of these grains were selected for further work from 1133 grains as follows: 21 from the Yenisey river, 30 from the Lena river, 92 from the Volga river, 14 from the Don river and 22 from the Pechora river. The breakdown of grains among the seven identified time intervals was as follows: 32 grains between 0.1–0.4 Ga, 25 grains between 0.4–0.55 Ga, 20 grains between 0.95–1.3 Ga, 20 grains between 1.45–1.7 Ga, 27 grains between 1.7–1.85 Ga, 29 grains between 1.85–2.0 Ga and 26 grains between 2.5–2.9 Ga. The U/Pb age results are listed in Table A1. The selected grains are concordant within 5% (including 2σ errors), show no age zonation and have no inclusions of apatite, rutile or titanite. These grains were then set in a larger than normal epoxy mount especially designed for high precision SHRIMP O isotope analyses and analyzed for first O and then Lu–Hf isotopes. This approach deliberately biased zircon selection towards grains most suitable for accurate O and Lu–Hf isotopic analyses.

3.2. O isotope analyses

The O isotope analytical method used in this study is described in detailed by Ickert et al. (2008). Briefly, chips of TEM-2 ($\delta^{18}O = 8.20 \pm 0.01$ (1σ)‰ VSMOW; Valley, 2003) were embedded into each mount and analyzed to bracket every three measurements of unknown zircons. Zircons separated from R33 ($\delta^{18}O = 5.55 \pm 0.04$ (1σ)‰ VSMOW; Valley, 2003) were analyzed as a secondary standard (Table A2). The analyses were carried out in May and August in 2007. The analytical uncertainties for individual analyses were 0.1–0.3‰ (95% c.l.) in May and 0.1–0.2‰ in August. The spot-to-spot reproducibility assuming isotopic homogeneity of TEM-2 zircons was ±0.50‰ (1σ) in May, and ±0.56‰ (1σ) in August. Summing the variance to the individual uncertainties gives mean R33 values of 5.06 ± 0.75‰ (1σ) for May, and 5.10 ± 0.55‰ for August. We analyzed O isotope of all 179 zircons, however, 20 analyses in the morning session on May 13, 2007 were rejected due to very large standard error difference (2.2 s.e.d > ± 1.0‰) for each of the analyses, which resulted from excessive machine drift. The $\delta^{18}O$ values for the other 159 grains are listed in Table A3.

3.3. Hf isotope analyses

Hf isotopic compositions of the zircon grains were measured using a ThermoFinnigan Neptune MC-ICP-MS coupled to a custom-built, second-generation laser-ablation system featuring an ArF excimer ($\lambda = 193$ nm) laser (Eggins et al., 2005). The laser ablation site for Hf isotope analysis was centered as close as possible to the spot where O isotope analysis was obtained, such that the region of the

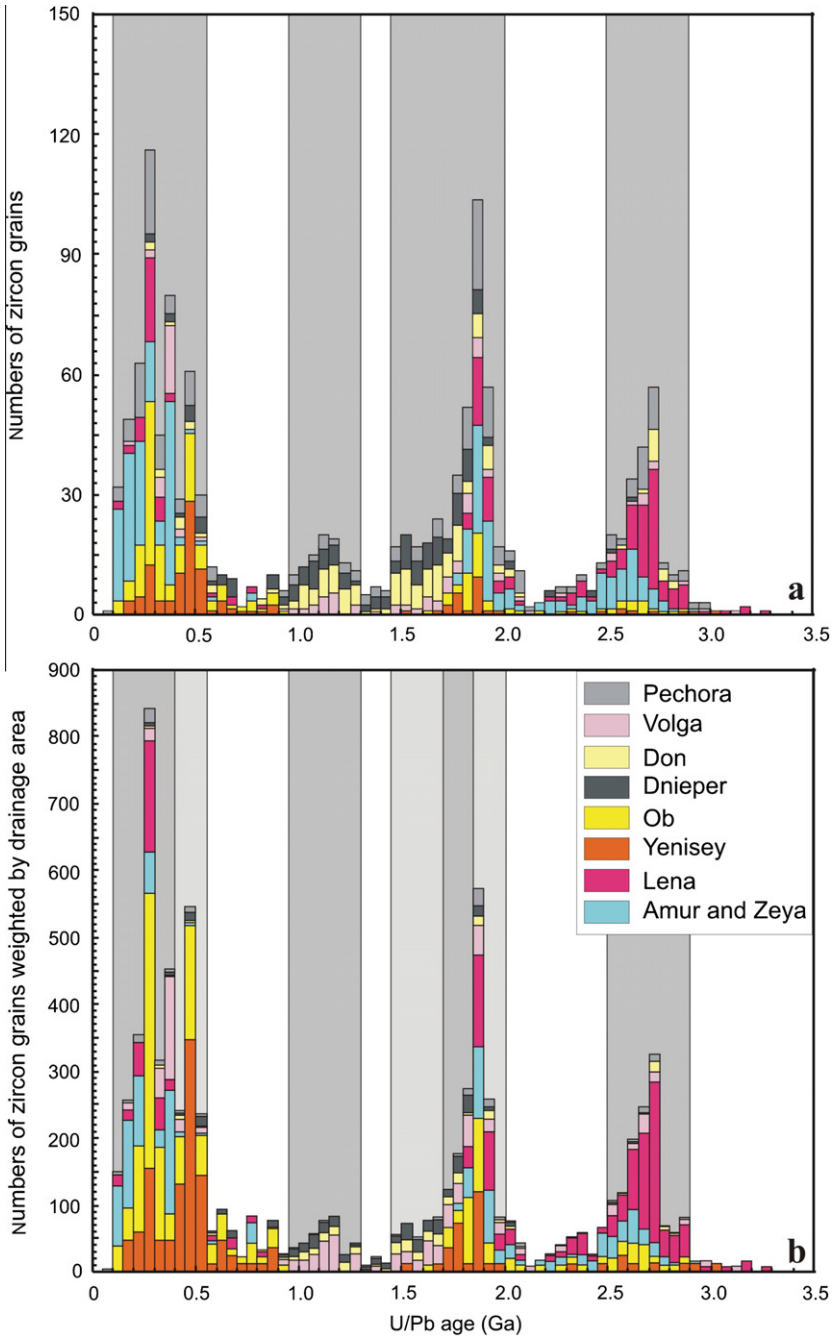

Fig. 3. (a) Unweighted U/Pb age histogram of 1366 zircons analyzed on electron probe mounts showing four U/Pb age peaks, and (b) the same data when the height of the bins is weighted by the drainage area of the eight rivers (taken from online Wikipedia Encyclopedia): Ob 2,972,497 km^2, Yenisey 2,554,482 km^2, Lena 2,306,772 km^2, Amur 1,929,981 km^2, Volga 1,410,994 km^2, Dnieper 531,817 km^2, Don 458,703 km^2, and Pechora 322,000 km^2. The weighting factor = (proportion of drainage area for each of the rivers × 250)/number of zircons analyzed for that river. The number 250 is arbitrary and is introduced to bring the minimum weighting factor close to 1. The bins have been grouped into seven time intervals (in grey) 0.1–0.40, 0.4–0.55, 0.95–1.3, 1.45–1.7, 1.75–1.85, 1.85–2.0 and 2.5–2.9 Ga as discussed in the text.

zircon analyzed for both Hf and O isotopes was almost identical. Most data were acquired by ablating a 62 μm (diameter) laser spot, but in some cases a 47 μm laser spot was used for small grains. The analytical method is described by Wang et al. (2009). A systematic bias of the instrument was confirmed by measuring a standard solution of the Hf isotope reference material JMC 475. The value obtained for $^{176}Hf/^{177}Hf$ was 0.282142 ± 5, which is 0.000018 below the accepted value of 0.282160. As a consequence, we have normalized our $^{176}Hf/^{177}Hf$ measurements to the weighted average of the 91500, Mud Tank and Temora standards measured in each analytical session to the solution values reported by Woodhead and Hergt (2005). A summary of the Lu–Hf isotopic data obtained over a six-month period for

four reference zircons during data collection, including normalized and un-normalized values, is shown in Table A4. The measured Lu–Hf isotopic ratios for the analyzed grains are listed in Table A3.

4. RESULTS

4.1. Zircon U/Pb ages

Histograms of U/Pb ages for zircons from the eight major rivers in Greater Russia analyzed for this study are shown in Fig. 2. They are arranged in order away from the Ural Mountains, to the west and southwest of the Urals the order is the Pechora, Volga, Don and Dnieper rivers (Fig. 2a–d), and to the east or southeast the Ob, Yenisey, Lena and Amur rivers (Fig. 2e–h). A brief discussion of zircon U/Pb age ranges, and the corresponding tectonic and thermal events for each of the river basins is given below.

4.1.1. Pechora River

The Pechora basin is located in the Timan block and is separated from the Russian platform by the Timan range to the southwest and from the Western Siberian platform to the east by the Ural Mountains. Significant portions of the zircons from the Pechora River are Archean (15%), Paleoproterozoic (30%) or Mesoproterozoic (6%) in age (Fig. 2a) and were probably recycled from the Russian platform basement. The age distribution of zircons from the Pechora River differs significantly from the other European Russian rivers. Most of Paleoproterozoic zircons from the Pechora River crystallized during the short time interval between 1.9–2.0 Ga, which is in sharp contrast with the much wider age distribution (1.54–2.0 Ga) of the Paleoproterozoic zircons from the Volga, Don and Dnieper rivers, indicating that the Pechora River sampled a different provenance to the Volga, Don and Dnieper rivers. Zircons with 500–700 Ma ages correspond to the Timanian orogeny, which form the basement of the Pechora basin (Kuznetsov et al., 2007; Pease and Scott, 2009). The peak at 250–270 Ma dates the collisional orogenic granites of the Northern Urals. Zircons with ages between these peaks (270–490 Ma) probably formed in arcs that developed during subduction of the Paleouralian ocean (Fershtater et al., 2007). The Pechora River also contains a significant fraction of Mesozoic zircons with ages between 120 and 250 Ma with a few grains as young as 85.9 Ma, which are absent from the other rivers in the Russian Platform. However, Mesozoic granites, the most likely source of these zircons, are located in Taymyr Peninsular and Kolyma regions, far from the Pechora river basin. Therefore the origin of Mesozoic zircons in Pechora is enigmatic.

4.1.2. Volga River

Archean zircons with ages ranging from 2.5 to 2.7 Ga form 10% of zircon population (Fig. 2b). Paleoproterozoic zircons are also abundant (30%) and range in age from 1.6 to 2.0 Ga without a distinct peak. Another significant period of zircon growth is recorded at 1.0–1.25 Ga (15%) but no tectonic event is recognized in the Volga basin during that period. The closest magmatic activity of Grenville age is in southwestern part of Baltica (Bogdanova et al., 2008). Phanerozoic zircons represent 22% of the Volga sediments and were derived from igneous activity in Urals, which occurred between 370 and 250 Ma (Fershtater et al., 2007). The early intrusions are interpreted to be subduction-related and the later ones are believed to have been produced during the collision. The majority of the Phanerozoic zircons formed between 370 and 340 Ma in arcs associated with the closure of the Paleourals Ocean, but the collision of these arcs with the Russian platform produced little zircon growth as there is only one grain with the arc age. The provenance of five zircons, with ages between 375 and 505 Ma, is problematic because granites older than Devonian are unknown in Urals. These grains may have originated from Kazakhstan. The intrusions that formed during Europe–Asia collision form the main age range of Urals (e.g. Main Granite Axis of the Urals), and the arc complexes that preceded the collision occur to the east of this range in the Ob River basin. It is unclear how zircons derived from these intrusions found their way into the Volga basin.

4.1.3. Don River

The Don River, with the exception of the Voronezh massif where the basement of the Sarmatia block is exposed (Shchipansky and Bogdanova, 1996), runs mainly through the sedimentary cover of the Russian platform. However, the Voronezh massif is unlikely to be a major contributor to the Don's zircon population because variations in elevation within the block are small and it is likely that most of the zircons from the Don River were recycled from sediments of the Russian platform. Archean zircons with a maximum at 2.7–2.8 Ga form 8% of zircon population. Early Proterozoic zircons are very abundant and make up 53% of the population and have a relatively uniform age range between 1.47–2.0 Ga (Fig. 2c). Mesoproterozoic zircons with ages mainly between 1.0 and 1.2 Ga make up 20% of population, whereas Phanerozoic zircons, with ages less than 540 Ma, make up only 7%. This population is too small to allow their source to be identified with confidence, although the Uralides and Variscides are most likely. The age distribution of zircons from the Don River shows some similarity with the Dnieper River except for a smaller fraction of Phanerozoic zircons in the Don.

4.1.4. Dnieper River

Exposure in the Dnieper River basin is dominated by the Ukrainian Shield, which includes extensive exposures of Archean rocks (Shchipansky and Bogdanova, 1996), but surprisingly the Dnieper River contains only two zircons with Archean ages. Proterozoic zircons, with a fairly uniform age distribution, from 2.0 to 0.9 Ga are dominant and form 76% of the population (Fig. 2d). Zircons younger than 700 Ma make up only 18% of the studied sample and most grains have ages between 500 and 675 Ma (10%), typical of the Timanian orogeny (Kuznetsov et al., 2007; Pease and Scott, 2009), which is an important event in the basin of the Pechora river, but unknown in the Dnieper basin. The youngest zircons have an age range from 260 to 500 Ma and could be derived from either the Urals or European Variscides.

Rocks with ages range from 1.5 to 1.0 Ga are unknown in the Volga, Don, Dnieper and Pechora river basins, so the source of zircons of this age in these basins is problematical. They are probably recycled zircons from Mesoproterozoic blocks in the Baltic shield, although the area of these blocks is small. Alternatively large rivers could have transported them across EEC at some earlier time or from other blocks, especially from adjacent Scythian and Barentz Blocks.

4.1.5. Ob River

The samples from the Ob River differ from the other rivers in that its detritus come from almost all areas of active erosion in the Paleozoic Central Asia fold belt. The lower course of the river with low gradient lies on the Western Siberian platform, where a thick layer of Mesozoic and Cenozoic sediments covers Paleozoic basement complexes. Zircon population of the Ob River includes two old peaks, a small Archean peak at 2.66–2.8 Ga and a larger early Proterozoic peak at 1.9–2.03 Ga (Fig. 2e). Rocks with these ages are not known in the Ob basin and it is likely that the zircons are recycled grains that originated from the Siberian craton. A significant portion of the zircons from the Ob River includes the grains between 0.5 and 1 Ga (12%) (Fig. 2e), which are also likely recycled grains originally derived from blocks of the Baikalian orogeny (Khain et al., 2003). Most of zircons from the Ob River are from two Phanerozoic peaks, one at ~500 Ma and the other at 300 Ma. Their source rocks are granitoids from Kazakhstan which formed during two discrete orogenic events, the 330–450 Ma Caledonian orogeny (Kostitsyn, 1996; Letnikov et al., 2009) and the 280–330 Ma Hercynian orogeny (Kostitsyn, 1996). The source of a few younger Mesozoic to early Cretaceous (250–120 Ma) zircons is likely to be rift-related granites in the Russian Altai (Vladimirov et al., 1997). Other parts of the Ob basin have been stable since the end of Permian (Zonenshain et al., 1990; Glukhan, 1996).

4.1.6. Yenisey River

The Yenisey River originates from Lake Baikal and the Sayan Mountains. Achean and Paleoproterozoic zircons from the Yenisey River were derived form the Siberian craton basement. Zircons of 900–600 Ma correspond to the Baikalian orogeny and may have originated mainly from the 880–860 Ma granites of the Yenisey ridge (Central Angara terrane) (Nozhkin et al., 1999; Vernikovsky et al., 2007), and some 700–770 Ma zircons are from 720 to 760 Ma granitoids that formed during accretion of the Central Angara terrane to Siberia (Vernikovsky et al., 2007). The majority of zircons from the Yenisey River (52%) formed between 400 and 500 Ma (Fig. 2f) and most of these grains were sourced from the Caledonian terranes of the Sayan Mountains. Grains of 400–250 Ma may have originated from Hercynian collisional complexes, which include the vast 340–270 Ma Angara-Vitim granite batholith (Tsygankov et al., 2007). Eight grains with a Mesozoic age could have originated from alkaline granites (Kovalenko et al.,1999) or core complexes in the Transbaikalia region (Donskaya et al., 2008).

4.1.7. Lena River

The Lena River basin flows through the Siberian craton and its sources are near Lake Baikal and the Aldan shield, where large areas of Archean and Proterozoic rocks are exposed. There is a significant elevation difference between the source of the Lena River and its mouth so erosion is active. The northern sections of the river mainly follow the sedimentary cover of the Siberian craton. The Lena is the only river in Greater Russia that carries a significant fraction of zircons older than 3.0 Ga and half of Lena zircons formed in Archean with a peak at 2.8–2.7 Ga (Fig. 2g). Paleoproterozoic zircons compose 24% of the population with most zircon ages between 1.85 and 1.95 Ga. Phanerozoic zircons make up 20% of zircons with most of these zircons have ages between 250–300 Ma, which corresponds to the Hercynian orogeny in south of the Lena basin, and in particular, the huge Angara-Vitim batholith.

4.1.8. Amur River

The Amur basin lies between the Siberian and North China cratons and mainly drains the complexes of the late Paleozoic-Mesozoic Mongol-Ohotsk belt. We analyzed zircons from two samples from the Amur basin: one sample from mouth of the Zeya River (large tributary of the Amur River) and another from the Amur River near its confluence with the Zeya River. Archean zircons from the Amur River have ages between 2.5 and 2.7 Ga, whereas most Paleoproterozoic zircons have ages between 1.75 and 2.0 Ga (Fig. 2h). These old zircons could have originated from the Siberian and/or North China cratons. However, Mesoproterozoic sediments derived from the North China craton contain abundant 2.4–2.5 Ga zircons (Li et al., 2007), a population that is not recognized in the zircons from the Amur River. On the other hand, Archean and Proterozoic zircons from the Amur River have ages similar to those from the Lena River, indicating that they may have originated from the Siberian craton, rather than the North China craton. Phanerozoic zircons compose 55% of the Amur sediments and 68% of the Zeya sediments. Devonian zircons are very abundant in the Amur River (36%) but are absent from the Zeya River (Fig. 2h). Mesozoic zircons, which mainly originated from the Mongol-Ohotsk belt, are very abundant in the Zeya sample (53%) and make up 15% of total Amur sample.

Note that Mesozoic fold belts, which are located near the periphery of the Siberian craton, were not effectively sampled because the samples of the relevant Siberian rivers were collected some distance from their mouth, above where they cut the Mesozoic fold belts (Fig. 1). These fold belts may therefore be underrepresented in this study.

4.1.9. A summary of the major U/Pb age ranges of zircons from the Greater Russian rivers

The total U/Pb age analyses on zircons from eight rivers yielded an age range from 0.085 to 3.3 Ga, with only five grains, four from Lena and one from Volga, having ages older than 3.0 Ga. Three strong broad peaks and one small peak were recognized in a histogram of all U/Pb ages: 0.1–0.55 Ga, 0.95–1.3 Ga, 1.45–2.0 Ga, and 2.5–2.9 Ga (Fig. 3a). Fig. 3b is a histogram in which the bins are

weighted by drainage area of the sampled rivers. In this case the two major populations shown in Fig. 3a have been arbitrarily subdivided to obtain better resolution as discussed previously; the 0.1–0.55 Ga peak into two narrower zones, and the 1.45–2.0 Ga peak into three smaller ones. We therefore resolve seven age ranges in the weighted Hf model age histogram, *i.e.*, 0.1–0.4 Ga, 0.4–0.55 Ga, 0.95–1.3 Ga, 1.45–1.7 Ga, 1.7–1.85 Ga, 1.85–2.0 Ga, and 2.5–2.9 Ga (Fig. 3b). The percentage of zircons for each of the seven age ranges, from the youngest to the oldest, is 25.0%, 18.7%, 6.7%, 6.4%, 8.6%, 17.6% and 16.9%.

Safonova et al. (2010) studied U/Pb ages of detrital zircons from Don, Volga, Ob, Yenisey and Amur rivers. The peaks and relative intensity of the age distribution histograms for most of the rivers they studied, are similar to ours, indicating that detrital grains analyzed in both studies are representative and reproducible.

4.2. O isotope

Most Archean zircons have $\delta^{18}O$ values lying between 4.53‰ and 7.33‰ (Fig. 4), with the two high exceptions having values of 7.73‰ and 8.45‰ and two low grains having values of 3.95–4.28‰. The Archean zircons yield an average of $\delta^{18}O = 6.05 \pm 1.09$ (1σ)‰. Proterozoic and Phanerozoic zircons show a dramatic increase in their maximum $\delta^{18}O$ values to 12‰ (Fig. 4). Compared with Archean zircons, Proterozoic and Phanerozoic zircons are more variable in $\delta^{18}O$ values than Archean zircons and have a larger range of $\delta^{18}O$ values in each of the time intervals (Fig. 4a). However,

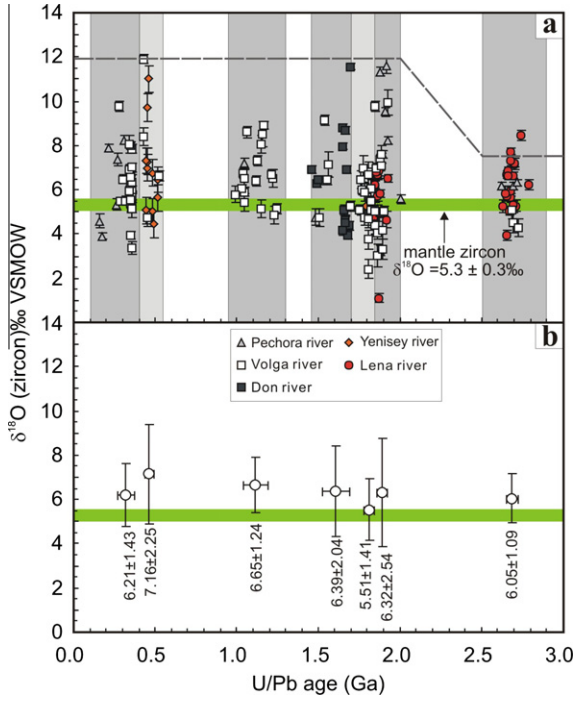

Fig. 4. (a). Plot of $\delta^{18}O$ values versus U/Pb ages for the detrital zircons from the major rivers in Greater Russia and (b). the average $\delta^{18}O$ vaules for the zircons from each of the time intervals. The heavy dashed line shows a step increase of $\delta^{18}O$ values from 2.5 to 2.0 Ga.

there is little evidence of a systematic change in their average $\delta^{18}O$ values with time. The average $\delta^{18}O$ values for zircons of the six time internals in Proterozoic and Phanerozoic are 6.21 ± 1.43‰ for 0.1–0.4 Ga, 7.16 ± 2.25‰ for 0.4–0.55 Ga, 6.65 ± 1.24‰ for 0.95–1.3 Ga, 6.39 ± 2.04‰ for 1.45–1.7 Ga, 5.51 ± 1.41‰ for 1.7–1.85 Ga, 6.32 ± 2.54‰ for 1.85–2.0 Ga, respectively (Fig. 4b). Valley et al. (2005) also found that most Archean zircons have lower maximum $\delta^{18}O$ (<7.5‰) than most Phanerozoic and Proterozoic zircons ($\delta 18O < 10$‰). However, instead of a continuous increase in $\delta^{18}O$ documented by Valley et al. (2005) and Kemp et al. (2006), our data, from both Greater Russia and Mississippi river basin (see Wang et al., 2009), suggest a step increase in the range of observed $\delta^{18}O$ values from 2.5 to 2.0 Ga, *i.e.*, most zircons older than 2.5 Ga have $\delta^{18}O$ lying between 4.5‰ and 7.5‰ whereas most zircons younger than 2.0 Ga vary more widely from 4.5‰ to 12‰ with some low $\delta^{18}O$ exceptions (Fig. 4a).

4.3. Lu–Hf isotopes

The Hf chondritic value of Blichert-Toft and Albarede (1997) was used to calculate εHf_i values and the depleted mantle $^{176}Hf/^{177}Hf$ growth line was calculated assuming a present-day $^{176}Hf/^{177}Hf = 0.283251$, similar to that of average mid-ocean ridge basalts, $^{176}Lu/^{177}Hf = 0.0384$ (Griffin et al., 2002) and a decay constant of 1.867×10^{-11} yr^{-1} for ^{176}Lu (Söderlund et al., 2004). Hf model ages were calculated from the measured Hf isotopic compositions and U/Pb ages of the zircons by projecting the $(^{176}Hf/^{177}Hf)_i$ of zircons back to the depleted mantle growth curve, assuming a $^{176}Lu/^{177}Hf$ ratio for the crustal source region that melted to form the melt from which the zircon crystallized. Two model ages were calculated. The first (T_{DM}^{C}, *constant*) assumes a mean crustal $^{176}Lu/^{177}Hf$ ratio of 0.0115 (Rudnick and Gao, 2003) for the zircon source region. The second Hf model age (T_{DM}^{V}, *variable*) was calculated using $^{176}Lu/^{177}Hf$ ratios that varied with measured $\delta^{18}O$ values of the analyzed grains. Because the $^{176}Lu/^{177}Hf$ ratio of the crust is highly variable and there are appreciable differences in this ratio between upper (0.00831), lower (0.0187) and average continental crust (0.0115) (Rudnick and Gao, 2003), the choice of the $^{176}Lu/^{177}Hf$ ratio used in the Hf model age calculations can have a profound influence on the results (see Fig. 5). We have therefore used O isotopes to reduce uncertainty in the choice of $^{176}Lu/^{177}Hf$ for individual grains. Zircons with near-mantle O isotope values are assumed to have crystallized from a melt derived by melting mafic igneous rocks or a mixture between such a melt and mantle derived melt. Zircons with high O isotope values are assumed to have crystallized from a magma derived from a crustal source region with high sedimentary component. We have assumed a $^{176}Lu/^{177}Hf = 0.021$ for the samples with the most primitive O isotope values ($\delta^{18}O \leqslant 5.5$‰), a value appropriate for mafic lower crust (Kemp et al., 2006) and 0.0083 for zircons with $\delta^{18}O > 9.5$‰, a value appropriate for the upper crust. $^{176}Lu/^{177}Hf$ values for zircons with O isotope values lying between these extremes have been determined by linear interpolation using an equation:

$$^{176}Lu/^{177}Hf = 0.0362 - 0.0028 \times \delta^{18}O$$

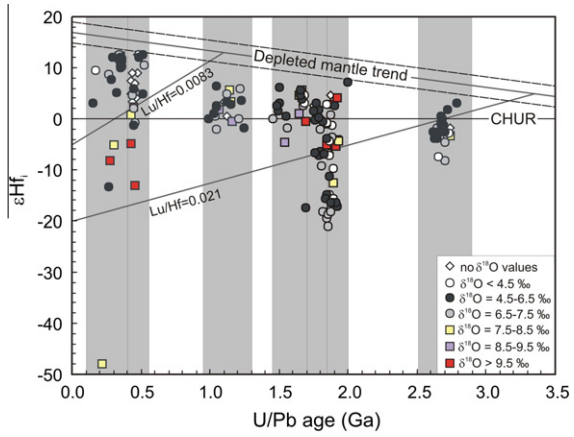

Fig. 5. Plot of εHf_i versus U/Pb ages, which also shows $\delta^{18}O$ values for each of the measured grains. The Hf chondritic value of Blichert-Toft and Albarede (1997) was used for the calculation of εHf_i values and the depleted mantle $^{176}Hf/^{177}Hf$ growth line was calculated assuming a present-day $^{176}Hf/^{177}Hf = 0.283251$, similar to that of average mid-ocean ridge basalts, $^{176}Lu/^{177}Hf = 0.0384$ (Griffin et al., 2002) and a decay constant of 1.867×10^{-11} yr^{-1} for ^{176}Lu (Söderlund et al., 2004).

where the $\delta^{18}O$ values were set as 5.5‰, 6‰, 7‰, 8‰, 9‰ and 10‰ to obtain the $^{176}Lu/^{177}Hf$ ratios for the zircons with $\delta^{18}O$ values within the intervals of <5.5‰, 5.6–6.5‰, 6.6–7.5‰, 7.6–8.5‰, 8.6–9.5‰ and >9.5‰.

The Hf model ages calculated for this study are subject to two qualifications. First, the widely accepted Griffin et al. (2002) model age is based on an average MORB $^{176}Hf/^{177}Hf = 0.283251$, well above the value of 0.283164 obtained by Chauvel et al. (2008) in a more recent compilation. Using the Chauvel et al. (2008) value lowers Hf model ages by 150–270 Myr depending on the ages and $^{176}Hf/^{177}Hf$ ratio of the zircon. It also ignores the widely held view that continental crust forms at arcs (Taylor, 1967), where the mantle has slightly lower $^{176}Hf/^{177}Hf$ ratio than MORB and other possible complications in the mantle growth curve for Hf (see Hawkesworth et al., 2010). Despite these reservations we present model ages calculated by the Griffin et al. (2002) value because they are compatible with other published data. Second, although the use of variable $^{176}Lu/^{177}Hf$ ratios (T_{DM}^{V}) produces more reliable Hf model ages than those based on a constant Lu/Hf ratio (T_{DM}^{C}), it still does not solve the smearing or hybrid age problem for zircons with high $\delta^{18}O$ values, which are interpreted to come from S-type granites. This problem will be discussed further below.

A plot of U/Pb ages versus εHf_i shows that grains in the 0.1–0.4, 0.4–0.55, 1.7–1.85 and 1.85–2.0 Ga U/Pb time intervals have more variable εHf_i values than those in other time ranges (Fig. 5).

5. DISCUSSION

5.1. Juvenile or reworked continental crust?

Zircons derived from juvenile crust should have εHf_i values lying within error of the depleted mantle growth curve for Hf and have $\delta^{18}O$ value close to the mantle value of 5.3 ± 0.3‰. If we define juvenile crust as having εHf_i value within 2 units of the Griffin et al. (2002) depleted mantle growth curve and $\delta^{18}O$ value between 4.5‰ and 6.5‰, none of the Greater Russian zircons are from juvenile crust (Fig. 5). However, if we use the lower average $^{176}Hf/^{177}Hf$ value for the mantle growth curve recommended by Chauvel et al. (2008) and recognize that juvenile magmas at continental margins commonly mix with crustal melts, as many as 6–10% of the zircons plotted on Fig. 5 could be reasonable be classified as originating from juvenile crust. Even so it is clear that zircons from juvenile continental crust are rare in Greater Russia and that the overwhelming majority of grains were produced by remelting of accreted oceanic arcs or older continental crust. This analysis ignores the contribution of juvenile basaltic rocks to the continental crust that do not crystallize zircons, such as continental tholeiitic and basaltic arc magmas.

Most zircons crystallize from quartz-saturated magma produced by partial melting of the continental crust. As a consequence a minimum of two stages are required in the formation of zircons: stage 1, the separation of a primitive continental crust from the mantle, and stage 2, cratonization, which involves widespread melting of the primitive continental crust to form granites (Campbell and Hill, 1988; McLaren and Sandiford, 2001). T_{DM}^{V} Hf model ages date stage one, separation of continental crust from the mantle, whereas U/Pb ages date stage two. U/Pb ages of the zircons are less than their T_{DM}^{V} ages and the difference between them is referred as crustal incubation time.

A plot of T_{DM}^{V} Hf model age versus U/Pb age for the zircons from the Pechora, Volga, Don, Yenisey and Lena rivers, contoured for incubation time, indicates that the majority of zircons have crustal incubation time of 300–1000 Myr, with only 12 grains having incubation time of less than 300 Myr (Fig. 6), again showing that juvenile crust

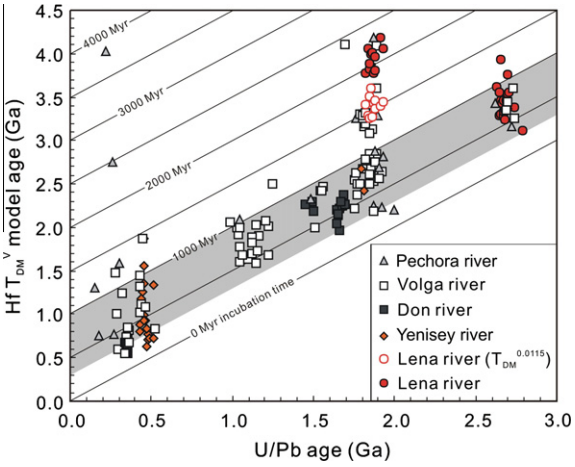

Fig. 6. A Plot of U/Pb ages versus Hf T_{DM}^{V} model ages for the detrital zircons from Greater Russia, contoured for crustal incubation time. The $T_{DM}^{0.0115}$ model ages were calculated using $^{176}Lu/^{177}Hf = 0.0115$ for the Lena Paleoproterozoic zircons to show that the model ages are lowered between 350 to 790 Myr when this ratio was used. Note that most zircons have incubation times of between 300 and 1000 Myr (grey field).

in Greater Russia is rare. T_{DM}^{V} ages for Paleoproterozoic zircons from the Pechora River indicate both young and Archean protoliths, whereas the late Paleozoic and Mesozoic zircons yield a wide range of T_{DM}^{V} ages and thus originated from heterogeneous protolith with a significant contribution from ancient crust. One grain from the Pechora River has extremely long crustal incubation time of 3.81 Gyr (Fig. 6). In this respect the Pechora zircons contrast with Mesoproterozoic grains of the Don River, which originated from a crust with short incubation time (Fig. 6).

Paleoproterozoic zircons of the Volga River show a large variation of T_{DM}^{V} ages (Fig. 6), reflecting formation by reworking of crust that ranged in age from young to Archean. Mesoproterozoic and Paleozoic zircons of the Volga River, on the other hand, formed during reworking of crust that was mainly >1000 Myr old and some of the Paleozoic zircons may have come directly from juvenile crust. These data are in a good agreement with the model of the eastern part of EEC by Bogdanova et al. (2008) and a Uralian orogen source for the Paleozoic zircons.

Paleoproterozoic zircons from the Yenisey River have shorter incubation time than those from the Lena River. These data, together with the absence of Archean zircons in the Yenisey, are inconsistent with models that assume an Archean basement for the western Siberian craton (Smelov and Timofeev, 2007). Late Neoproterozoic to Early Paleozoic zircons from the Yenisey River have T_{DM}^{V} ages in the range of 0.5–1.8 Ga (Fig. 6). These data show that the Paleozoic granitic rocks formed by melting a heterogeneous basement that included juvenile or very young crust, Neoproterozoic (Baikalian orogeny) blocks, and ancient Siberian craton crust.

Most Archean zircons from the Lena River have T_{DM}^{V} ages ranging from 3.1 to 3.6 Ga, which shows that the Archean crust of the Siberian craton extends back to that period (Rosen and Turkina, 2007). Paleoproterozoic zircons, on the other hand, have T_{DM}^{V} ages (3.8–4.2 Ga) that are appreciably older than Archean zircons (Fig. 6). Although they overlap in time, the two periods of crust formation have an average model age difference of 430 Myr. Surprisingly, it is the crust with the younger model age that melted first. This scenario is unexpected.

There are two alternative explanations for the unexpected old Hf model ages of the Lena Paleoproterozoic zircons. The first is that an inappropriate $^{176}Lu/^{177}Hf$ ratio was used to calculate the T_{DM}^{V} Hf model ages. If it is assumed that Paleoproterozoic and Archean granitic rocks in the Lena basin formed by melting protoliths of the same age at different times the T_{DM}^{V} ages of their zircons should be similar. The $^{176}Lu/^{177}Hf$ ratio required to bring the T_{DM}^{V} ages of the Paleoproterozoic grains into line with the Archean zircons is 0.0115, that of the average continental crust (Fig. 6). This is appreciably less than the value of 0.021 we used in the T_{DM}^{V} age calculations for the Lena Paleoproterozoic zircons, which was based on the mantle-like O isotopic ratios of the zircons.

We cannot offer a compelling explanation as to why an average crustal $^{176}Lu/^{177}Hf$ ratio should apply to the apparently primitive Lena Paleoproterozoic zircons with $\delta^{18}O < 6.5$. Our preferred interpretation of the Lena Paleoproterozoic zircons is that the O isotopic composition of these zircons was reset by a later thermal event and that 0.0115 is an appropriate $^{176}Lu/^{177}Hf$ ratio to use in the Hf model age calculations for these grains. There are three lines of evidence supporting a low $^{176}Lu/^{177}Hf$ for the Lena Paleoproterozoic zircon T_{DM}^{V} Hf model age calculation. First, the average $^{176}Lu/^{177}Hf$ ratio for the Lena Archean zircons is 0.000619 compared with 0.000313 for the Paleoproterozoic zircons. This observation is assumed to be consistent with the source region for Paleoproterozoic zircons having lower $^{176}Lu/^{177}Hf$ ratios than that of the Archean zircons. It does not prove this point because other factors such as fractionation of Lu/Hf ratios during partial melting and fractional crystallization of the magma from which the zircon crystallized can also influence the relationship between the $^{176}Lu/^{177}Hf$ ratios of the zircons and its protolith source. Secondly, Nd model ages of the oldest igneous rocks in the Lena River basin range from 2.9 to 3.7 Ga (Rosen and Turkina, 2007) and thus provide no evidence for a protolith older than 3.7 Ga in the region. Nd model ages for igneous rocks are more reliable than zircon Hf model ages because the Sm/Nd ratios used in Nd model age calculations are better constrained than the Lu/Hf ratios used in the Hf calculations. However, the agreement between the igneous rock-based Nd model ages and the zircon-based Hf model ages, using 0.0115 for the $^{176}Lu/^{177}Hf$ ratio, could still be fortuitous because there is considerable uncertainty regarding the nature of the mantle growth curves for both isotopic systems as discussed earlier in connection with the Lu–Hf system. Thirdly, the cathodoluminescence images of the Lena Paleoproterozoic zircons show that the grains may have been subjected to a high temperature thermal event (Fig. 7). The fine banding, typical of zircon from felsic igneous rocks and courser banding typical of zircons from mafic rocks, has faded to varying degrees and in two cases, LNT-004 and LNT-065, has totally been obliterated. The alternatively low $^{176}Lu/^{177}Hf$ ratio for the Lena Paleoproterozoic zircons source region lowers the T_{DM}^{V} age range from 3.8 to 4.2 Ga to 3.3 to 3.6 Ga and the mean from 3.9 to 3.4 Ga.

Although we emphasize that our preferred interpretation is principally based on the consistency of Hf model age with Nd model ages of the oldest igneous rocks within the Lena basin, another possibility is also considered. A second explanation for the anomalously old Hf model ages of the Lena Paleoproterozoic zircons is that these zircons initially crystallized at ca. 2.7 Ga but had their U/Pb system reset during a metamorphic event at ca. 1.85 Ga, resulting in the model age calculations incorporating an inappropriate $^{176}Lu/^{177}Hf$ ratio between 1.9 and 2.7 Ga and in an overestimation of the Hf model ages. This explanation is unlikely for two reasons. First, incorporating an initial zircon crystallization age of 2.7 Ga into the Hf model age calculation lowers the model ages by an average of ca. 800 Myr and the range to 2.9–3.3 Ga, well below the range of the 3.1–3.6 Ga for the Archean Lena zircons that we were expecting to replicate. Second, although resetting of the U/Pb system is common in Archean zircons, it only occurs if the U content of the grains exceeds ca. 300 ppm (e.g. Squire et al., 2010). The reason for the reset of U/Pb

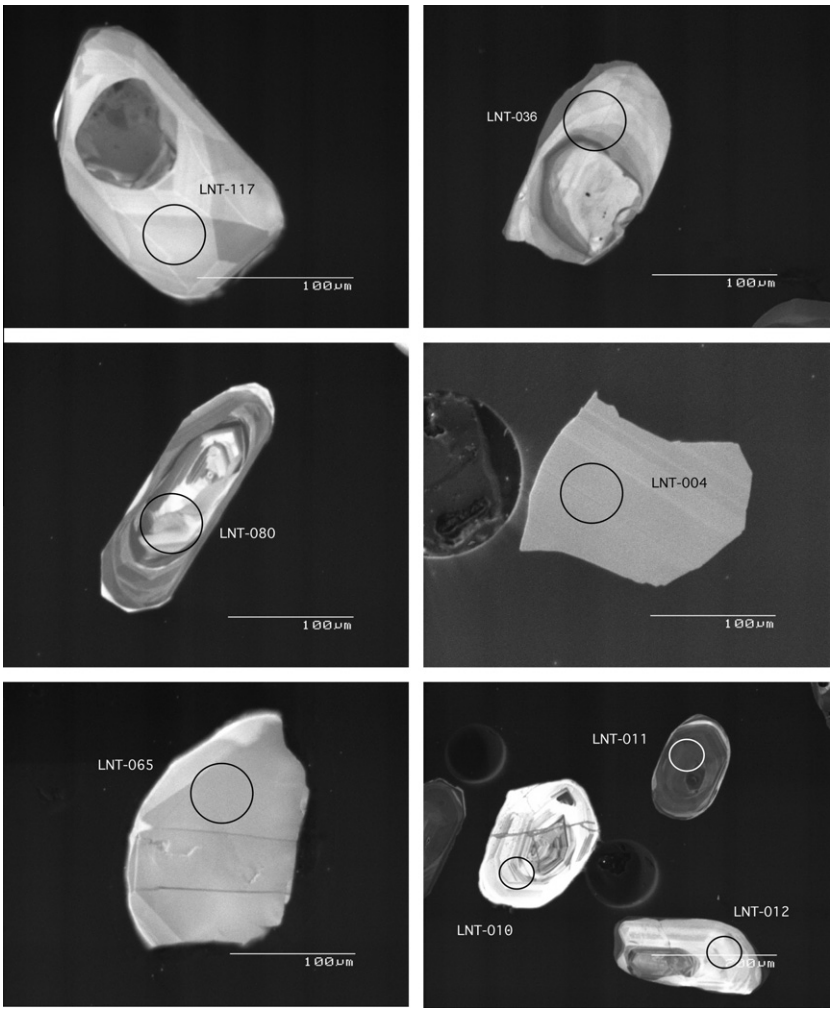

Fig. 7. Cathodoluminescence images of representative Lena Paleoproterozoic zircons. Note that the igneous banding is faint and in two cases, LNT-004 and LNT-065, has almost been obliterated. Two grains, LNT-117 and LNT-036, show a core and rim, but the U/Pb age and Hf isotope on the rim of the grains were analyzed. Two grains, LNT-080 and LNT-012, have cores that are the same age as the rims. LNT-010 and LNT-011 are Archean zircons.

system is that high U grains become metamict if they are held for an extended period below the zircon annealing temperature of ca. 220°C, and therefore readily lose Pb. Crystalline zircon, however, is resilient to Pb loss, even at the temperature of granitic magmas, due to the low diffusion rate of Pb in zircon (Lee et al., 1997). The abundance of xenocrysts in granitic rocks testifies to the resilience of the U/Pb system in zircon to thermal resetting. Only one of the Lena Paleoproterozoic zircons has an U content above 300 ppm. The remainder have U contents between 20 and 205 ppm with an average value of 100 ppm, making it unlikely that these zircons became metamict and therefore susceptible to Pb loss.

However, we suggest that the use of $^{176}Lu/^{177}Hf = 0.0115$ for zircons with mantle-like O isotopes is a unique occurrence that should not be applied to other low $\delta^{18}O$ zircons. Hawkesworth et al. (2010) compiled data for zircons with mantle-like $\delta^{18}O$ values and identified three crustal arrays with slopes corresponding to $^{176}Lu/^{177}Hf$ ratios between 0.19 and 0.24. We therefore see no reason to abandon our general conclusion that the appropriate $^{176}Lu/^{177}Hf$ ratio for zircons with mantle-like $\delta^{18}O$ value is ~0.021.

5.2. Continuous or episodic continental crust growth?

The average Hf model crustal formation age for each of the U/Pb age time intervals recognized in Greater Russia is listed in Table 1. The average Hf model ages were weighted by the fraction of zircons in each of the selected U/Pb age populations (load-weighted) as shown in Fig. 3b, which in turn, were weighted by river drainage area as previously noted. The average weighted T_{DM}^{V} age for crust growth is 2.12 Ga, which is identical to the average load-weighted T_{DM}^{V} age of 2.13 Ga for the Mississippi river basin (Wang et al., 2009), indicating that Archean was an important period of continental crustal growth in both continents. However, the load-weighted T_{DM}^{V} age of 2.12 Ga is a minimum estimate because older zircons are more likely to suffer radiation damage and be destroyed during multiple cycles of erosion and sedimentation. In addition, rivers derive a

Table 1
Average variable Lu/Hf (T_{DM}^{V}) and fixed Lu/Hf (T_{DM}^{C}) Hf model ages for each of time intervals resolved by zircon U/Pb ages for Greater Russia.

Column	1 U/Pb age time intervals (Ga)	2 Average T_{DM}^{v} (Ga)[a]	3 Average T_{DM}^{v} (Ga)[b]	4 Average T_{DM}^{C} (Ga)[c]	5 Fraction of zircons[d]	6 Proportion of outcrop area of source rocks[e]	7 Weighted T_{DM}^{v} by load (Ga)[f]	8 Weighted T_{DM}^{v} by area (Ga)[g]	9 Weighted T_{DM}^{v} by load (Ga)[h]	10 Weighted T_{DM}^{v} by area (Ga)[i]	11 Weighted T_{DM}^{C} by load (Ga)[f]
1	0.1–0.4	0.95 ± 0.71	0.95 ± 0.71	0.81 ± 0.62	0.250	0.03	0.24	0.03	0.24	0.03	0.20
2	0.4–0.55	1.09 ± 0.34	1.09 ± 0.34	1.03 ± 0.33	0.187	0.37	0.20	0.40	0.20	0.40	0.19
3	0.95–1.3	1.89 ± 0.22	1.89 ± 0.22	1.72 ± 0.14	0.067	0.05	0.13	0.09	0.13	0.09	0.12
4	1.45–1.7	2.33 ± 0.44	2.33 ± 0.44	2.16 ± 0.30	0.064	0.02	0.15	0.05	0.15	0.05	0.14
5	1.75–1.85	3.00 ± 0.50	2.92 ± 0.38	2.66 ± 0.37	0.086	0.30	0.26	0.90	0.25	0.88	0.23
6	1.85–2.1	3.21 ± 0.69	3.08 ± 0.56	2.90 ± 0.45	0.176	0.06	0.57	0.19	0.54	0.18	0.52
7	2.45–2.9	3.43 ± 0.18	3.43 ± 0.18	3.23 ± 0.12	0.169	0.17	0.58	0.58	0.58	0.58	0.55
					Average crustal formation age		**2.12**	**2.25**	**2.09**	**2.22**	**1.94**

[a] Hf model ages calculated with $^{176}Lu/^{177}Hf$ ratios that vary with the O isotopic values of the individual grains.
[b] Hf model ages calculated with $^{176}Lu/^{177}Hf$ ratios that vary with the O isotopic values of the individual grains and a $^{176}Lu/^{177}Hf$ ratio of 0.0115 is used for the Hf model age calculations of the Lena Paleoproterozoic zircons.
[c] Hf model ages calculated with a fixed average crustal $^{176}Lu/^{177}Hf$ ratios of 0.0115.
[d] The fraction of zircons that lie within the designated U/Pb time intervals shown in the weighted histogram of Fig. 3.
[e] The fraction used for weighting by area has been determined by measuring the outcrop area of the orogenic events shown in Fig. 1.
[f] Weighted T_{DM}^{v} and T_{DM}^{C} ages are the average T_{DM}^{v} ages in column 2 and T_{DM}^{C} ages in column 4 weighted by the fraction of zircons in each of the selected U/Pb age time intervals.
[g] Weighted T_{DM}^{v} ages are the average T_{DM}^{v} in column 2 weighted by the area in each of the selected U/Pb age time intervals.
[h] Weighted T_{DM}^{V} ages are the average T_{DM}^{V} in column 3 weighted by the fraction of zircons in each of the selected U/Pb age time intervals.
[i] Weighted T_{DM}^{V} ages are the average T_{DM}^{V} in column 3 weighted by the area in each of the selected U/Pb age time intervals.

disproportionate fraction of their load from rapidly eroding young orogenic areas that will normally include a high fraction of young crust. As an alternative a second average T_{DM}^{V} age was calculated that was weighted by the area covered by the different aged orogenic events shown in Fig. 1. The area-weighted average T_{DM}^{V} age is 2.25 Ga (Table 1), which may give a better estimation of the average age of formation of Greater Russia. When our preferred low $^{176}Lu/^{177}Hf$ model ages are used for the Lena Paleoproterozoic zircons the load- and area-weighted ages fall to 2.09 and 2.22 Ga, respectively.

If a crustal source region for the granitic melt from which a zircon crystallizes contains a significant sedimentary component, Hf model ages will be smeared by the sedimentary component and will represent an average or hybrid model age of the components that make up the sediments, and not a specific crustal extraction age (Hawkesworth and Kemp, 2006b; Pietranik et al., 2008; Wang et al., 2009). Therefore, it is important to identify zircons that crystallized from a melt produced by melting a source rock with high fraction of sediments when using Hf model ages to date discrete periods of continental growth. The O isotopic composition of igneous zircons provides a record of intracrustal recycling of sediments (Valley et al., 2005). Zircons in equilibrium with pristine mantle-derived melts should have a $\delta^{18}O$ value of $5.3 \pm 0.3‰$ (Valley et al., 1998), whereas zircons derived from a mixed magma source with both mantle-derived and sedimentary components should have $\delta^{18}O$ values higher than $5.3 \pm 0.3‰$. The low $\delta^{18}O$ values (4.53–7.33‰) of Archean zircons of Greater Russia indicate only minor amount of sediments in the source regions of the Archean zircons. Highly variable $\delta^{18}O$ values (4.5–12‰) of Proterozoic and Phanerozoic zircons can be attributed to a combination of higher $\delta^{18}O$ values in sediments after 2.5 Ga, and higher ratios of sedimentary to igneous rocks in the source region of the magma from which the zircons crystallized (Land and Lynch, 1996; Shields and Veizer, 2002; Perry and Lefticariu, 2003; Valley et al., 2005), indicating that sediments became increasingly important in the source region of Proterozoic and Phanerozoic granitic melts after cratonization of continents in the late Archean. In the case of Greater Russia, zircons with ages between 0.4 and 0.55 Ga and between 1.8 and 2.0 Ga have significantly higher and more variable $\delta^{18}O$ values than zircons of other periods (Fig. 4), implying an unusually high sedimentary fraction in the source region of some of the granites during these two periods.

Ideally only the zircons with O isotopic values lying within the mantle range ($\delta^{18}O = 5.3 \pm 0.3‰$) can be interpreted to have come from a magmatic precursor that contain no sedimentary component, and therefore, only grains with $\delta^{18}O$ values between 5.0‰ and 5.6‰ should be considered when calculating the model age of discrete crustal extraction events. Incorporating zircon Hf model ages of grains with $\delta^{18}O > 5.6‰$ smears the crustal extraction ages by mixing the discrete model crustal extraction age of the magmatic component in the continental crust with the average or mixed model age of the sedimentary component. In practice, the range has been extended to 4.5–6.5‰, taking into account the errors associated with the analyses of O isotope by SHRIMP and recognizing that incorporating a small fraction of sediment in the source region will produce minimal smearing. ~41% zircons analyzed in this study have $\delta^{18}O$ values between 4.5‰ and 6.5‰. Fig. 8 shows histograms of T_{DM}^{V} model ages: Fig. 8a shows the T_{DM}^{V} ages for all grains, assuming $^{176}Lu/^{177}Hf$ of 0.0115 for the Lena Paleoproterozoic zircons; Fig. 8b shows only grains with $\delta^{18}O$ values between 4.5‰ and 6.5‰ with the Lena Paleoproterozoic zircons omitted because of uncertainty as to the appropriate $^{176}Lu/^{177}Hf$ used for the Hf model age calculations; Fig. 8c shows the Hf model ages of all the zircons calculated using a $^{176}Lu/^{177}Hf$ that varies with the $\delta^{18}O$ of the zircons; and Fig. 8d is the same as Fig. 8c but includes only zircons with mantle $\delta^{18}O$ values. The number of zircons for each of the age bins in Fig. 8 is weighted by the fraction of zircon U/Pb ages in each of the seven time intervals as discussed in connection with Fig. 3b (load-weighted). The T_{DM}^{V} ages of the zircons in Fig. 8a spread nearly continuously between 0.5 and 4.2 Ga with a major peak at 0.5–0.9 Ga, and a slightly smaller peak at 3.2–3.5 Ga. Both peaks are dominated by zircons with mantle-like $\delta^{18}O$ values, which suggests minimal sediment involvement. The young strong period of crustal growth occurred during closure of oceans, whose complexes now form Central Asia fold belt. We suggest that the closing oceans brought proto-igneous crust, probably in the form of island arcs that formed between 0.5 and 0.9 Ga, into the Cental Asia fold belt where it was melted by mantle derived magmas to provide the principal constituents of granitic rocks of the Cental Asia fold belt. By analogy the zircons with Hf model ages of around 3.4 Ga are thought to have formed as arcs that were reworked by mantle-derived magmas at ca. 2.65 Ga. For grains with mantle-like $\delta^{18}O$ values (Fig. 8b) the prominent peaks are sharper than in Fig. 8a, and reduce to 0.6–0.8 Ga and 3.3–3.5 Ga, indicating that some smearing occurs if all grains are included. Fig. 8c and d are similar to Fig. 8a and b except that at the old end of the diagram the prominent peak becomes broader due to the Lena Paleoproterozoic zircons being moved from the 3.4 Ga peak to older ages.

Calculated growth curves for the Greater Russian continental crust are shown in Fig. 9. Because the T_{DM}^{V} Hf model age of crust extraction periods can be distorted by smearing, as discussed in connection with Fig. 8, curves were calculated for all grains and for grains with near mantle $\delta^{18}O$ values. Four different growth curves are given: (1) load-weighted T_{DM}^{V} Hf model ages (curve 3 in Fig. 9a and b), (2) area-weighted T_{DM}^{V} Hf model ages (curve 4 in Fig. 9a and b), (3) load-weighted T_{DM}^{C} Hf model ages (curve 5 in Fig. 9a and b), and (4) load-weighted T_{DM}^{V} Hf model ages in which an average $^{176}Lu/^{177}Hf$ ratio of 0.0115 was used to calculate the model age for the Lena Paleoproterozic zircons (curve 6 in Fig. 9a and b). Curve 6 gives our preferred interpretation of reason discussed in connection with Fig. 8. All curves lie closer to the continuous growth model of McLennan and Taylor (1982) (curve 2 in Fig. 9) than to the steady-

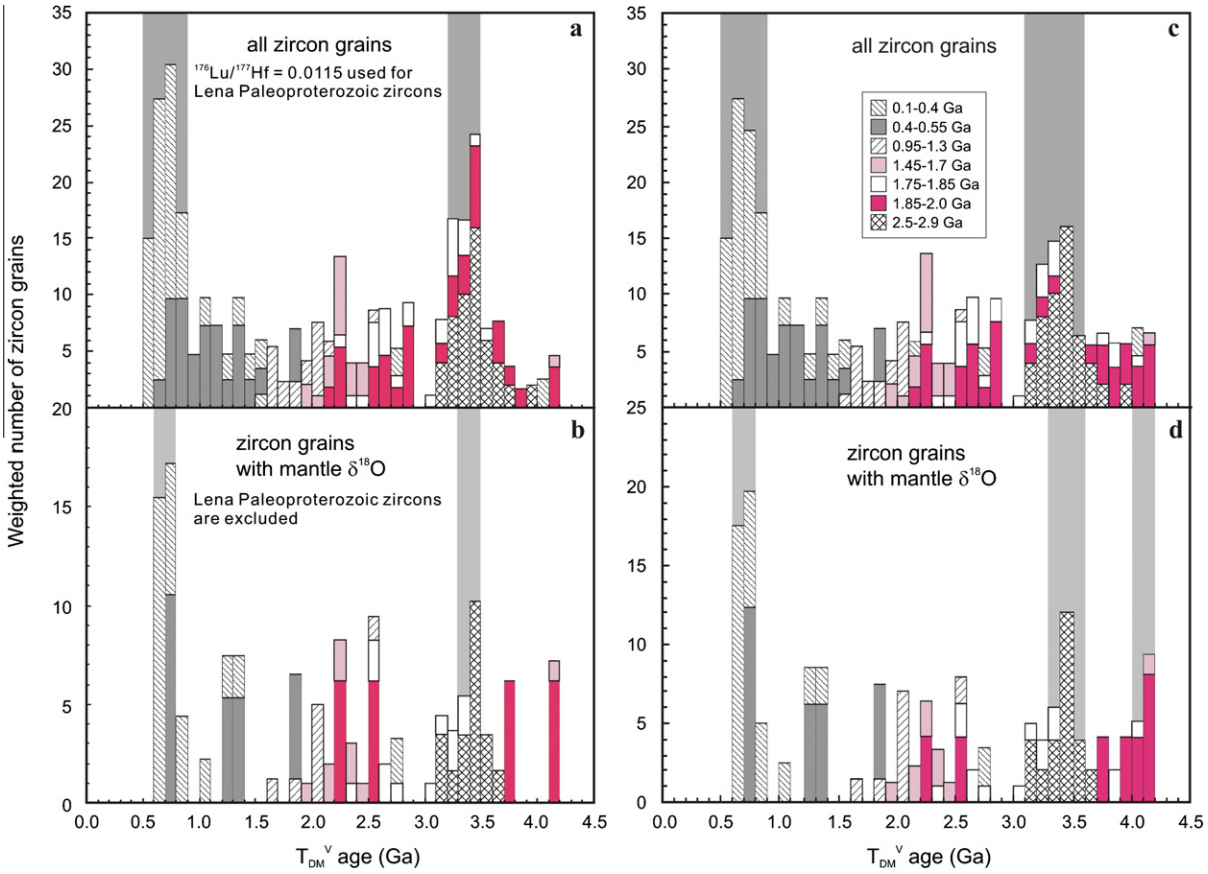

Fig. 8. (a). Histogram showing Hf T_{DM}^{V} model ages for all zircons, for which the model ages of the Lena Paleoproterozoic zircons were calculated using the $^{176}Lu/^{177}Hf$ ratio of 0.0115; (b). T_{DM}^{V} model ages for zircons with $\delta^{18}O = 4.5–6.5‰$, with the Lena Paleoproterozoic zircons being excluded because of uncertainty regarding the appropriate usage of $^{176}Lu/^{177}Hf$ ratios; (c) T_{DM}^{V} model ages for all zircons and (d) T_{DM}^{V} model ages for zircons with $\delta^{18}O = 4.5–6.5‰$. The T_{DM}^{V} ages have been weighted according to the fraction of zircons in whichever of the seven U/Pb age time intervals recognized in Fig. 3b the zircon fall as follows: weighting factor = (percentage of zircons in the U/Pb age time interval × 30)/number of zircons analyzed for Hf analyses from that age interval. The number 30 is arbitrary and is introduced to bring the minimum weighting factor close to 1.

state crustal growth curve of Armstrong (1981, 1991) (curve 1 in Fig. 9) between 4.1 and 2.7 Ga, but are well below McLennan and Taylor's curve between 2.7 and 0.6 Ga. The T_{DM}^{V} Hf model age curves are similar in shape to the constant Lu/Hf T_{DM}^{C} Hf model age curves (Fig. 9), but for a given fraction of continental growth the T_{DM}^{V} Hf model ages are 100–200 Myr older than the T_{DM}^{C} model ages, except at model ages greater that 3.0 Ga, where the difference can be greater than 500 Myr. The growth curves for all of the T_{DM}^{V} Hf model ages are remarkably similar between 3.3 and 4.2 Ga. Growth starts at 4.2 Ga, reaches ~30% of the present volume by 3.3 Ga, ~72% by 0.9 Ga and was completed by 0.6 Ga. However our preferred interpretation of curve 6 in Fig. 9 differs from the other T_{DM}^{V} curves between 3.3 and 4.2 Ga. Although some growth may start as early as 4.2 Ga, significant growth was delayed until 3.5 Ga, showing two principal periods of crustal growth, 3.5–3.3 Ga and 0.8–0.6 Ga, which are separated by an interval of low but more or less continuous growth (Fig. 9b).

The interpretation of peaks in continental growth, inferred from zircon Hf model ages, could be complicated by variable preservation. Campbell and Allen (2008) have shown that peaks in the U/Pb ages of zircons coincided with periods of supercontinent formation. This observation can be interpreted to mean that more crustal melting and therefore more zircon growth occurs during periods of continent amalgamation, or that continental amalgamation resulted in better preservation of newly formed continental crust (Hawkesworth et al., 2009). If the latter interpretation is correct preferential preservation of zircons during supercontinent formation could bias the Hf model ages. That is growth of the continental crust could be continuous, whereas the peaks and troughs in zircon Hf model ages histograms could be due to respective periods of enhanced and diminished crustal preservation. Our data favor the first interpretation. There is no obvious correlation between supercontinent formation and zircon Hf model ages (Fig. 10). Furthermore the Hf model ages of the zircons that crystallized during the 250–500 Ma and 1.85 Ga

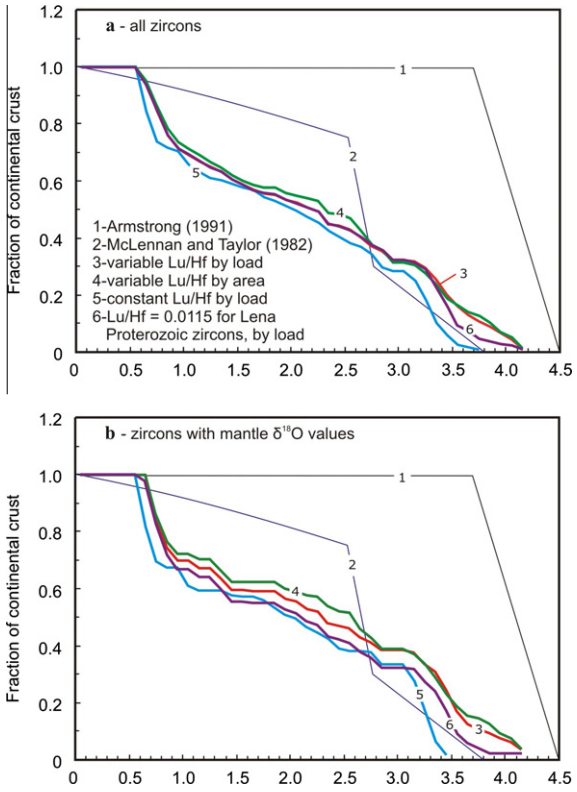

Fig. 9. Cumulative continental crust growth curves of Greater Russia. Data were weighted by the fraction of zircons in each of time intervals as shown in Fig. 3b or by the basement area of the orogenic events with the corresponding age as shown in Fig. 1. Zircon Hf model ages were calculated to use both $^{176}Lu/^{177}Hf$ ratios that vary with the measured $\delta^{18}O$ values of the zircons and a constant average crustal $^{176}Lu/^{177}Hf$ ratio of 0.0115. The Hf model ages for the Lena Paleoproterozoic zircons are calculated using the $^{176}Lu/^{177}Hf$ ratio of 0.0115. The upper figure (a) gives the growth curves calculated from all zircons, whereas the lower figure (b) uses only grains with near mantle $\delta^{18}O$ values, from which the Lena paleoproterozoic zircons are excluded.

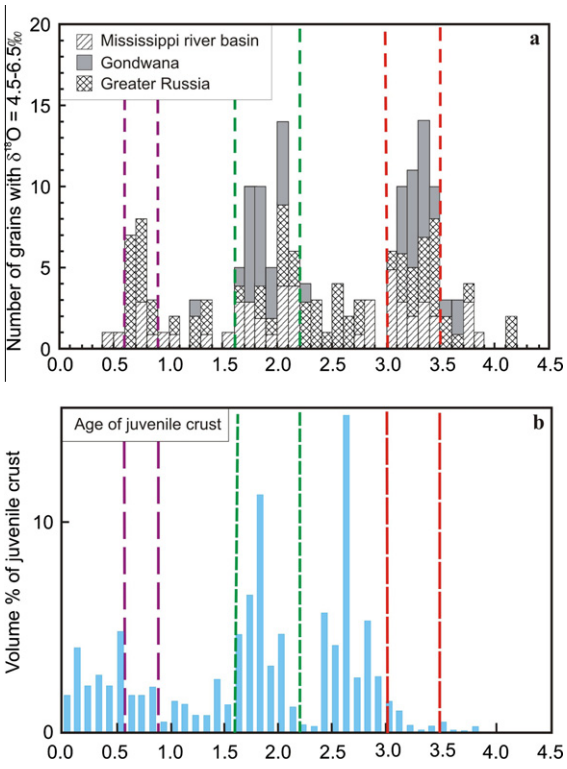

Fig. 10. A comparison of major periods of crustal growth of Greater Russia, Mississippi river basin and Gondwana. The upper figure shows detrital zircon grains with mantle $\delta^{18}O$ values (4.5–6.5‰) from Greater Russia, Mississippi river basin and Gondwana. Note the Lena Paleoproterozoic zircons are excluded from the Greater Russian group. Data source: Greater Russia, this study; Mississippi river basin, Wang et al. (2009); Gondwana, Kemp et al. (2006). The lower figure shows variation in the volume of juvenile crust production with age from Condie (2005), based on a compilation of U/Pb zircon dates of samples with juvenile Nd model ages.

supercontinental formation events in Greater Russia (Fig. 6) range semi-continuously over at least 1000 and 1500 Myr respectively, with only a small break at 3.0 Ga in the 1.85 Ga zircons. The continuity of Hf model ages for these periods suggests that preservation was not a problem.

5.3. Implications for growth of continental crusts

Previous zircon Hf model age studies suggest that the continental growth was episodic in both Gondwana and the Mississippi river basin; two pronounced peaks were recognized at 1.9–1.7 and 3.1–2.9 Ga in part of eastern Gondwana (Hawkesworth and Kemp, 2006a) and 2.2–1.6 and 3.4–2.9 Ga in the Mississippi river basin (Wang et al., 2009). Pietranik et al. (2008) identified two peaks in detrital zircons from the Archean Slave craton of Canada, one at 3.4 Ga and the other at 3.8 Ga. The two principal growth periods recognized in Greater Russia differ from those seen in Gondwana and the Mississippi river basin; the older 3.5–3.3 Ga peak being slightly older than the older Gondwana–Mississippi peaks, whereas the younger 0.8–0.6 Ga peak is distinctly younger than the younger peaks in either Gondwana or the Mississippi river basin. This shows that continental growth in Greater Russia finished later (at ~0.6 Ga) than it did in North America and Gondwana, and that the major periods of crustal growth may differ from continent to continent although it should be noted that the position of the Gondwana peaks is based on limited data. Therefore, the two peaks of crustal growth identified in Gondwana and the Mississippi river basin may not be global periods of enhanced growth of the continental crusts. More data are needed from other continents to resolve this issue.

The zircon T_{DM}^{V} Hf model ages for Gondwana, the Mississippi river basin and Greater Russia have been compiled in Fig. 10a. The combined data set shows three periods of enhanced crustal growth; 3.5–3.0 Ga, 2.2–1.6 Ga and 0.9–0.6 Ga. The strong peak between 3.5 and 3.0 Ga suggests that growth of the continental crust was rapid in

the Archean as proposed by McLennan and Taylor (1982). However, in the McLennan and Taylor's model the fastest growth occurred between 2.8 and 2.5 Ga, which is a period of slow growth in our compilation. Available zircon Hf model ages suggest that the preserved continental crust began to form at about 4.0 Ga, the age of the oldest known continental crust (Bowring and Williams, 1999), and possibly as early as 4.2 Ga. There is no evidence for growth of the continental crust prior to 4.2 Ga in the zircon Hf model ages reported in this study, in Nd model ages of Earth's oldest sediments (Jacobsen and Dymek, 1987) or in the U/Pb ages of the zircons derived from them (Nutman, 2001). Rare detrital zircons as old as 4.4 Ga in sediments from Western Australia (Wilde et al., 2001), provide unambiguous evidence that felsic crust existed at that time but not that it was extensive. If extensive continental crust existed prior to 4.0 Ga, it had been destroyed by recycling into the mantle. If crustal processes, for example crustal melting, destroyed large amounts of pre-4.0 Ga continental crust some evidence for its prior existence would have been preserved in the zircon Hf isotopic record of the Greater Russian, Mississippi or Gondwana detrital zircons. It is unclear how a large mass of buoyant continent crust could be recycled into the mantle prior to 4.0 Ga, especially if subduction was not active at that time.

Fig. 10a and b compares our compilation with one by Condie (2005) for juvenile crust based on U/Pb zircon dates of rocks, which on the basis of εNd values lying within two of the Nd depleted mantle growth curves, are interpreted to be juvenile. The Condie's compilation shows little evidence for growth of the continental crust prior to 3.0 Ga and identifies the period between 3.0 and 2.4 Ga as a major growth period whereas our compilation shows 3.5–3.0 Ga to be an important period of growth and 3.0–2.4 Ga to be a period of slow growth. It is not clear whether these differences are due to differences in approach or to sampling different terranes. However, if both data sets are taken at face value our compiled data show periods of strong crustal growth where Condie's compilation sees none, and show periods of slow crustal growth where Condie sees rapid growth (Fig. 10). These observations weaken the case for episodic crustal growth and cast doubts on models for major overturns in the mantle and stop-start plate tectonics. If growth of the continental crust was controlled by major mantle overturns, which must be global in scale, we would expect a strong correlation between peaks in the crustal growth on different continents. We emphasize the need for caution when evaluating the global significance of zircon Hf model age growth peaks from limited data sets.

6. CONCLUSIONS

The formation of small amounts of the preserved continental crust may have started as earlier as 4.2 Ga in Greater Russia, compared with 3.9 Ga in the Mississippi basin (Wang et al., 2009), but in both cases significant growth started sometimes later; 3.5 Ga in Greater Russia and 3.4 Ga in the Mississippi. Growth of the continental crust also finished later in Greater Russia, at about 0.6 Ga compared with 1.5 Ga for 90% of the crust in the Mississippi basin, but here minor growth continued for a further 1.0 Gyr. Most of the peaks in continental growth for Greater Russia do not correlate with the principle growth peaks recognized for Gondwana or North America, or with the peaks in a compilation of ages of juvenile crust by Condie (2005), a notable exception being the 3.4 Ga peak that correlates with peak of similar age in the Slave craton. The oldest peak recognized in the Greater Russian data (3.5–3.3 Ga) is slightly older than the Archean peaks observed in the Mississippi and Gondwana data and the youngest peak (0.8–0.6 Ga) is distinctly younger than the youngest period of significant growth periods recognized in the other data sets. The lack of correlation between peaks in growth of the continental crust on the different continents does not support the Condie (2005) hypothesis of episodic crustal growth controlled by major overturns in the mantle. The crustal incubation time for most of the Greater Russian zircons lies between 300 and 1000 Myr.

ACKNOWLEDGEMENT

ARC Discovery Project Grant DP 0556923 to I.H.C. supported this study, which was a joint initiative between the Laboratory of Regional Mineralogy, Institute of Geology, Komi and The Australian National University. We would especially like to thank Academician Nicolai Yushkin who arranged the sample collection for this project. Without his help this project would not have been possible. Karl Musser and Jeremy Wykes helped with the GIS software used to draw the map. Olga Turkina and Fedor Zhimulev are thanked for their insight and advice on Russian geology. The Hundred Talent Program of the Chinese Academy of Sciences to C.Y.W. is also appreciated. Finally, we thank Chris Hawkesworth and Tony Kemp for constructive reviews of our paper and AE Steve Shirey for some helpful suggestions. This is contribution No. IS-1270 from GIGCAS.

APPENDIX A

See Tables A1–A4.

Table A1
ELA-ICP-MS U–Th–Pb age determinations for detrital zircons mounted in epoxy from Greater Russia.

Analysis ID	Pb^* (ppm)	U (ppm)	Atomic Th/U	Uncorr'd $^{206}Pb/^{238}U$ ratio	±	Uncorr'd $^{207}Pb/^{235}U$ ratio	±	Uncorr'd $^{207}Pb/^{206}Pb$ ratio	±	Uncorr'd $^{208}Pb/^{232}Th$ ratio	±	%Common ^{206}Pb using ^{208}Pb	%Common ^{206}Pb using ^{207}Pb
070330\lnt-002	149	252	0.520	0.5139	0.0020	12.9604	0.0727	0.1829	0.0007	0.1437	0.0010	0.09	0.10
070330\lnt-004	77.8	205	0.750	0.3278	0.0012	5.1208	0.0372	0.1133	0.0007	0.0953	0.0005	0.08	0.20
070330\lnt-006	57.6	89.8	0.797	0.5245	0.0020	13.2325	0.0946	0.1830	0.0011	0.1394	0.0010	−0.20	−0.65
070330\lnt-010	26.6	34.9	2.143	0.4966	0.0029	12.2887	0.1651	0.1795	0.0022	0.1335	0.0011	−0.81	0.76
070330\lnt-011	111	157	1.359	0.5196	0.0020	13.1521	0.0869	0.1836	0.0010	0.1373	0.0008	−0.63	−0.20
070330\lnt-012	7.49	21.1	0.084	0.3549	0.0038	5.7419	0.1588	0.1173	0.0030	0.1687	0.0092	0.67	−0.36
070330\lnt-020	14.7	45.1	0.120	0.3279	0.0021	5.1006	0.0802	0.1128	0.0016	0.0998	0.0032	0.06	0.14
070330\lnt-024	180	312	0.019	0.5506	0.0021	14.8386	0.0840	0.1955	0.0008	0.1944	0.0083	0.05	−0.74
070330\lnt-029	65.6	164	0.854	0.3361	0.0013	5.2315	0.0435	0.1129	0.0008	0.0971	0.0006	−0.06	−0.17
070330\lnt-030	329	602	0.198	0.5096	0.0023	12.6769	0.0735	0.1804	0.0006	0.1429	0.0010	0.05	0.03
070330\lnt-031	107	172	0.753	0.5170	0.0018	13.2047	0.0772	0.1852	0.0009	0.1391	0.0008	−0.18	0.23
070330\lnt-033	140	250	0.544	0.4885	0.0018	11.9560	0.0749	0.1775	0.0009	0.1355	0.0010	0.00	0.99
070330\lnt-036	21.3	57.0	0.526	0.3379	0.0018	5.4468	0.0695	0.1169	0.0014	0.1024	0.0016	0.37	0.27
070330\lnt-038	108	191	0.473	0.4985	0.0024	12.8712	0.0836	0.1873	0.0008	0.1505	0.0014	0.52	1.80
070330\lnt-042	59.8	146	0.915	0.3408	0.0020	5.2948	0.0631	0.1127	0.0012	0.0965	0.0010	−0.25	−0.38
070330\lnt-044	118	215	0.184	0.5134	0.0021	12.7505	0.0817	0.1801	0.0009	0.1535	0.0014	0.19	−0.28
070330\lnt-046	181	326	0.305	0.5058	0.0022	12.7043	0.0798	0.1822	0.0008	0.1471	0.0017	0.14	0.55
070330\lnt-049	65.6	180	0.469	0.3359	0.0013	5.2943	0.0365	0.1143	0.0006	0.0967	0.0007	0.00	0.02
070330\lnt-051	67.1	95.4	1.641	0.4978	0.0036	12.7108	0.1289	0.1852	0.0013	0.1371	0.0012	−0.05	1.53
070330\lnt-057	71.4	113	0.701	0.5250	0.0020	13.2023	0.0865	0.1824	0.0010	0.1432	0.0008	−0.05	−0.78
070330\lnt-060	46.8	107	1.072	0.3493	0.0017	5.6812	0.0652	0.1180	0.0012	0.1042	0.0009	0.64	−0.04
070330\lnt-064	27.3	48.8	0.394	0.5006	0.0029	12.9995	0.1350	0.1883	0.0016	0.1538	0.0022	0.51	1.81
070330\lnt-065	22.3	47.1	1.950	0.3229	0.0018	5.0264	0.0691	0.1129	0.0014	0.0936	0.0007	0.18	0.33
070330\lnt-066	163	302	0.290	0.4983	0.0016	12.5386	0.0663	0.1825	0.0008	0.1368	0.0009	−0.02	1.10
070330\lnt-069	197	293	1.235	0.5075	0.0017	12.7188	0.0730	0.1817	0.0008	0.1396	0.0007	−0.03	0.37
070330\lnt-071	111	190	0.537	0.5099	0.0017	12.9286	0.0696	0.1839	0.0008	0.1389	0.0009	−0.07	0.52
070330\lnt-072	251	448	0.319	0.5081	0.0022	12.6605	0.0750	0.1807	0.0007	0.1410	0.0008	0.03	0.18
070330\lnt-080	196	607	0.119	0.3262	0.0012	5.1291	0.0285	0.1141	0.0005	0.0914	0.0010	−0.06	0.36
070330\lnt-117	40.0	90.2	1.378	0.3359	0.0018	5.3085	0.0581	0.1146	0.0011	0.0965	0.0007	−0.04	0.05
070330\lnt-119	126	220	0.428	0.5076	0.0018	12.5247	0.0735	0.1790	0.0008	0.1465	0.0017	0.09	−0.05
070330\vgt-071	4.57	22.8	0.715	0.1785	0.0014	1.8255	0.0576	0.0742	0.0023	0.0542	0.0009	0.11	−0.06
070330\vgt-077	31.7	105	0.227	0.2967	0.0017	4.3973	0.0581	0.1075	0.0013	0.0877	0.0015	0.04	0.59
070330\vgt-079	19.6	333	0.506	0.0561	0.0003	0.4199	0.0071	0.0543	0.0009	0.0168	0.0002	−0.35	0.09
070330\vgt-080	44.5	221	0.394	0.1938	0.0007	2.0976	0.0216	0.0785	0.0008	0.0575	0.0005	−0.06	0.09
070330\vgt-082	37.7	136	1.134	0.2221	0.0010	2.5113	0.0351	0.0820	0.0011	0.0662	0.0005	0.02	−0.24
070330\vgt-083	13.1	235	1.126	0.0456	0.0003	0.3524	0.0072	0.0561	0.0011	0.0145	0.0002	0.33	0.50
070330\vgt-084	15.7	245	0.820	0.0564	0.0003	0.4324	0.0082	0.0556	0.0010	0.0172	0.0001	−0.30	0.24
070330\vgt-089	17.6	303	0.448	0.0561	0.0003	0.4139	0.0069	0.0535	0.0009	0.0174	0.0002	−0.05	−0.01
070330\vgt-090	17.0	290	0.549	0.0550	0.0003	0.4021	0.0073	0.0531	0.0009	0.0174	0.0002	0.15	−0.04
070330\vgt-091	38.7	120	0.583	0.2915	0.0011	4.1949	0.0361	0.1044	0.0008	0.0858	0.0006	0.07	0.38
070330\vgt-092	5.35	89.0	0.577	0.0560	0.0004	0.4044	0.0135	0.0524	0.0017	0.0174	0.0003	−0.09	−0.14
070330\vgt-096	45.4	215	0.687	0.1893	0.0012	2.0080	0.0241	0.0769	0.0008	0.0547	0.0006	−0.41	0.01
070330\vgt-098	50.8	135	0.717	0.3277	0.0013	5.1171	0.0368	0.1133	0.0007	0.0934	0.0006	−0.13	0.20

070330\vgt-100	32.6	181	0.324	0.1776	0.0007	1.8083	0.0173	0.0739	0.0006	0.0538	0.0006	0.02	−0.07
070330\vgt-103	5.86	93.2	0.695	0.0569	0.0004	0.4241	0.0147	0.0540	0.0018	0.0173	0.0003	−0.35	0.04
070330\vgt-104	12.9	213	1.035	0.0507	0.0003	0.3700	0.0074	0.0529	0.0010	0.0157	0.0001	−0.11	0.02
070330\vgt-107	27.0	409	0.885	0.0570	0.0003	0.4103	0.0066	0.0522	0.0008	0.0175	0.0001	−0.27	−0.17
070330\vgt-113	12.5	172	0.439	0.0702	0.0004	0.5529	0.0114	0.0571	0.0011	0.0217	0.0003	−0.07	0.18
070330\vgt-115	33.1	78.1	1.281	0.3279	0.0017	5.3805	0.0596	0.1190	0.0012	0.0976	0.0008	0.67	0.93
070330\vgt-118	30.3	88.8	0.509	0.3116	0.0014	4.6022	0.0449	0.1071	0.0009	0.0932	0.0011	0.15	0.02
070330\vgt-119	8.16	40.3	0.435	0.1926	0.0011	2.0833	0.0454	0.0785	0.0016	0.0595	0.0011	0.18	0.11
070330\vgt-121	9.52	46.5	0.969	0.1725	0.0013	1.8114	0.0441	0.0762	0.0018	0.0511	0.0006	−0.27	0.34
070330\vgt-122	55.1	141	0.749	0.3381	0.0016	5.3433	0.0476	0.1146	0.0009	0.0971	0.0011	−0.14	−0.03
070330\vgt-125	8.07	139	0.469	0.0555	0.0004	0.4131	0.0097	0.0540	0.0012	0.0172	0.0003	−0.05	0.06
070330\vgt-128	8.94	160	0.470	0.0537	0.0004	0.4012	0.0091	0.0542	0.0012	0.0169	0.0003	0.10	0.12
070330\vgt-129	54.1	161	0.458	0.3122	0.0012	4.8275	0.0436	0.1122	0.0009	0.0939	0.0007	0.24	0.64
070330\vgt-134	11.1	166	0.176	0.0691	0.0004	0.5200	0.0126	0.0546	0.0013	0.0226	0.0005	0.14	−0.10
070330\vgt-137	7.53	164	0.205	0.0473	0.0003	0.3354	0.0089	0.0514	0.0013	0.0150	0.0004	0.02	−0.10
070330\vgt-138	41.8	132	1.096	0.2571	0.0011	3.3863	0.0374	0.0955	0.0010	0.0732	0.0006	−0.57	0.39
070330\vgt-139	8.49	137	0.641	0.0566	0.0004	0.4134	0.0115	0.0530	0.0014	0.0179	0.0002	0.16	−0.07
070330\vgt-141	6.88	125	0.308	0.0550	0.0004	0.4171	0.0114	0.0550	0.0015	0.0182	0.0004	0.31	0.20
070330\vgt-142	28.0	103	1.738	0.1938	0.0011	2.0607	0.0281	0.0771	0.0010	0.0581	0.0005	−0.02	−0.08
070330\vgt-143	5.30	95.8	0.380	0.0541	0.0005	0.4108	0.0146	0.0550	0.0019	0.0183	0.0005	0.49	0.22
070330\vgt-146	5.08	26.6	0.470	0.1802	0.0016	1.8294	0.0515	0.0736	0.0020	0.0549	0.0013	0.10	−0.16
070426\DNt-166	10.3	38.0	0.660	0.2434	0.0021	3.1472	0.0634	0.0938	0.0017	0.0725	0.0009	0.08	0.59
070426\DNt-188	68.2	210	0.851	0.2771	0.0011	3.8642	0.0299	0.1011	0.0007	0.0808	0.0006	−0.05	0.45
070426\DNt-189	17.2	57.3	0.587	0.2719	0.0021	3.8240	0.0559	0.1020	0.0013	0.0798	0.0010	0.01	0.73
070426\DNt-196	24.6	74.1	0.798	0.2861	0.0015	4.1011	0.0475	0.1040	0.0011	0.0840	0.0007	0.05	0.51
070426\DNt-199	8.25	23.0	1.203	0.2841	0.0021	4.0376	0.0724	0.1031	0.0017	0.0818	0.0009	−0.26	0.46
070426\DNt-201	41.7	146	0.387	0.2723	0.0012	3.8024	0.0338	0.1013	0.0008	0.0784	0.0007	−0.08	0.62
070426\DNt-202	24.4	75.1	0.871	0.2763	0.0014	3.8966	0.0491	0.1023	0.0012	0.0807	0.0009	−0.05	0.62
070505\DNt-208	68.4	229	0.444	0.2808	0.0012	4.0266	0.0256	0.1040	0.0005	0.0821	0.0007	0.02	0.69
070505\DNt-209	19.0	66.0	0.348	0.2772	0.0014	3.9465	0.0535	0.1033	0.0013	0.0837	0.0012	0.15	0.72
070505\DNt-210	63.2	213	0.317	0.2862	0.0009	4.0194	0.0234	0.1018	0.0005	0.0859	0.0010	0.07	0.24
070505\DNt-216	27.6	96.7	0.661	0.2539	0.0015	3.1966	0.0369	0.0913	0.0009	0.0775	0.0008	0.35	−0.03
070505\DNt-222	55.0	207	0.470	0.2493	0.0008	3.2237	0.0261	0.0938	0.0007	0.0738	0.0005	0.02	0.42
070505\DNt-240	108	369	0.419	0.2756	0.0009	3.8832	0.0231	0.1022	0.0005	0.0800	0.0005	−0.05	0.64
070505\DNt-242	40.7	132	0.573	0.2810	0.0010	3.9290	0.0316	0.1014	0.0007	0.0795	0.0006	−0.25	0.36
070725\LNt-143	85.8	155	0.483	0.4897	0.0028	12.4792	0.0991	0.1848	0.0010	0.1374	0.0012	0.04	2.02
070725\sey-01	13.3	173	0.260	0.0776	0.0005	0.6117	0.0106	0.0572	0.0009	0.0247	0.0004	0.10	0.05
070725\sey-03	9.24	118	0.329	0.0778	0.0005	0.6279	0.0129	0.0586	0.0011	0.0253	0.0005	0.29	0.22
070725\sey-05	29.2	379	0.518	0.0730	0.0005	0.5614	0.0112	0.0558	0.0011	0.0219	0.0002	−0.31	−0.03
070725\sey-11	22.2	198	1.521	0.0834	0.0006	0.6730	0.0111	0.0585	0.0009	0.0266	0.0002	0.79	0.11
070725\sey-15	16.9	227	0.123	0.0787	0.0005	0.6308	0.0114	0.0581	0.0010	0.0251	0.0005	0.05	0.15
070725\sey-21	13.2	159	0.864	0.0712	0.0004	0.5464	0.0141	0.0556	0.0014	0.0231	0.0002	0.63	−0.02
070725\sey-24	19.1	244	0.568	0.0728	0.0004	0.5829	0.0119	0.0580	0.0011	0.0235	0.0002	0.38	0.25
070725\sey-25	151	453	0.339	0.3194	0.0013	5.0077	0.0327	0.1137	0.0006	0.0920	0.0006	−0.02	0.57
070725\sey-30	23.3	312	0.344	0.0739	0.0004	0.5696	0.0085	0.0559	0.0008	0.0235	0.0003	0.12	−0.03
070725\sey-31	20.0	242	1.063	0.0683	0.0003	0.5376	0.0092	0.0571	0.0009	0.0218	0.0002	0.48	0.22
070725\sey-32	16.1	196	0.583	0.0762	0.0006	0.5919	0.0103	0.0564	0.0009	0.0241	0.0002	0.16	−0.02
070725\sey-34	135	411	0.440	0.3077	0.0014	4.7986	0.0341	0.1131	0.0006	0.0914	0.0007	0.24	0.92

(*continued on next page*)

Table A1 (*continued*)

Analysis ID	Pb^* (ppm)	U (ppm)	Atomic Th/U	Uncorr'd $^{206}Pb/^{238}U$ ratio	±	Uncorr'd $^{207}Pb/^{235}U$ ratio	±	Uncorr'd $^{207}Pb/^{206}Pb$ ratio	±	Uncorr'd $^{208}Pb/^{232}Th$ ratio	±	%Common ^{206}Pb using ^{208}Pb	%Common ^{206}Pb using ^{207}Pb
070725\sey-37	7.48	94.8	0.413	0.0764	0.0005	0.6058	0.0154	0.0575	0.0014	0.0253	0.0004	0.42	0.11
070725\sey-44	10.4	151	0.271	0.0695	0.0004	0.5450	0.0115	0.0569	0.0011	0.0225	0.0004	0.17	0.16
070725\sey-50	21.6	280	0.502	0.0732	0.0003	0.5827	0.0083	0.0577	0.0008	0.0231	0.0003	0.04	0.20
070725\sey-52	15.6	170	0.692	0.0830	0.0008	0.7328	0.0248	0.0640	0.0021	0.0244	0.0004	−0.54	0.79
070725\sey-54	13.3	151	1.046	0.0726	0.0005	0.5706	0.0117	0.0570	0.0011	0.0237	0.0003	0.92	0.13
070725\sey-62	39.0	121	0.421	0.3021	0.0014	4.5942	0.0424	0.1103	0.0009	0.0892	0.0008	0.09	0.76
070725\sey-69	21.5	305	0.220	0.0721	0.0003	0.5745	0.0089	0.0578	0.0009	0.0227	0.0002	0.04	0.23
070725\sey-70	12.6	146	1.080	0.0706	0.0006	0.5533	0.0144	0.0569	0.0014	0.0229	0.0003	0.76	0.14
070725\sey-71	32.7	446	0.305	0.0734	0.0004	0.5730	0.0090	0.0566	0.0008	0.0231	0.0003	0.03	0.06
070725\VGt-164	33.5	171	0.244	0.1961	0.0012	2.1874	0.0288	0.0809	0.0010	0.0640	0.0011	0.31	0.32
070725\VGt-182	33.9	98.9	0.627	0.3057	0.0019	4.7214	0.0520	0.1120	0.0010	0.0932	0.0009	0.41	0.85
070725\VGt-206	43.9	526	0.695	0.0751	0.0004	0.6235	0.0090	0.0602	0.0008	0.0246	0.0003	0.57	0.47
070725\VGt-226	68.0	108	0.987	0.5014	0.0025	13.4305	0.1049	0.1943	0.0012	0.1440	0.0009	0.52	2.65
070725\VGt-236	43.7	122	1.266	0.2772	0.0014	3.9353	0.0399	0.1029	0.0009	0.0843	0.0007	0.74	0.68
070725\VGt-240	24.7	64.8	0.789	0.3276	0.0019	5.3534	0.0759	0.1185	0.0015	0.0952	0.0010	0.07	0.87
070725\VGt-260	14.7	39.5	0.912	0.3111	0.0022	4.8752	0.0831	0.1136	0.0018	0.0929	0.0010	0.35	0.86
070725\VGt-292	27.1	71.2	0.616	0.3379	0.0031	5.3756	0.0836	0.1154	0.0014	0.0998	0.0017	0.23	0.08
070731\VGt-301	27.0	68.6	0.969	0.3253	0.0015	5.1078	0.0619	0.1139	0.0013	0.0938	0.0009	0.00	0.37
070731\VGt-321	15.7	43.0	0.626	0.3239	0.0019	5.2009	0.0748	0.1164	0.0015	0.1013	0.0013	0.71	0.75
070731\VGt-323	43.3	242	0.416	0.1718	0.0007	1.7778	0.0191	0.0751	0.0007	0.0526	0.0004	0.09	0.22
070731\VGt-353	7.67	135	0.447	0.0546	0.0004	0.4138	0.0127	0.0550	0.0016	0.0183	0.0004	0.52	0.20
070731\VGt-356	47.0	116	0.994	0.3331	0.0015	5.1621	0.0511	0.1124	0.0010	0.0948	0.0006	−0.17	−0.12
070731\VGt-366	90.0	432	0.307	0.2046	0.0010	2.3346	0.0239	0.0827	0.0007	0.0638	0.0005	0.19	0.32
070731\VGt-368	25.8	73.2	0.464	0.3266	0.0016	5.2372	0.0575	0.1163	0.0011	0.0955	0.0012	0.09	0.63
070731\VGt-384	41.8	200	0.399	0.2010	0.0008	2.2943	0.0242	0.0828	0.0008	0.0624	0.0006	0.23	0.43
070731\VGt-393	30.2	49.1	0.746	0.5107	0.0026	13.0813	0.1339	0.1858	0.0017	0.1429	0.0014	0.15	0.75
070731\VGt-398	21.3	56.7	0.663	0.3304	0.0017	5.4189	0.0864	0.1190	0.0018	0.1022	0.0014	0.69	0.83
070731\VGt-399	8.36	136	0.660	0.0558	0.0004	0.4266	0.0111	0.0554	0.0014	0.0179	0.0002	0.28	0.23
070731\VGt-432	40.0	140	0.587	0.2598	0.0012	3.3623	0.0359	0.0939	0.0009	0.0783	0.0008	0.20	0.10
070731\VGt-434	26.6	150	0.366	0.1715	0.0008	1.7535	0.0206	0.0741	0.0008	0.0560	0.0008	0.44	0.11
070731\VGt-435	15.0	35.6	1.420	0.3182	0.0023	5.0047	0.0993	0.1141	0.0021	0.0933	0.0008	0.32	0.65
070731\VGt-436	9.01	153	0.517	0.0555	0.0003	0.4232	0.0109	0.0553	0.0014	0.0180	0.0003	0.30	0.22
070731\VGt-438	22.8	63.0	0.771	0.3130	0.0016	4.7066	0.0569	0.1091	0.0012	0.0898	0.0009	−0.11	0.21
070731\VGt-439	12.2	193	0.854	0.0550	0.0003	0.4049	0.0092	0.0534	0.0012	0.0169	0.0002	−0.24	0.00
070731\VGt-441	15.5	207	0.423	0.0724	0.0004	0.5584	0.0106	0.0559	0.0010	0.0226	0.0003	0.01	−0.01
070731\VGt-448	31.6	162	0.398	0.1867	0.0020	2.0071	0.0379	0.0780	0.0012	0.0601	0.0012	0.44	0.20
070731\VGt-457	14.4	77.4	0.598	0.1710	0.0016	1.6806	0.0377	0.0713	0.0014	0.0510	0.0007	−0.09	−0.22
070731\VGt-459	40.6	114	0.433	0.3305	0.0016	5.1412	0.0522	0.1128	0.0010	0.0982	0.0010	0.18	0.04
070731\VGt-462	84.3	246	0.356	0.3245	0.0013	4.9998	0.0378	0.1117	0.0007	0.0948	0.0007	0.06	0.12
070731\VGt-468	53.2	151	0.580	0.3170	0.0014	4.8737	0.0407	0.1115	0.0008	0.0936	0.0009	0.15	0.38
070731\VGt-470	9.47	157	0.505	0.0570	0.0003	0.4491	0.0136	0.0571	0.0017	0.0193	0.0005	0.68	0.42
070731\VGt-474	17.0	41.5	0.926	0.3401	0.0024	5.7383	0.0997	0.1224	0.0019	0.1035	0.0014	0.76	0.89
070731\VGt-489	8.01	137	0.530	0.0552	0.0005	0.4333	0.0127	0.0569	0.0016	0.0180	0.0004	0.39	0.43
070731\VGt-506	57.1	141	1.108	0.3240	0.0014	5.1761	0.0510	0.1159	0.0010	0.0956	0.0006	0.36	0.67

070731\VGt-507	4.41	70.2	0.738	0.0559	0.0005	0.4300	0.0183	0.0558	0.0023	0.0183	0.0004	0.58	0.28
070731\VGt-510	72.6	256	0.420	0.2676	0.0010	3.5500	0.0314	0.0962	0.0008	0.0785	0.0006	0.00	0.15
070731\VGt-512	27.2	319	0.352	0.0842	0.0004	0.6484	0.0094	0.0558	0.0008	0.0260	0.0003	−0.02	−0.23
070731\VGt-514	11.2	49.2	0.645	0.2048	0.0014	2.2845	0.0443	0.0809	0.0015	0.0615	0.0009	0.05	0.09
070731\VGt-516	11.5	181	0.707	0.0570	0.0004	0.4347	0.0124	0.0553	0.0015	0.0181	0.0002	0.25	0.19
070731\VGt-518	106	322	0.349	0.3138	0.0013	4.7314	0.0323	0.1094	0.0006	0.0937	0.0006	0.14	0.22
070731\VGt-525	25.1	65.7	0.837	0.3240	0.0019	5.0530	0.0672	0.1131	0.0013	0.0960	0.0010	0.30	0.32
070731\VGt-531	33.8	457	0.599	0.0685	0.0003	0.5163	0.0079	0.0546	0.0008	0.0212	0.0002	−0.07	−0.09
070731\VGt-535	30.8	96.4	0.344	0.3049	0.0018	4.5022	0.0545	0.1071	0.0011	0.0924	0.0013	0.17	0.25
070731\VGt-541	16.7	26.4	0.784	0.5172	0.0038	13.0975	0.2230	0.1837	0.0028	0.1491	0.0022	0.46	−0.01
070731\VGt-543	4.29	68.8	0.688	0.0563	0.0004	0.4517	0.0170	0.0582	0.0021	0.0183	0.0003	0.46	0.57
070731\VGt-544	30.0	87.1	0.440	0.3204	0.0017	5.0715	0.0570	0.1148	0.0011	0.0933	0.0009	0.04	0.67
070731\VGt-546	65.3	96.7	0.949	0.5319	0.0026	13.8020	0.1169	0.1882	0.0013	0.1481	0.0013	0.19	−0.41
070731\VGt-547	110	333	0.291	0.3182	0.0012	4.7166	0.0289	0.1075	0.0005	0.0922	0.0006	0.00	−0.17
070731\VGt-549	10.5	50.9	0.377	0.1985	0.0022	2.1318	0.0878	0.0779	0.0031	0.0596	0.0019	0.01	−0.11
070731\VGt-550	22.8	448	0.078	0.0544	0.0004	0.4096	0.0066	0.0546	0.0008	0.0204	0.0004	0.24	0.15
070731\VGt-552	46.4	132	0.539	0.3176	0.0014	5.0694	0.0444	0.1158	0.0009	0.1013	0.0009	0.76	0.89
070731\VGt-556	11.5	30.7	0.779	0.3226	0.0026	4.9281	0.1009	0.1108	0.0021	0.0927	0.0015	−0.07	0.08
070731\VGt-560	16.1	239	0.243	0.0683	0.0004	0.5180	0.0108	0.0550	0.0011	0.0215	0.0003	0.04	−0.04
070731\VGt-563	6.35	123	0.923	0.0444	0.0003	0.3269	0.0095	0.0534	0.0015	0.0136	0.0002	−0.41	0.19
070731\VGt-565	59.0	295	0.748	0.1763	0.0006	1.8161	0.0166	0.0747	0.0006	0.0536	0.0003	0.11	0.07
070731\VGt-571	55.8	158	0.238	0.3429	0.0021	5.5092	0.0550	0.1165	0.0009	0.0976	0.0010	−0.03	0.02
070731\VGt-572	40.7	98.9	0.870	0.3448	0.0017	5.3531	0.0600	0.1126	0.0011	0.0991	0.0008	0.01	−0.55
090715\p11-102	11.9	67.8	0.278	0.1757	0.0009	1.7935	0.0296	0.0741	0.0012	0.0504	0.0008	−0.20	0.00
090715\p11-104	1.7	60.7	0.836	0.0243	0.0003	0.1561	0.0102	0.0467	0.0030	0.0080	0.0002	0.57	−0.30
090715\p11-110	30.5	48.5	1.202	0.4840	0.0044	11.7605	0.1413	0.1762	0.0014	0.1277	0.0016	−0.87	1.10
090715\p11-111	13.9	89.5	1.178	0.1247	0.0011	1.1160	0.0262	0.0649	0.0014	0.0372	0.0006	−0.87	0.05
090715\p11-113	49.3	120	0.961	0.3398	0.0020	5.4745	0.0519	0.1168	0.0009	0.0944	0.0009	−0.46	0.19
090715\p11-114	59.5	161	0.480	0.3386	0.0019	5.2606	0.0459	0.1127	0.0007	0.0998	0.0011	0.13	−0.29
090715\p11-116	8.0	167	0.862	0.0417	0.0003	0.3030	0.0076	0.0527	0.0013	0.0130	0.0001	−0.10	0.15
090715\p11-118	97.6	206	1.712	0.3360	0.0026	5.3708	0.0521	0.1159	0.0007	0.0991	0.0012	0.58	0.22
090715\p11-119	144	331	0.051	0.4303	0.0023	8.7127	0.0667	0.1469	0.0008	0.1762	0.0052	0.22	0.03
090715\p11-120	2.8	68.8	0.978	0.0342	0.0004	0.2590	0.0129	0.0550	0.0027	0.0107	0.0002	−0.05	0.56
090715\p11-121	55.4	145	0.199	0.3730	0.0021	6.3035	0.0566	0.1226	0.0009	0.1051	0.0012	−0.04	−0.45
090715\p11-127	41.7	117	0.383	0.3366	0.0021	5.4787	0.0597	0.1181	0.0011	0.0958	0.0011	−0.06	0.47
090715\p11-131	3.1	62.8	0.428	0.0486	0.0005	0.3770	0.0187	0.0562	0.0027	0.0146	0.0004	−0.29	0.46
090715\p11-133	120	356	0.314	0.3245	0.0020	5.1308	0.0407	0.1147	0.0006	0.0906	0.0008	−0.13	0.50
090715\p11-135	3.2	106	0.727	0.0273	0.0003	0.1883	0.0082	0.0501	0.0021	0.0088	0.0002	0.34	0.07
090715\p11-136	45.1	74.2	0.715	0.5075	0.0046	13.0292	0.1577	0.1862	0.0015	0.1449	0.0016	0.18	1.05
090715\p11-140	9.0	197.5	0.585	0.0422	0.0004	0.3125	0.0074	0.0537	0.0012	0.0135	0.0003	−0.10	0.27
090715\p11-141	10.4	35.1	0.731	0.2602	0.0021	3.3847	0.0578	0.0943	0.0014	0.0779	0.0010	0.18	0.14
090715\p11-142	163	259	0.693	0.5238	0.0027	13.5202	0.0959	0.1872	0.0009	0.1460	0.0012	0.13	0.05
090715\p11-144	75.0	186	1.022	0.3290	0.0024	5.2521	0.0490	0.1158	0.0007	0.0958	0.0009	0.14	0.47
090715\p11-147	87.0	216	0.776	0.3449	0.0021	5.5977	0.0493	0.1177	0.0007	0.1015	0.0011	0.25	0.10
090715\p11-149	107	334	0.243	0.3130	0.0017	4.6400	0.0367	0.1075	0.0006	0.0892	0.0008	−0.05	0.01
090715\p11-150	237	655	0.308	0.3454	0.0021	5.5929	0.0435	0.1174	0.0006	0.1021	0.0011	0.08	0.04
090715\p11-156	42.3	103	1.011	0.3332	0.0023	5.4470	0.0613	0.1186	0.0011	0.0996	0.0011	0.54	0.67
090715\p11-157	137	375	0.425	0.3385	0.0018	5.3638	0.0425	0.1149	0.0007	0.1015	0.0010	0.23	−0.01

(*continued on next page*)

Table A1 (*continued*)

Analysis ID	Uncorr'd $^{206}Pb/^{238}U$ age (Ma)	±	Uncorr'd $^{207}Pb/^{235}U$ age (Ma)	±	Uncorr'd $^{207}Pb/^{206}Pb$ age (Ma)	±	^{208}Pb corr'd $^{206}Pb^*/^{238}U$ age (Ma)	±	^{208}Pb corr'd $^{207}Pb^*/^{235}U$ age (Ma)	±	^{208}Pb corr'd $^{207}Pb^*/^{206}Pb^*$ age (Ma)	±	Selected age (Ma)	Selected age	±
070330\lnt-002	2673.2	33.2	2676.8	32.6	2679.4	32.4	2677.7	33.6	2672.0	34.3	2672.5	34.1	2672.5	oc	34.1
070330\lnt-004	1827.9	22.7	1839.6	22.9	1852.7	22.9	1833.5	22.8	1833.5	23.4	1841.4	23.2	1841.4	oc	23.2
070330\lnt-006	2718.4	33.7	2696.4	33.1	2679.9	32.7	2731.3	35.0	2707.7	38.4	2696.4	37.9	2696.4	oc	37.9
070330\lnt-010	2599.3	33.6	2626.7	34.0	2647.9	33.8	2646.1	37.6	2671.8	48.7	2713.6	48.3	2647.9	ou	33.8
070330\lnt-011	2697.4	33.4	2690.6	32.9	2685.5	32.6	2727.3	34.9	2725.2	38.5	2735.4	38.2	2735.4	oc	38.2
070330\lnt-012	1958.2	29.6	1937.7	33.4	1915.9	31.8	1948.5	29.5	1887.1	34.2	1821.9	32.2	1915.9	ou	31.8
070330\lnt-020	1828.1	24.2	1836.2	25.8	1845.3	25.3	1828.3	24.2	1831.6	26.0	1836.7	25.5	1836.7	oc	25.5
070330\lnt-024	2827.5	35.1	2804.9	34.1	2788.8	33.7	2826.0	35.0	2802.4	34.1	2785.2	33.7	2788.8	ou	33.7
070330\lnt-029	1868.0	23.2	1857.8	23.4	1846.4	23.0	1877.9	25.6	1862.2	50.0	1854.7	49.4	1846.4	ou	23.0
070330\lnt-030	2654.8	33.4	2655.9	32.3	2656.8	32.1	2653.6	33.4	2653.0	32.3	2652.4	32.0	2652.4	oc	32.0
070330\lnt-031	2686.6	33.1	2694.4	32.8	2700.2	32.7	2699.1	33.4	2704.3	33.6	2714.5	33.5	2700.2	ou	32.7
070330\lnt-033	2564.4	31.7	2601.0	31.8	2629.5	31.9	2571.6	31.9	2601.0	32.5	2629.5	32.6	2629.5	oc	32.6
070330\lnt-036	1876.4	24.2	1892.3	25.2	1909.7	25.0	1875.4	24.2	1864.6	26.1	1858.1	25.6	1858.1	oc	25.6
070330\lnt-038	2607.1	32.9	2670.3	32.6	2718.3	32.9	2601.4	32.9	2641.7	32.4	2676.9	32.5	2676.9	oc	32.5
070330\lnt-042	1890.5	24.6	1868.0	24.6	1843.1	23.8	1903.0	25.7	1886.8	37.9	1878.2	37.3	1878.2	oc	37.3
070330\lnt-044	2671.0	33.2	2661.4	32.5	2654.1	32.2	2669.2	33.2	2650.9	32.4	2638.7	32.0	2654.1	ou	32.2
070330\lnt-046	2638.5	33.1	2658.0	32.4	2672.8	32.4	2639.4	33.3	2650.0	33.4	2661.1	33.2	2661.1	oc	33.2
070330\lnt-049	1866.8	23.3	1867.9	23.2	1869.1	22.9	1871.1	23.4	1867.9	24.0	1869.0	23.8	1869.0	oc	23.8
070330\lnt-051	2604.2	34.8	2658.5	33.3	2699.9	33.1	2625.7	35.3	2661.2	34.6	2703.9	34.4	2703.9	oc	34.4
070330\lnt-057	2720.5	33.8	2694.2	32.9	2674.6	32.5	2728.4	34.3	2696.9	34.9	2678.5	34.4	2674.6	ou	32.5
070330\lnt-060	1931.1	24.6	1928.5	25.2	1925.8	24.8	1933.9	24.7	1880.2	27.2	1836.1	26.4	1925.8	ou	24.8
070330\lnt-064	2616.5	33.8	2679.6	33.6	2727.5	33.7	2609.2	34.0	2651.9	34.9	2687.5	34.8	2687.5	oc	34.8
070330\lnt-065	1804.1	23.3	1823.8	24.8	1846.3	24.6	1823.7	23.9	1810.0	32.6	1820.1	32.3	1820.1	oc	32.3
070330\lnt-066	2606.3	32.0	2645.6	32.1	2675.8	32.4	2609.7	32.3	2646.6	33.4	2677.2	33.6	2677.2	oc	33.6
070330\lnt-069	2646.2	32.6	2659.0	32.4	2668.8	32.3	2663.1	33.0	2660.5	33.8	2670.9	33.7	2670.9	oc	33.7
070330\lnt-071	2656.3	32.7	2674.5	32.5	2688.2	32.5	2664.4	32.8	2678.3	32.7	2693.7	32.7	2693.7	oc	32.7
070330\lnt-072	2648.4	33.2	2654.7	32.3	2659.6	32.1	2651.9	33.2	2653.0	32.5	2657.0	32.3	2657.0	oc	32.3
070330\lnt-080	1819.8	22.6	1840.9	22.6	1864.9	22.7	1821.7	22.6	1845.0	22.7	1872.6	22.8	1864.9	ou	22.7
070330\lnt-117	1867.1	24.0	1870.2	24.3	1873.7	23.9	1883.5	24.5	1873.2	30.7	1879.2	30.3	1879.2	oc	30.3
070330\lnt-119	2646.2	32.7	2644.6	32.2	2643.3	32.0	2653.5	33.7	2639.6	37.0	2636.1	36.6	2643.3	ou	32.0
070330\vgt-071	1059.0	14.9	1054.7	24.3	1045.9	23.6	1062.1	15.0	1045.3	29.2	1019.1	28.2	1045.9	ou	23.6
070330\vgt-077	1675.1	21.8	1711.8	23.3	1757.0	23.3	1676.3	21.8	1708.5	23.6	1750.4	23.6	1750.4	oc	23.6
070330\vgt-079	351.9	4.6	356.0	6.7	382.1	6.9	354.0	4.6	373.2	8.3	499.3	10.4	351.9	yu	4.6
070330\vgt-080	1141.7	14.2	1148.0	15.5	1160.0	15.4	1144.4	14.3	1152.7	16.1	1172.3	16.2	1160.0	ou	15.4
070330\vgt-082	1292.7	16.3	1275.3	18.4	1246.2	17.7	1301.9	16.5	1273.9	22.6	1242.6	21.9	1246.2	ou	17.7
070330\vgt-083	287.3	3.9	306.5	6.6	454.7	9.0	288.5	4.0	292.7	14.2	343.3	16.2	288.5	yc	4.0
070330\vgt-084	353.8	4.6	364.9	7.3	435.4	8.3	356.6	4.8	379.4	19.6	531.5	25.6	353.8	yu	4.6
070330\vgt-089	352.1	4.5	351.7	6.5	349.4	6.3	353.2	4.5	354.0	7.5	365.3	7.6	352.1	yu	4.5
070330\vgt-090	344.9	4.5	343.2	6.7	331.9	6.3	345.8	4.6	335.8	8.8	277.1	7.3	344.9	yu	4.5
070330\vgt-091	1649.0	20.6	1673.0	21.3	1703.2	21.4	1652.4	20.6	1667.9	21.7	1693.0	21.8	1693.0	oc	21.8
070330\vgt-092	351.2	4.9	344.8	10.6	302.5	9.3	352.7	5.0	349.2	12.7	333.6	12.1	352.7	yc	5.0

070330\vgt-096	1117.7	14.9	1118.2	15.7	1119.1	15.1	1126.2	15.1	1151.5	21.8	1207.6	22.0	1119.1	ou	15.1
070330\vgt-098	1827.1	22.8	1838.9	22.9	1852.3	22.8	1834.8	23.1	1848.3	26.1	1870.0	26.1	1852.3	ou	22.8
070330\vgt-100	1053.6	13.2	1048.5	14.1	1037.8	13.7	1055.1	13.2	1047.1	15.7	1033.8	15.3	1037.8	ou	13.7
070330\vgt-103	357.0	4.9	359.0	11.3	371.3	11.4	359.8	5.0	376.1	14.9	487.4	18.2	357.0	yu	4.9
070330\vgt-104	318.7	4.2	319.6	6.7	325.7	6.6	322.2	4.5	324.6	23.3	363.9	25.5	318.7	yu	4.2
070330\vgt-107	357.1	4.6	349.1	6.3	296.8	5.3	360.1	4.6	362.3	8.7	390.0	9.1	360.1	yc	4.6
070330\vgt-113	437.6	5.8	446.9	9.2	494.9	9.7	439.0	5.8	450.6	11.7	515.9	12.9	437.6	yu	5.8
070330\vgt-115	1828.3	23.4	1881.8	24.5	1941.2	24.8	1831.6	23.7	1833.1	28.3	1850.6	28.1	1850.6	oc	28.1
070330\vgt-118	1748.6	22.0	1749.7	22.5	1750.9	22.2	1751.0	22.5	1738.4	31.5	1728.9	31.0	1750.9	ou	22.2
070330\vgt-119	1135.2	15.0	1143.3	20.3	1158.7	20.1	1135.9	15.0	1128.2	22.9	1118.5	22.4	1118.5	oc	22.4
070330\vgt-121	1025.7	14.3	1049.6	20.3	1099.5	20.4	1033.8	14.6	1070.7	25.3	1158.1	26.1	1099.5	ou	20.4
070330\vgt-122	1877.7	23.7	1875.8	23.8	1873.7	23.4	1886.9	24.6	1886.6	34.0	1893.8	33.7	1873.7	ou	23.4
070330\vgt-125	348.3	4.8	351.1	8.1	369.2	8.2	349.5	4.8	353.4	10.8	385.4	11.4	348.3		4.8
070330\vgt-128	337.2	4.6	342.6	7.8	378.1	8.2	337.9	4.7	338.0	10.5	344.9	10.5	337.9	yc	4.7
070330\vgt-129	1751.3	21.8	1789.7	22.8	1834.7	23.1	1751.7	21.9	1772.1	23.0	1801.0	23.1	1801.0	oc	23.1
070330\vgt-134	430.6	5.7	425.2	9.8	396.0	9.0	430.6	5.7	417.2	10.5	347.2	8.8	430.6	yu	5.7
070330\vgt-137	297.8	4.1	293.6	7.6	261.7	6.7	298.1	4.1	292.6	9.4	252.5	8.1	297.8	yu	4.1
070330\vgt-138	1474.9	18.6	1501.2	20.0	1538.6	20.2	1490.8	18.8	1545.7	22.4	1633.4	23.1	1538.6	ou	20.2
070330\vgt-139	354.7	5.1	351.3	9.3	329.3	8.5	355.6	5.1	343.4	11.7	271.5	9.3	354.7	yu	5.1
070330\vgt-141	345.0	4.8	354.0	9.2	413.4	10.3	344.7	4.8	339.2	10.4	307.0	9.3	344.7	yc	4.8
070330\vgt-142	1141.7	14.9	1135.8	16.5	1124.8	15.9	1155.2	15.4	1137.8	30.0	1130.1	29.5	1124.8	ou	15.9
070330\vgt-143	339.9	5.1	349.5	11.3	412.8	12.6	339.0	5.2	326.3	18.5	241.7	14.1	339.9	yu	5.1
070330\vgt-146	1068.1	15.6	1056.1	22.4	1031.4	21.2	1069.8	15.8	1047.8	25.9	1007.8	24.5	1031.4	ou	21.2
070426\DNt-166	1404.2	20.2	1444.3	23.3	1503.8	23.0	1409.3	20.3	1438.1	25.5	1490.0	25.2	1490.0	oc	25.2
070426\DNt-188	1576.9	19.8	1606.2	20.3	1644.9	20.5	1587.9	19.9	1609.8	21.4	1652.2	21.7	1652.2	oc	21.7
070426\DNt-189	1550.5	21.4	1597.8	22.5	1660.7	22.4	1557.2	21.6	1597.2	23.9	1659.5	23.8	1659.5	oc	23.8
070426\DNt-196	1622.2	20.9	1654.5	22.0	1695.8	22.0	1630.7	21.1	1650.3	23.2	1687.3	23.2	1687.3	oc	23.2
070426\DNt-199	1612.2	21.9	1641.8	24.5	1679.9	24.2	1630.1	22.4	1662.0	28.8	1720.6	28.8	1679.9	ou	24.2
070426\DNt-201	1552.7	19.6	1593.2	20.4	1647.3	20.7	1558.1	19.8	1599.8	22.2	1660.7	22.6	1647.3	ou	20.7
070426\DNt-202	1572.7	20.2	1613.0	21.9	1665.9	22.1	1583.9	20.6	1617.0	26.9	1674.1	27.2	1674.1	oc	27.2
070505\DNt-208	1595.5	20.0	1639.6	20.3	1696.6	20.7	1599.3	20.1	1638.0	21.0	1693.4	21.4	1693.4	oc	21.4
070505\DNt-209	1577.0	20.2	1623.3	22.4	1683.7	22.7	1578.2	20.3	1611.8	22.9	1660.3	23.1	1660.3	oc	23.1
070505\DNt-210	1622.6	20.0	1638.1	20.2	1658.0	20.3	1624.8	20.1	1632.5	22.6	1646.5	22.6	1646.5	oc	22.6
070505\DNt-216	1458.6	19.1	1456.3	19.6	1453.1	19.1	1461.1	19.2	1427.0	23.1	1387.1	22.1	1453.1	ou	19.1
070505\DNt-222	1434.6	17.7	1462.9	18.6	1504.1	19.0	1438.4	17.7	1460.9	19.0	1499.8	19.3	1499.8	oc	19.3
070505\DNt-240	1569.0	19.4	1610.2	19.9	1664.5	20.4	1573.5	19.5	1614.1	20.3	1672.4	20.8	1664.5	ou	20.4
070505\DNt-242	1596.2	19.7	1619.7	20.5	1650.3	20.7	1605.0	19.9	1639.4	21.4	1690.4	21.8	1650.3	ou	20.7
070725\LNt-143	2569.2	33.1	2641.2	32.6	2696.8	32.8	2576.3	33.7	2639.2	35.2	2693.9	35.4	2693.9	oc	35.4
070725\sey-01	481.7	6.6	484.7	8.9	498.3	8.7	482.3	6.6	478.5	12.1	465.5	11.6	481.7	yu	6.6
070725\sey-03	482.8	6.5	494.8	10.0	550.4	10.6	483.0	6.6	477.5	12.3	458.7	11.6	483.0		6.6
070725\sey-05	454.2	6.1	452.5	9.1	443.9	8.7	457.7	6.2	470.5	13.4	543.8	14.9	454.2	yu	6.1
070725\sey-11	516.5	7.1	522.5	9.2	548.6	9.1	521.2	7.3	472.7	22.3	283.6	14.4	516.5	yu	7.1
070725\sey-15	488.4	6.7	496.6	9.3	534.2	9.5	488.8	6.7	493.5	9.6	518.2	9.6	488.8	yc	6.7
070725\sey-21	443.7	5.9	442.6	10.6	437.7	10.4	444.7	5.9	406.3	14.5	213.8	8.2	443.7	yu	5.9
070725\sey-24	453.3	6.0	466.3	9.5	531.1	10.3	454.3	6.1	444.6	12.5	408.9	11.5	454.3	yc	6.1
070725\sey-25	1786.8	22.4	1820.6	22.5	1859.5	22.7	1791.3	22.4	1821.8	22.7	1861.6	22.9	1861.6	oc	22.9
070725\sey-30	459.6	5.9	457.8	7.8	448.9	7.4	460.5	6.0	451.0	9.0	410.4	8.1	459.6	yu	5.9
070725\sey-31	425.8	5.4	436.9	8.0	495.1	8.8	428.5	5.6	410.1	17.7	333.7	14.8	425.8	yu	5.4

(*continued on next page*)

Table A1 (*continued*)

Analysis ID	Uncorr'd $^{206}Pb/^{238}U$ age (Ma)	±	Uncorr'd $^{207}Pb/^{235}U$ age (Ma)	±	Uncorr'd $^{207}Pb/^{206}Pb$ age (Ma)	±	^{208}Pb corr'd $^{206}Pb^{*}/^{238}U$ age (Ma)	±	^{208}Pb corr'd $^{207}Pb^{*}/^{235}U$ age (Ma)	±	^{208}Pb corr'd $^{207}Pb^{*}/^{206}Pb^{*}$ age (Ma)	±	Selected age (Ma)	Selected age	±
070725\sey-32	473.2	6.6	472.0	8.7	466.8	8.2	475.0	6.6	462.6	10.9	414.0	9.6	473.2	yu	6.6
070725\sey-34	1729.5	21.8	1784.7	22.2	1849.7	22.7	1731.4	21.9	1767.0	23.3	1815.9	23.5	1815.9	oc	23.5
070725\sey-37	474.6	6.4	480.9	11.3	510.7	11.6	474.5	6.4	455.8	13.7	371.6	11.4	474.6	yu	6.4
070725\sey-44	433.3	5.8	441.7	9.3	485.5	9.7	433.7	5.9	432.5	10.1	432.0	9.8	433.7	yc	5.9
070725\sey-50	455.6	5.8	466.2	7.7	518.4	8.3	457.4	6.0	464.0	17.8	506.4	19.0	457.4	yc	6.0
070725\sey-52	514.3	7.9	558.2	16.0	741.4	19.2	520.2	8.1	590.1	20.3	882.5	26.4	514.3	yu	7.9
070725\sey-54	451.6	6.3	458.4	9.4	492.2	9.5	452.5	6.4	404.6	18.9	166.4	8.5	451.6	yu	6.3
070725\sey-62	1701.9	21.5	1748.2	22.3	1804.0	22.7	1705.5	21.6	1741.4	22.6	1790.8	22.9	1790.8	oc	22.9
070725\sey-69	448.9	5.7	460.9	8.0	521.2	8.7	449.6	5.7	458.5	8.8	507.9	9.4	449.6	yc	5.7
070725\sey-70	439.6	6.4	447.1	10.9	485.8	11.1	441.5	6.6	404.0	20.0	223.1	11.8	439.6	yu	6.4
070725\sey-71	456.6	5.9	460.0	8.0	476.6	8.0	457.2	6.0	457.9	11.7	465.5	11.7	457.2	yc	6.0
070725\VGt-164	1154.5	15.2	1177.0	16.8	1218.7	16.8	1153.5	15.2	1151.6	17.4	1152.4	16.9	1152.4	oc	16.9
070725\VGt-182	1719.7	22.7	1771.1	23.2	1832.1	23.3	1720.9	22.7	1740.2	24.4	1772.3	24.2	1772.3	oc	24.2
070725\VGt-206	466.7	6.1	492.0	8.2	611.5	9.6	467.1	6.1	458.9	10.4	432.7	9.7	467.1	yc	6.1
070725\VGt-226	2619.9	33.2	2710.4	33.4	2778.4	33.8	2624.2	33.3	2683.1	33.3	2739.5	33.6	2739.5	oc	33.6
070725\VGt-236	1577.5	20.2	1621.0	21.1	1677.9	21.4	1583.2	20.6	1563.2	28.3	1558.0	27.9	1558.0	oc	27.9
070725\VGt-240	1826.9	23.7	1877.4	25.6	1933.8	25.8	1834.5	23.9	1872.1	27.1	1924.0	27.2	1924.0	oc	27.2
070725\VGt-260	1746.2	23.7	1798.0	25.9	1858.5	25.9	1750.8	24.0	1771.7	31.4	1808.3	31.2	1808.3	oc	31.2
070725\VGt-292	1876.6	27.1	1881.0	26.2	1885.7	25.0	1880.6	27.2	1863.9	27.9	1853.9	26.7	1885.7	ou	25.0
070731\VGt-301	1815.6	22.9	1837.4	24.3	1862.1	24.3	1823.6	23.1	1837.8	27.0	1862.8	27.0	1862.8	oc	27.0
070731\VGt-321	1809.0	23.7	1852.8	25.4	1902.3	25.4	1803.3	23.7	1799.9	26.6	1802.4	26.1	1802.4	oc	26.1
070731\VGt-323	1021.9	12.9	1037.4	14.3	1069.9	14.4	1023.4	13.0	1029.9	14.9	1048.7	14.8	1048.7	oc	14.8
070731\VGt-353	342.6	4.8	351.6	10.0	411.1	11.2	341.9	4.8	326.8	12.8	228.0	9.2	342.6	yu	4.8
070731\VGt-356	1853.2	23.3	1846.4	23.7	1838.7	23.3	1865.2	23.5	1859.1	25.3	1862.6	25.0	1862.6	oc	25.0
070731\VGt-366	1200.2	15.3	1222.9	16.4	1263.1	16.5	1199.9	15.3	1207.7	16.7	1224.8	16.5	1224.8	oc	16.5
070731\VGt-368	1821.8	23.3	1858.7	24.2	1900.2	24.3	1824.7	23.3	1852.4	24.8	1888.4	24.9	1888.4	oc	24.9
070731\VGt-384	1180.4	14.8	1210.5	16.3	1264.6	16.7	1180.8	14.8	1192.2	16.9	1218.0	17.0	1218.0	oc	17.0
070731\VGt-393	2659.8	33.7	2685.5	33.6	2704.9	33.5	2665.5	33.9	2677.6	34.0	2693.4	33.8	2693.4	oc	33.8
070731\VGt-398	1840.2	23.5	1887.9	26.5	1940.6	26.7	1836.4	23.6	1837.3	27.9	1846.5	27.7	1846.5	oc	27.7
070731\VGt-399	350.3	4.8	360.8	9.0	428.2	10.1	351.1	4.8	347.3	12.0	333.7	11.4	351.1	yc	4.8
070731\VGt-432	1488.8	18.8	1495.7	19.8	1505.3	19.6	1491.6	18.9	1479.4	20.7	1469.7	20.3	1505.3	ou	19.6
070731\VGt-434	1020.6	13.0	1028.5	14.5	1045.1	14.4	1019.0	13.0	992.5	15.5	940.1	14.6	1045.1	ou	14.4
070731\VGt-435	1781.2	24.2	1820.1	27.5	1864.9	27.4	1792.9	24.6	1796.2	32.9	1819.5	32.5	1819.5	oc	32.5
070731\VGt-436	348.4	4.7	358.3	8.9	422.6	10.0	348.8	4.7	343.8	11.0	319.5	10.2	348.8	yc	4.7
070731\VGt-438	1755.5	22.5	1768.4	23.5	1783.6	23.3	1765.2	22.7	1776.9	25.1	1800.2	24.9	1783.6	ou	23.3
070731\VGt-439	345.3	4.6	345.2	7.9	344.7	7.6	348.3	4.7	356.5	11.3	424.8	12.9	345.3	yu	4.6
070731\VGt-441	450.8	6.0	450.5	8.8	449.4	8.5	452.1	6.0	449.8	10.0	445.2	9.7	450.8	yu	6.0
070731\VGt-448	1103.3	17.3	1117.9	18.6	1146.4	17.4	1102.0	17.3	1081.8	21.5	1047.7	19.8	1146.4	ou	17.4
070731\VGt-457	1017.5	15.2	1001.2	18.7	966.0	17.1	1022.5	15.3	1008.7	21.8	987.9	20.6	987.9	oc	20.6
070731\VGt-459	1840.8	23.4	1842.9	23.7	1845.3	23.4	1842.8	23.4	1829.5	24.1	1819.9	23.6	1845.3	ou	23.4
070731\VGt-462	1811.8	22.7	1819.3	22.8	1827.8	22.6	1814.6	22.7	1814.9	23.0	1819.5	22.8	1819.5	oc	22.8
070731\VGt-468	1775.1	22.3	1797.7	22.7	1824.0	22.7	1779.1	22.4	1786.2	23.3	1801.9	23.2	1801.9	oc	23.2

070731\VGt-470	357.6	4.7	376.6	10.5	495.2	13.1	356.7	4.7	343.6	14.5	265.8	11.5	356.7	yc	4.7
070731\VGt-474	1887.2	25.4	1937.2	27.7	1991.0	27.6	1886.4	25.6	1882.2	31.2	1890.4	30.7	1890.4	oc	30.7
070731\VGt-489	346.3	5.0	365.5	10.0	489.0	12.4	346.6	5.0	347.1	13.0	361.7	13.2	346.6	yc	5.0
070731\VGt-506	1809.2	22.8	1848.7	23.7	1893.4	23.9	1817.5	23.0	1821.8	25.3	1842.9	25.2	1842.9	oc	25.2
070731\VGt-507	350.5	5.3	363.2	13.7	444.8	15.9	350.8	5.4	335.3	19.6	244.5	14.7	350.5	yu	5.3
070731\VGt-510	1528.6	19.0	1538.4	19.7	1551.9	19.7	1532.9	19.1	1538.8	20.2	1552.6	20.1	1552.6	oc	20.1
070731\VGt-512	521.2	6.8	507.5	8.4	446.5	7.2	522.7	6.8	509.0	9.4	454.2	8.3	521.2	yu	6.8
070731\VGt-514	1200.9	16.3	1207.5	19.9	1219.2	19.4	1206.1	16.5	1203.2	23.4	1208.2	22.9	1208.2	oc	22.9
070731\VGt-516	357.6	5.1	366.5	9.8	422.6	10.8	359.0	5.1	354.4	12.2	339.3	11.5	359.0	yc	5.1
070731\VGt-518	1759.4	22.0	1772.8	22.0	1788.5	21.9	1761.1	22.1	1762.0	22.2	1767.7	22.0	1767.7	oc	22.0
070731\VGt-525	1809.3	23.7	1828.2	24.7	1849.8	24.4	1814.9	23.8	1805.3	26.2	1806.3	25.7	1806.3	oc	25.7
070731\VGt-531	427.4	5.4	422.7	7.3	397.5	6.8	429.9	5.5	426.7	9.3	421.7	9.0	429.9	yc	5.5
070731\VGt-535	1715.8	22.4	1731.4	23.1	1750.3	22.8	1717.2	22.6	1718.3	26.2	1724.6	25.8	1724.6	oc	25.8
070731\VGt-541	2687.2	36.1	2686.7	36.0	2686.4	35.3	2689.6	36.2	2660.9	36.7	2648.8	35.8	2686.4	ou	35.3
070731\VGt-543	353.2	5.0	378.5	12.7	536.1	16.6	353.9	5.1	356.4	16.3	387.8	17.3	353.9	yc	5.1
070731\VGt-544	1791.8	23.0	1831.4	24.0	1876.6	24.1	1796.3	23.1	1828.1	24.7	1870.5	24.8	1870.5	oc	24.8
070731\VGt-546	2749.6	34.8	2736.2	33.8	2726.4	33.4	2760.2	35.0	2725.7	34.2	2711.3	33.7	2726.4	ou	33.4
070731\VGt-547	1780.9	22.1	1770.2	21.9	1757.6	21.5	1784.2	22.2	1769.8	21.9	1756.8	21.6	1757.6	ou	21.5
070731\VGt-549	1167.4	18.2	1159.2	31.7	1144.0	30.5	1170.7	18.4	1158.1	34.7	1141.2	33.5	1144.0	ou	30.5
070731\VGt-550	341.8	4.7	348.6	6.3	394.2	6.7	341.2	4.7	337.4	6.6	312.8	5.8	341.2	yc	4.7
070731\VGt-552	1778.2	22.4	1831.0	23.2	1891.5	23.6	1773.7	22.3	1774.6	23.3	1784.3	23.1	1784.3	oc	23.1
070731\VGt-556	1802.4	25.1	1807.1	27.7	1812.4	26.9	1813.2	25.9	1812.0	37.9	1821.9	37.2	1821.9	oc	37.2
070731\VGt-560	425.8	5.6	423.8	8.8	413.3	8.4	426.5	5.7	421.6	10.7	399.8	10.0	425.8	yu	5.6
070731\VGt-563	280.0	4.0	287.2	8.1	345.0	9.2	283.6	4.1	304.0	12.3	482.6	17.8	280.0	yu	4.0
070731\VGt-565	1046.5	13.0	1051.3	14.0	1061.0	13.9	1051.8	13.1	1042.6	15.2	1036.5	15.0	1061.0	ou	13.9
070731\VGt-571	1900.8	25.0	1902.0	24.4	1903.4	23.8	1904.2	25.1	1904.4	24.6	1907.8	24.1	1903.4	ou	23.8
070731\VGt-572	1909.5	24.3	1877.4	24.5	1842.1	23.7	1921.0	24.6	1876.9	26.4	1841.1	25.6	1842.1	ou	23.7
090715\p11-102	1043.2	14.4	1043.1	17.3	1042.9	17.0	1044.1	14.4	1059.1	18.0	1088.1	18.1	1042.9	ou	17.0
090715\p11-104	154.6	2.9	147.3	9.2	37.6	2.4	153.2	2.9	132.8	13.6	0.5	0.0	154.6	yu	2.9
090715\p11-110	2544.6	38.3	2585.5	35.4	2617.7	34.8	2565.1	39.7	2633.9	40.6	2688.9	40.2	2617.7	ou	34.8
090715\p11-111	757.5	11.8	761.1	16.0	771.5	15.4	761.9	14.6	824.5	78.1	992.1	87.2	757.5	yu	11.8
090715\pll-113	1885.9	26.4	1896.6	26.0	1908.3	25.6	1891.7	26.6	1930.0	28.3	1969.5	28.2	1908.3	ou	25.6
090715\p11-114	1879.9	26.2	1862.5	25.3	1843.2	24.6	1877.1	26.2	1852.8	26.8	1824.9	26.0	1843.2	ou	24.6
090715\p11-116	263.2	4.0	268.8	6.9	316.7	7.7	263.2	4.0	272.8	11.4	353.3	14.0	263.2	yu	4.0
090715\p11-118	1867.6	27.2	1880.2	25.8	1894.1	25.2	1857.9	27.3	1836.4	32.8	1811.8	31.8	1894.1	ou	25.2
090715\p11-119	2306.9	31.8	2308.4	30.8	2309.7	30.4	2302.7	31.7	2294.3	30.7	2286.9	30.2	2309.7	ou	30.4
090715\p11-120	216.6	3.7	233.9	10.8	410.9	17.2	216.8	3.8	235.6	16.0	428.6	26.4	216.6	yu	3.7
090715\p11-121	2043.4	28.3	2018.9	27.4	1994.1	26.7	2044.1	28.3	2022.2	28.3	1999.8	27.6	1999.8	oc	27.6
090715\p11-127	1870.2	26.3	1897.3	26.4	1927.0	26.2	1872.2	26.5	1901.5	28.6	1934.9	28.5	1927.0	ou	26.2
090715\p11-131	306.1	5.1	324.8	14.4	460.7	18.9	307.3	5.2	337.1	17.1	550.6	25.1	306.1	yu	5.1
090715\p11-133	1811.7	25.5	1841.2	24.9	1874.7	24.7	1815.1	25.5	1850.9	25.3	1893.0	25.3	1874.7	oc	24.7
090715\p11-135	173.4	3.1	175.2	7.4	197.3	7.9	173.3	3.2	165.5	15.1	63.8	6.0	173.4	yu	3.1
090715\p11-136	2645.9	39.5	2681.8	36.7	2708.9	36.0	2646.0	39.6	2671.8	37.2	2694.4	36.5	2694.4	oc	36.5
090715\p11-140	266.3	4.3	276.1	6.7	359.3	8.0	267.2	4.5	280.2	19.5	394.9	25.9	266.3	yu	4.3
090715\p11-141	1491.1	22.1	1500.9	23.7	1514.6	23.0	1493.2	22.3	1486.4	27.3	1483.1	26.5	1483.1	oc	26.5
090715\p11-142	2715.2	37.1	2716.7	35.9	2717.8	35.6	2718.7	37.3	2709.8	36.3	2707.9	35.9	2717.8	ou	35.6
090715\p11-144	1833.6	26.4	1861.1	25.5	1892.0	25.1	1840.0	26.6	1850.8	27.5	1872.6	27.0	1872.6	oc	27.0

(*continued on next page*)

Table A1 (*continued*)

Analysis ID	Uncorr'd $^{206}Pb/^{238}U$ age (Ma)	±	Uncorr'd $^{207}Pb/^{235}U$ age (Ma)	±	Uncorr'd $^{207}Pb/^{206}Pb$ age (Ma)	±	^{208}Pb corr'd $^{206}Pb^{*}/^{238}U$ age (Ma)	±	^{208}Pb corr'd $^{207}Pb^{*}/^{235}U$ age (Ma)	±	^{208}Pb corr'd $^{207}Pb^{*}/^{206}Pb^{*}$ age (Ma)	±	Selected age (Ma)	Selected age	±
090715\p11-147	1910.2	26.8	1915.7	26.0	1921.7	25.6	1913.4	26.9	1897.6	26.8	1888.2	26.1	1921.7	ou	25.6
090715\p11-149	1755.6	24.4	1756.5	23.8	1757.5	23.3	1758.5	24.4	1760.7	23.9	1765.6	23.5	1757.5	ou	23.3
090715\p11-150	1912.6	26.8	1915.0	25.8	1917.6	25.3	1914.1	26.9	1908.8	27.1	1906.3	26.6	1917.6	ou	25.3
090715\p11-156	1853.8	26.5	1892.3	26.4	1934.8	26.3	1857.9	26.6	1852.4	28.8	1860.7	28.3	1860.7	oc	28.3
090715\p11-157	1879.4	25.8	1879.1	25.4	1878.8	25.0	1880.7	25.9	1861.8	26.5	1846.4	25.9	1878.8	ou	25.0

Note: The common Pb correction was determined by the ^{208}Pb method (Compston et al., 1984) and the age-dependent Pb model of Cumming and Richards (1975). Whether a common Pb-uncorrected age or a common Pb-corrected age was chosen depends on which one brought the analysis closer to Concordia (Campbell et al. (2005)). $^{206}U/^{238}Pb$ ages were used for zircons younger than 0.9 Ga, and $^{207}Pb/^{206}Pb$ ages for older grains. In Table A1, "yc" indicates that common Pb corrected $^{206}Pb/^{238}U$ age has been used, "yu" for uncorrected $^{206}Pb/^{238}U$ age, "oc" for corrected $^{207}Pb/^{206}Pb$ age and "ou" for uncorrected $^{207}Pb/^{206}Pb$ age.

References:

Campbell I. H., Reiners W., Allen C. M. Nicolescu S. and Upadhyay R. (2005) He–Pb double dating of detrital zircons from the Ganges and Indus Rivers: implication for quantifying sediment recycling and provenance studies. *Earth Planet. Sci. Lett.* **237**, 402–432.

Compston W., Williams I. S. and Meyer C. (1984) U–Pb geochronology of zircons from lunar breccia 73217 using a sensitive high mass-resolution ion micro-probe. *J. Geophys. Res.* **89** (Suppl.), B525–B534.

Cumming G. L. and Richards J. R. (1975) Ore lead isotopes ratios in a continuously changing earth. *Earth Planet. Sci. Lett.* **28**, 155–171.

Table A2
$\delta^{18}O$ values for standard material TEM-2 and R33 on five analytical sessions.

No.	Sessions	TEM-2		No.	Sessions	TEM-2	
		‰oVSMOW	2.2 s.e.m.			‰oVSMOW	2.2 s.e.m.
1	2007.05.03	8.20	0.17	33	2007.08.13 PM	7.97	0.16
2		8.25	0.11	34		8.08	0.10
3		8.20	0.14	35		8.64	0.11
4		8.01	0.10	36		7.89	0.11
5		8.48	0.23	37		9.40	0.10
6		7.62	0.08	38		6.94	0.15
7		8.65	0.14	39		8.48	0.10
8		9.09	0.11		Ave.	8.20	
9		7.51	0.10		SD (1σ)	0.76	
10		7.67	0.14				
11		8.22	0.12	40	2007.08.13 night	7.48	0.14
12		8.96	0.10	41		8.06	0.07
13		7.59	0.26	42		8.92	0.12
14		8.41	0.10	43		8.82	0.11
15		8.15	0.14	44		9.34	0.14
	Ave.	8.20		45		7.94	0.15
	SD (1σ)	0.48		46		8.26	0.09
				47		7.17	0.14
16	2007.05.25	8.03	0.12	48		7.28	0.17
17		9.05	0.12	49		7.24	0.10
18		7.45	0.13	50		8.46	0.10
19		7.93	0.18	51		9.01	0.14
20		8.20	0.20	52		8.79	0.18
21		8.31	0.23	53		8.02	0.19
22		9.19	0.12		Ave.	8.20	
23		8.15	0.08		SD (1σ)	0.72	
24		7.86	0.14				
25		7.85	0.13	54	2007.08.16	8.19	0.14
26		7.82	0.22	55		8.20	0.07
27		8.10	0.17	56		8.55	0.08
28		9.33	0.14	57		8.01	0.12
29		8.35	0.20	58		8.31	0.13
30		8.05	0.16	59		7.88	0.13
31		8.46	0.14	60		8.43	0.08
32		7.67	0.12	61		7.71	0.12
	Ave.	8.22		62		8.53	0.10
	SD (1σ)	0.53		63		8.34	0.09
				64		8.05	0.13
				65		8.42	0.08
				66		7.70	0.12
				67		8.52	0.10
				68		8.33	0.09

(*continued on next page*)

Table A2 (*continued*)

No.	Sessions	TEM-2		No.	Sessions	TEM-2	
				69		8.04	0.13
					Ave.	8.20	
					SD (1σ)	0.28	
No.	Sessions	R33		No.	Sessions	R33	
		‰oVSMOW	2.2 s.e.d			‰oVSMOW	2.2 s.e.d
1	2007.05.03	5.32	0.18	12	2007.08.13.PM	4.79	0.59
2		4.53	0.15	13		5.30	0.59
3		3.68	0.19	14		4.55	0.58
4		4.52	0.15		**Ave.**	**4.88**	
5		4.34	0.17		**SD (1σ)**	**0.39**	
6		5.87	0.17				
	Ave.	**4.71**		15	2007.08.13.night	4.99	0.41
	SD (1σ)	**0.77**		16		5.01	0.39
				17		4.29	0.41
7	2007.05.25	5.57	0.14	18		5.63	0.39
8		5.84	0.18	19		3.85	0.43
9		5.76	0.17		**Ave.**	**4.76**	
10		5.61	0.24		**SD (1σ)**	**0.69**	
11		4.62	0.21				
	Ave.	**5.48**		20	2007.08.16	5.32	0.21
	SD (1σ)	**0.50**		21		5.84	0.20
				22		5.48	0.21
				23		5.64	0.19
				24		5.12	0.18
				25		5.63	0.32
				26		5.11	0.31
					Ave.	**5.45**	
					SD (1σ)	**0.30**	

Table A3
Lu–Hf and O isotopic data for the detrital zircons from Greater Russia.

Analysis N	$^{176}Lu/^{177}Hf$	+ (2σ)	$^{176}Hf/^{177}Hf$	+ (2σ)	U/Pb age (Ma)	^{176}Lu decay constant (1.867×10^{-11})					$\delta^{18}O$ VSMOW (‰)	± (s.e.d.)[c]
						Initial Hf	εHf_i	± (1σ)	T_{DM}^{C} (Ga)[a]	T_{DM}^{V} (Ga)[b]		
DNt-166	0.000744	0.000032	0.281900	0.000018	1490.0	0.281879	1.5	0.3	2.06	2.30	6.30	0.18
DNt-188	0.000684	0.000015	0.281909	0.000016	1652.2	0.281887	5.5	0.3	1.97	2.14	5.10	0.23
DNt-189	0.000683	0.000011	0.281882	0.000016	1659.5	0.281861	4.7	0.3	2.02	2.22	4.65	0.20
DNt-196	0.001500	0.000057	0.281843	0.000022	1687.3	0.281795	3.0	0.4	2.14	2.38	4.39	0.20
DNt-199	0.001345	0.000024	0.281885	0.000032	1679.9	0.281842	4.5	0.6	2.05	2.25	3.97	0.19
DNt-201	0.001306	0.000065	0.281806	0.000032	1647.3	0.281765	1.1	0.5	2.22	2.21	8.79	0.18
DNt-202	0.001092	0.000032	0.281827	0.000020	1674.1	0.281792	2.6	0.3	2.15	2.26	6.89	0.17
DNt-208	0.000131	0.000038	0.281698	0.000024	1693.4	0.281693	−0.4	0.4	2.33	2.27	11.57	0.14
DNt-209	0.000817	0.000095	0.281912	0.000058	1660.3	0.281886	5.6	1.0	1.97	1.96	8.68	0.18
DNt-210	0.000618	0.000010	0.281886	0.000024	1646.5	0.281867	4.7	0.5	2.01	2.05	7.97	0.16
DNt-216	0.000857	0.000037	0.281886	0.000028	1453.1	0.281863	0.1	0.5	2.11	2.26	6.90	0.17
DNt-222	0.000753	0.000004	0.281934	0.000026	1499.8	0.281913	3.0	0.4	1.99	2.19	6.43	0.19
DNt-240	0.000703	0.000012	0.281857	0.000030	1664.5	0.281834	3.9	0.5	2.07	2.29	4.51	0.27
DNt-242	0.001316	0.000041	0.281924	0.000068	1650.3	0.281882	5.3	1.2	1.98	2.16	4.15	0.18
lnt-002	0.000443	0.000030	0.281024	0.000032	2672.5	0.281002	−2.5	0.6	3.24	3.47	5.63	0.20
lnt-004[d]	0.000471	0.000001	0.281207	0.000012	1841.4	0.281190	−14.9	0.2	3.25	3.83	6.18	0.27
lnt-006	0.000447	0.000009	0.280852	0.000022	2696.4	0.280829	−8.1	0.4	3.56	3.76	7.15	0.25
lnt-010	0.000116	0.000001	0.281047	0.000014	2647.9	0.281041	−1.7	0.2	3.17	3.29	6.66	0.17
lnt-011	0.000126	0.000006	0.280945	0.000022	2735.4	0.280938	−3.3	0.4	3.33	3.39	8.45	0.23
lnt-012[d]	0.000151	0.000007	0.281104	0.000018	1915.9	0.281099	−16.5	0.3	3.40	4.19	4.64	0.37
lnt-020[d]	0.000010	0.000002	0.281173	0.000016	1836.7	0.281172	−15.7	0.3	3.29	4.06	4.72	0.31
lnt-024	0.000392	0.000056	0.281103	0.000020	2788.8	0.281082	3.0	0.4	3.02	3.12	6.23	0.23
lnt-029[d]	0.000298	0.000013	0.281066	0.000016	1846.4	0.281056	−19.6	0.3	3.51	3.88	6.61	3.47
lnt-030	0.001520	0.000126	0.281090	0.000016	2652.4	0.281013	−2.6	0.3	3.22	3.46	5.73	0.19
lnt-031	0.000608	0.000032	0.280954	0.000018	2700.2	0.280922	−4.7	0.3	3.38	3.53	7.22	0.21
lnt-033	0.000478	0.000012	0.281018	0.000014	2629.5	0.280994	−3.8	0.3	3.27	3.62	5.25	0.28
lnt-036[d]	0.000247	0.000003	0.281013	0.000034	1858.1	0.281005	−21.1	0.6	3.60	3.99	6.67	0.23
lnt-038	0.000290	0.000012	0.281065	0.000016	2676.9	0.281050	−0.7	0.3	3.14	3.24	7.33	0.23
lnt-042[d]	0.000505	0.000003	0.281092	0.000024	1878.2	0.281074	−18.2	0.4	3.46	3.82	7.03	0.19
lnt-044	0.000371	0.000060	0.280896	0.000018	2654.1	0.280878	−7.4	0.3	3.49	3.94	3.95	0.22
lnt-046	0.000376	0.000014	0.281000	0.000020	2661.1	0.280981	−3.6	0.4	3.28	3.42	6.85	0.18
lnt-049[d]	0.000204	0.000003	0.281102	0.000046	1869.0	0.281094	−17.7	0.8	3.43	3.77	6.84	0.19
lnt-051	0.000266	0.000019	0.280997	0.000014	2703.9	0.280983	−2.5	0.2	3.26	3.56	5.28	0.24
lnt-057	0.002199	0.000090	0.281093	0.000020	2674.6	0.280980	−3.3	0.3	3.28	3.33	7.73	0.15
lnt-060[d]	0.000181	0.000002	0.281080	0.000014	1925.8	0.281073	−17.2	0.2	3.44	4.06	6.50	0.17
lnt-064	0.000632	0.000012	0.281055	0.000012	2687.5	0.281023	−1.5	0.2	3.19	3.46	5.29	0.18
lnt-065[d]	0.000771	0.000013	0.281138	0.000014	1820.1	0.281111	−18.2	0.3	3.41	3.77	6.75	0.21
lnt-066	0.000992	0.000049	0.281094	0.000016	2677.2	0.281043	−1.0	0.3	3.15	3.35	5.92	0.20
lnt-069	0.000265	0.000013	0.281100	0.000016	2670.9	0.281087	0.4	0.3	3.07	3.29	5.03	0.17
lnt-071	0.001195	0.000007	0.281017	0.000012	2693.7	0.280955	−3.7	0.2	3.32	3.46	6.65	0.16
lnt-072	0.000569	0.000009	0.281062	0.000012	2657.0	0.281033	−1.8	0.2	3.18	3.30	6.64	0.18
lnt-080[d]	0.000118	0.000028	0.281181	0.000036	1864.9	0.281177	−14.9	0.6	3.27	4.02	1.11	0.19

(*continued on next page*)

Table A3 (*continued*)

Analysis N	$^{176}Lu/^{177}Hf$	+ (2σ)	$^{176}Hf/^{177}Hf$	+ (2σ)	U/Pb age (Ma)	^{176}Lu decay constant (1.867×10^{-11})					$\delta^{18}O$ VSMOW (‰)	± (s.e.d.)[c]
						Initial Hf	εHf_i	± (1σ)	T_{DM}^{C} (Ga)[a]	T_{DM}^{V} (Ga)[b]		
lnt-117[d]	0.000342	0.000014	0.281137	0.000014	1879.2	0.281125	−16.4	0.2	3.36	3.97	5.83	0.20
lnt-119	0.000484	0.000026	0.281008	0.000016	2643.3	0.280983	−3.9	0.3	3.29	3.55	5.83	0.34
sey-01	0.000825	0.000006	0.282819	0.000018	481.7	0.282811	12.0	0.3	0.67	0.77	5.03	0.57
sey-03	0.000887	0.000005	0.282817	0.000018	483.0	0.282809	12.0	0.3	0.67	0.71	6.77	0.58
sey-05	0.000771	0.000028	0.282477	0.000024	454.2	0.282471	−0.7	0.4	1.35	1.55	6.99	0.60
sey-11	0.000762	0.000012	0.282593	0.000016	516.5	0.282585	4.8	0.3	1.10	1.34	5.63	0.59
sey-15	0.001525	0.000024	0.282836	0.000012	488.8	0.282822	12.5	0.2	0.64	0.73	4.44	0.59
sey-21	0.001530	0.000030	0.282677	0.000016	443.7	0.282665	6.0	0.3	0.97	1.26	5.06	0.58
sey-24	0.001448	0.000055	0.282662	0.000020	454.3	0.282649	5.7	0.4	1.00	1.00		
sey-25	0.000596	0.000013	0.281435	0.000012	1861.6	0.281414	−6.5	0.2	2.81	2.81		
sey-30	0.001000	0.000038	0.282691	0.000018	459.6	0.282682	7.0	0.3	0.93	0.93		
sey-31	0.001426	0.000058	0.282728	0.000020	425.8	0.282716	7.4	0.3	0.88	0.88		
sey-32	0.000858	0.000038	0.282736	0.000018	473.2	0.282728	8.9	0.3	0.83	0.83		
sey-34	0.000739	0.000016	0.281643	0.000012	1815.9	0.281617	−0.3	0.2	2.43	2.43		
sey-37	0.000532	0.000008	0.282834	0.000012	474.6	0.282830	12.5	0.2	0.63	0.63		
sey-44	0.001165	0.000029	0.282765	0.000018	433.7	0.282755	9.0	0.3	0.80	0.80		
sey-50	0.001076	0.000027	0.282695	0.000016	457.4	0.282686	7.0	0.3	0.92	0.92		
sey-52	0.001711	0.000036	0.282822	0.000016	514.3	0.282805	12.5	0.3	0.66	0.73	6.47	0.58
sey-54	0.000588	0.000035	0.282556	0.000024	451.6	0.282551	2.1	0.4	1.19	1.36	7.28	0.58
sey-62	0.001036	0.000004	0.281689	0.000018	1790.8	0.281654	0.4	0.3	2.37	2.68	5.23	0.59
sey-69	0.000618	0.000008	0.282564	0.000014	449.6	0.282559	2.4	0.2	1.18	1.10	9.71	0.62
sey-70	0.000955	0.000048	0.282639	0.000022	439.6	0.282631	4.7	0.4	1.04	1.18	7.32	0.57
sey-71	0.000501	0.000014	0.282120	0.000020	457.2	0.282116	−13.2	0.3	2.04	1.87	11.01	0.58
vgt-071	0.000463	0.000002	0.282306	0.000168	1045.9	0.282297	6.4	2.9	1.44	1.60	5.89	0.20
vgt-077	0.001607	0.000015	0.281765	0.000020	1750.4	0.281712	1.5	0.3	2.27	2.55	5.11	0.21
vgt-079	0.000505	0.000015	0.282865	0.000014	351.9	0.282862	10.9	0.3	0.62	0.68	6.63	0.17
vgt-080	0.000597	0.000002	0.282042	0.000014	1160.0	0.282029	−0.6	0.3	1.91	1.90	8.93	0.16
vgt-082	0.000705	0.000015	0.281953	0.000020	1246.2	0.281937	−1.9	0.3	2.06	2.50	5.15	0.22
vgt-083	0.000385	0.000004	0.282809	0.000016	288.5	0.282807	7.6	0.3	0.76	1.01	5.49	0.17
vgt-084	0.000485	0.000004	0.282843	0.000016	353.8	0.282840	10.2	0.3	0.66	0.83	5.21	0.23
vgt-089	0.000592	0.000003	0.282895	0.000012	352.1	0.282891	11.9	0.2	0.56	0.65	6.45	0.20
vgt-090	0.000518	0.000002	0.282885	0.000014	344.9	0.282882	11.5	0.3	0.59	0.72	3.96	0.17
vgt-091	0.000441	0.000002	0.281228	0.000014	1693.0	0.281214	−17.5	0.2	3.27	4.11	5.28	0.22
vgt-092	0.000464	0.000005	0.282854	0.000014	352.7	0.282851	10.6	0.2	0.64	0.76	6.00	0.20
vgt-096	0.001103	0.000030	0.282189	0.000018	1119.1	0.282166	3.4	0.3	1.66	1.89	6.42	0.23
vgt-098	0.000003	0.000000	0.281074	0.000016	1852.3	0.281074	−18.8	0.3	3.47	3.84	6.96	0.23
vgt-100	0.000609	0.000010	0.282147	0.000016	1037.8	0.282135	0.5	0.3	1.76	1.92	6.75	0.22
vgt-103	0.000930	0.000025	0.282890	0.000018	357.0	0.282884	11.8	0.3	0.58	0.67	5.64	0.23
vgt-104	0.002032	0.000099	0.282732	0.000022	318.7	0.282720	5.2	0.4	0.92	1.24	5.50	0.20
vgt-107	0.000398	0.000001	0.282843	0.000014	360.1	0.282840	10.3	0.2	0.66	0.83	3.34	0.29
vgt-113	0.001579	0.000053	0.282604	0.000016	437.6	0.282591	3.2	0.3	1.12	1.12		
vgt-115	0.001310	0.000034	0.281528	0.000018	1850.6	0.281482	−4.4	0.3	2.68	2.68		
vgt-118	0.001033	0.000017	0.281774	0.000018	1750.9	0.281740	2.5	0.3	2.22	2.22		
vgt-119	0.000719	0.000016	0.282103	0.000014	1118.5	0.282087	0.6	0.3	1.82	1.82		

vgt-121	0.000537	0.000007	0.282191	0.000016	1099.5	0.282180	3.4	0.3	1.64	1.64		
vgt-122	0.000446	0.000045	0.281630	0.000016	1873.7	0.281614	0.9	0.3	2.41	2.53	7.38	0.20
vgt-125	0.000582	0.000012	0.282895	0.000016	348.3	0.282892	11.9	0.3	0.56	0.56		
vgt-128	0.000718	0.000011	0.282898	0.000012	337.9	0.282894	11.7	0.2	0.57	0.57		
vgt-129	0.001592	0.000032	0.281630	0.000018	1801.0	0.281575	−2.2	0.3	2.52	2.68	6.78	0.17
vgt-134	0.000737	0.000009	0.282644	0.000016	430.6	0.282638	4.8	0.3	1.03	1.03		
vgt-137	0.000809	0.000012	0.282934	0.000014	297.8	0.282930	12.1	0.2	0.51	0.60	6.48	0.21
vgt-138	0.000521	0.000004	0.281690	0.000012	1538.6	0.281675	−4.6	0.2	2.44	2.42	9.14	0.22
vgt-139	0.000802	0.000022	0.282908	0.000016	354.7	0.282903	12.4	0.3	0.54	0.56	7.84	0.20
vgt-141	0.000604	0.000011	0.282899	0.000016	344.7	0.282895	11.9	0.3	0.56	0.58	8.00	0.17
vgt-142	0.001963	0.000078	0.282244	0.000018	1124.8	0.282202	4.8	0.3	1.59	1.69	7.31	0.22
vgt-143	0.000410	0.000029	0.282890	0.000014	339.9	0.282888	11.6	0.3	0.58	0.67	5.93	0.23
vgt-146	0.000656	0.000006	0.282172	0.000016	1031.4	0.282159	1.1	0.3	1.72	2.00	6.05	0.20
VGt-164	0.000575	0.000007	0.282160	0.000012	1152.4	0.282147	3.4	0.2	1.69	1.73	8.49	0.58
VGt-182	0.000750	0.000011	0.281685	0.000012	1772.3	0.281660	0.2	0.2	2.37	2.50	6.95	0.60
VGt-206	0.001057	0.000002	0.282610	0.000012	467.1	0.282600	4.2	0.2	1.09	1.09		
VGt-226	0.000672	0.000009	0.281011	0.000012	2739.5	0.280976	−1.9	0.2	3.25	3.25		
VGt-236	0.001438	0.000068	0.281783	0.000016	1558.0	0.281741	−1.8	0.3	2.30	2.47	7.14	0.59
VGt-240	0.000017	0.000000	0.281440	0.000012	1924.0	0.281439	−4.2	0.2	2.73	2.64	9.94	0.57
VGt-260	0.000871	0.000015	0.281403	0.000018	1808.3	0.281373	−9.2	0.3	2.91	3.16	6.66	0.60
VGt-292	0.000507	0.000004	0.281498	0.000016	1885.7	0.281480	−3.7	0.3	2.67	2.84	7.07	0.57
VGt-301	0.000773	0.000013	0.281503	0.000016	1862.8	0.281476	−4.3	0.3	2.69	3.13	3.01	0.50
VGt-321	0.001095	0.000063	0.281480	0.000018	1802.4	0.281443	−6.9	0.3	2.78	3.30	3.75	0.41
VGt-323	0.000585	0.000019	0.282190	0.000014	1048.7	0.282179	2.2	0.2	1.67	2.00	5.41	0.41
VGt-353	0.000719	0.000008	0.282916	0.000016	342.6	0.282911	12.5	0.3	0.53	0.57	6.90	0.22
VGt-356	0.000337	0.000004	0.281410	0.000014	1862.6	0.281398	−7.1	0.2	2.84	3.36	4.05	0.28
VGt-366	0.000770	0.000017	0.282123	0.000016	1224.8	0.282105	3.6	0.3	1.74	2.01	4.84	0.39
VGt-368	0.000380	0.000007	0.281320	0.000014	1888.4	0.281306	−9.7	0.2	3.00	3.60	3.32	0.44
VGt-384	0.000642	0.000016	0.282188	0.000012	1218.0	0.282173	5.9	0.2	1.60	1.69	6.51	0.39
VGt-393	0.000411	0.000015	0.281045	0.000016	2693.4	0.281024	−1.3	0.3	3.18	3.45	4.53	0.45
VGt-398	0.000530	0.000001	0.281708	0.000014	1846.5	0.281689	2.9	0.2	2.27	2.50	4.45	0.44
VGt-399	0.000656	0.000013	0.282884	0.000014	351.1	0.282880	11.5	0.3	0.59	0.72	5.41	0.40
VGt-432	0.000456	0.000005	0.282010	0.000016	1505.3	0.281997	6.1	0.3	1.82	1.99	4.74	0.39
VGt-434	0.000513	0.000006	0.282200	0.000014	1045.1	0.282190	2.5	0.2	1.65	1.78	6.53	0.41
VGt-435	0.000529	0.000024	0.281448	0.000016	1819.5	0.281430	−6.9	0.3	2.79	3.19	6.08	0.39
VGt-436	0.000751	0.000003	0.282875	0.000012	348.8	0.282870	11.2	0.2	0.61	0.75	5.37	0.42
VGt-438	0.000407	0.000000	0.281462	0.000016	1783.6	0.281448	−7.1	0.3	2.78	3.31	4.77	0.39
VGt-439	0.000672	0.000005	0.282897	0.000012	345.3	0.282893	11.9	0.2	0.56	0.65	6.29	0.42
VGt-441	0.000690	0.000023	0.282464	0.000014	450.8	0.282459	−1.2	0.3	1.37	1.87	4.76	0.40
VGt-448	0.000479	0.000001	0.282141	0.000014	1146.4	0.282131	2.7	0.2	1.72	2.03	5.13	0.39
VGt-457	0.000474	0.000005	0.282160	0.000014	987.9	0.282151	−0.1	0.2	1.75	2.06	5.80	0.40
VGt-459	0.000492	0.000004	0.281593	0.000016	1845.3	0.281576	−1.2	0.3	2.50	2.85	4.40	0.39
VGt-462	0.000716	0.000023	0.281632	0.000014	1819.5	0.281608	−0.6	0.2	2.45	2.79	5.10	0.40
VGt-468	0.000242	0.000009	0.281464	0.000016	1801.9	0.281456	−6.4	0.3	2.75	3.26	4.70	0.41
VGt-470	0.000505	0.000005	0.282884	0.000014	356.7	0.282880	11.7	0.3	0.58	0.68	6.32	0.39
VGt-474	0.000815	0.000036	0.281169	0.000018	1890.4	0.281140	−15.6	0.3	3.33	4.10	4.17	0.42
VGt-489	0.000497	0.000007	0.282890	0.000020	346.6	0.282886	11.7	0.3	0.58	0.67	5.54	0.39

(*continued on next page*)

Table A3 (*continued*)

Analysis N	$^{176}Lu/^{177}Hf$	+ (2σ)	$^{176}Hf/^{177}Hf$	+ (2σ)	U/Pb age (Ma)	^{176}Lu decay constant (1.867×10^{-11})					$\delta^{18}O$ VSMOW (‰)	± (s.e.d.)[c]
						Initial Hf	εHf_i	± (1σ)	$T_{DM}{}^{C}$ (Ga)[a]	$T_{DM}{}^{V}$ (Ga)[b]		
VGt-506	0.002918	0.000002	0.281604	0.000018	1842.9	0.281501	−3.8	0.3	2.64	3.08	5.05	0.41
VGt-507	0.000623	0.000008	0.282878	0.000016	350.5	0.282874	11.3	0.3	0.60	0.65	6.59	0.22
VGt-510	0.000775	0.000026	0.281832	0.000018	1552.6	0.281809	0.5	0.3	2.17	2.43	6.44	0.21
VGt-512	0.000705	0.000007	0.282752	0.000018	521.2	0.282745	10.5	0.3	0.78	0.84	6.64	0.23
VGt-514	0.000448	0.000008	0.282025	0.000018	1208.2	0.282015	0.0	0.3	1.92	2.08	6.70	0.20
VGt-516	0.000704	0.000002	0.282869	0.000014	359.0	0.282864	11.2	0.2	0.61	0.67	7.02	0.20
VGt-518	0.001938	0.000083	0.281808	0.000022	1767.7	0.281743	3.0	0.4	2.20	2.38	6.02	0.26
VGt-525	0.000638	0.000010	0.281466	0.000014	1806.3	0.281444	−6.7	0.2	2.77	3.29	2.42	0.45
VGt-531	0.000822	0.000007	0.282533	0.000016	429.9	0.282527	0.8	0.3	1.25	1.33	8.43	0.40
VGt-539	0.000198	0.000003	0.281478	0.000014	1881.4	0.281471	−4.0	0.3	2.69	2.76	7.58	0.40
VGt-541	0.000328	0.000007	0.281078	0.000014	2686.4	0.281061	−0.1	0.2	3.11	3.34	5.11	0.41
VGt-543	0.000319	0.000017	0.282838	0.000016	353.9	0.282836	10.0	0.3	0.67	0.85	5.16	0.40
VGt-544	0.000271	0.000011	0.281733	0.000016	1870.5	0.281724	4.7	0.3	2.19	2.19		
VGt-546	0.000906	0.000013	0.281004	0.000016	2726.4	0.280957	−2.9	0.3	3.30	3.61	4.28	0.42
VGt-547	0.001853	0.000059	0.281718	0.000018	1757.6	0.281657	−0.3	0.3	2.38	2.63	6.47	0.39
VGt-549	0.000757	0.000050	0.282232	0.000018	1144.0	0.282216	5.7	0.3	1.55	1.59	8.06	0.41
VGt-550	0.000363	0.000012	0.282908	0.000016	341.2	0.282906	12.2	0.3	0.54	0.56	8.06	0.40
VGt-552	0.000628	0.000026	0.281716	0.000016	1784.3	0.281695	1.7	0.3	2.29	2.50	5.87	0.40
VGt-556	0.000455	0.000006	0.281447	0.000016	1821.9	0.281431	−6.8	0.3	2.79	3.31	5.48	0.25
VGt-560	0.000298	0.000003	0.282371	0.000014	425.8	0.282369	−4.9	0.2	1.56	1.44	11.91	0.23
VGt-563	0.000488	0.000004	0.282372	0.000020	280.0	0.282369	−8.1	0.3	1.62	1.48	9.76	0.25
VGt-565	0.000737	0.000006	0.282175	0.000016	1061.0	0.282160	1.8	0.3	1.70	1.69	8.60	0.24
VGt-571	0.000710	0.000007	0.281672	0.000014	1903.4	0.281646	2.7	0.2	2.33	2.56	5.02	0.23
VGt-572	0.000180	0.000000	0.281475	0.000014	1842.1	0.281469	−5.0	0.2	2.71	2.62	9.77	0.24
p11-102	0.000033	0.000000	0.282060	0.000012	1042.9	0.282060	−2.1	0.2	1.90	2.10	7.22	0.39
p11-104	0.000516	0.000023	0.282762	0.000018	154.6	0.282761	3.0	0.3	0.90	1.31	4.59	0.38

p11-110	0.000601	0.000011	0.281070	0.000014	2617.7	0.281039	−2.5	0.2	3.19	3.42	6.17	0.31
p11-113	0.000281	0.000001	0.281421	0.000014	1908.3	0.281411	−5.6	0.2	2.79	2.69	9.54	0.46
p11-114	0.000847	0.000070	0.281617	0.000020	1843.2	0.281587	−0.8	0.4	2.48	2.82	4.44	0.31
p11-116	0.000589	0.000006	0.282235	0.000014	263.2	0.282232	−13.3	0.2	1.89	2.76	5.34	0.34
p11-118	0.000216	0.000001	0.281231	0.000014	1894.1	0.281223	−12.6	0.2	3.16	3.28	7.60	0.37
p11-120	0.000769	0.000017	0.281286	0.000014	216.6	0.281283	−47.9	0.3	3.71	4.02	7.87	0.38
p11-121	0.001985	0.000030	0.281792	0.000020	1999.8	0.281716	7.4	0.4	2.15	2.21	5.58	0.30
p11-127	0.000357	0.000009	0.281443	0.000014	1927.0	0.281430	−4.5	0.2	2.75	2.82	8.22	0.41
p11-131	0.000671	0.000031	0.282442	0.000018	306.1	0.282438	−5.1	0.3	1.47	1.58	8.25	0.42
p11-133	0.000431	0.000025	0.281686	0.000016	1874.7	0.281671	2.9	0.3	2.30	2.25	11.33	0.53
p11-135	0.000645	0.000025	0.282936	0.000018	173.4	0.282934	9.6	0.3	0.55	0.76	3.91	0.23
p11-136	0.000498	0.000011	0.281038	0.000014	2694.4	0.281013	−1.7	0.2	3.20	3.41	6.16	0.31
pll-140	0.001594	0.000061	0.282858	0.000020	266.3	0.282850	8.6	0.4	0.68	0.78	7.38	0.42
pll-141	0.000909	0.000029	0.281919	0.000018	1483.1	0.281893	1.9	0.3	2.04	2.34	4.75	0.43
pll-142	0.000751	0.000003	0.281134	0.000016	2717.8	0.281095	1.8	0.3	3.03	3.16	6.32	0.32
pll-144	0.0004ll	0.000002	0.281131	0.000014	1872.6	0.281117	−16.8	0.3	3.38	4.19	4.97	0.32
pll-149	0.000242	0.000004	0.28l483	0.000014	1757.5	0.281475	−6.7	0.3	2.73	3.26	5.09	0.33
pll-150	0.000622	0.000015	0.281698	0.000012	1917.6	0.281675	4.0	0.2	2.27	2.23	11.61	0.61
pll-156	0.000076	0.000000	0.281239	0.000012	1860.7	0.281236	−12.9	0.2	3.15	3.85	5.14	0.27
pll-157	0.000494	0.000010	0.281569	0.000014	1878.8	0.281551	−1.3	0.2	2.53	2.88	3.25	0.26

[a] T_{DM}^{C} ages are calculated using a constant average crustal $^{176}Lu/^{177}Hf$ value of 0.0115.

[b] T_{DM}^{V} ages are calculated using $^{176}Lu/^{177}Hf$ values that vary with the O isotopic values of each of the grains, $^{176}Lu/^{177}Hf = 0.021$, 0.0194, 0.0165, 0.0138, 0.0110, and 0.0083 when O isotope <5.5‰, 5.6–6.5‰, 6.6–7.5‰, 7.6–8.5‰, 8.6–9.5‰, and >9.5‰, respectively. For those without measured O isotopic compositions, the T_{DM}^{V} ages are calculated using $^{176}Lu/^{177}Hf = 0.0115$.

[c] The uncertainty of O isotope of the samples is expressed as s.e.d. (standard error difference) by taking into the consideration of standard error of means for both unknown and Temora. s.e.d. = SQRT (s.e.m.$_{sample}$^2 + s.e.m.$_{Temora}$^2).

[d] They are the Lena Paleoproterozoic zircons, the $T_{DM}^{0.0115}$ model ages are used in Figs. 6, 8 and 9.

Table A4
Analytical results for four reference zircons obtained over a period of 6 months. A summary of the Lu–Hf data obtained over a six-month period for four reference zircons is shown in the Table and are compared with the $^{176}Lu/^{177}Hf$ and $^{176}Hf/^{177}Hf$ reported by Woodhead and Hergt (2005). Their solution values are taken as "known" and are the basis of our $^{176}Hf/^{177}Hf$ normalization procedure. Both measured and normalized values are given for $^{176}Hf/^{177}Hf$. $^{174}Hf/^{177}Hf$ values, a ratio strongly affected by Yb interference, are also listed. They match well the natural ratio of 0.008674 ± 32 (Chu et al., 2002) confirming that our correction for Yb interference on the more important ^{176}Hf has worked satisfactorily.

	Mean $^{176}Lu/^{177}Hf$	Mean $^{176}Hf/^{177}Hf$	Mean $^{174}Hf/^{177}Hf$
91500			
This study (un-normalized)	0.000324 ± 46	0.282279 ± 45 ($n = 16$)	0.008668 ± 63
This study (normalized)		0.282300 ± 41	
WH (2005) (solution)	0.000311	0.282306 ± 8	
WH (2005) (laser)		0.282296 ± 28	
Temora-2			
This study (un-normalized)	0.00125 ± 72	0.282669 ± 24 ($n = 33$)	0.008663 ± 65
This study (normalized)		0.282687 ± 39	
WH (2005) (solution)	0.00109	0.282686 ± 8	
WH (2005) (laser)		0.282680 ± 22	
Mud Tank			
This study (un-normalized)	0.000051 ± 5	0.282487 ± 22 ($n = 20$)	0.008662 ± 16
This study (normalized)		0.282509 ± 18	
WH (2005) (solution)	0.000042	0.282507 ± 6	
WH (2005) (laser)		0.282504 ± 44	
Monastery			
This study (un-normalized)	0.000008 ± 8	0.282699 ± 26 ($n = 21$)	0.008660 ± 12
This study (normalized)		0.282724 ± 20	
WH (2005) (solution)	0.000009	0.282738 ± 8	
WH (2005) (laser)		0.282739 ± 26	

*WH (2005) is Woodhead and Hergt (2005); all uncertainties are 2σ.

A graphical representation of the standard data with error bars on individual analyses shown as 2 standard errors. The errors shown for the full data sets are 2 standard deviations.

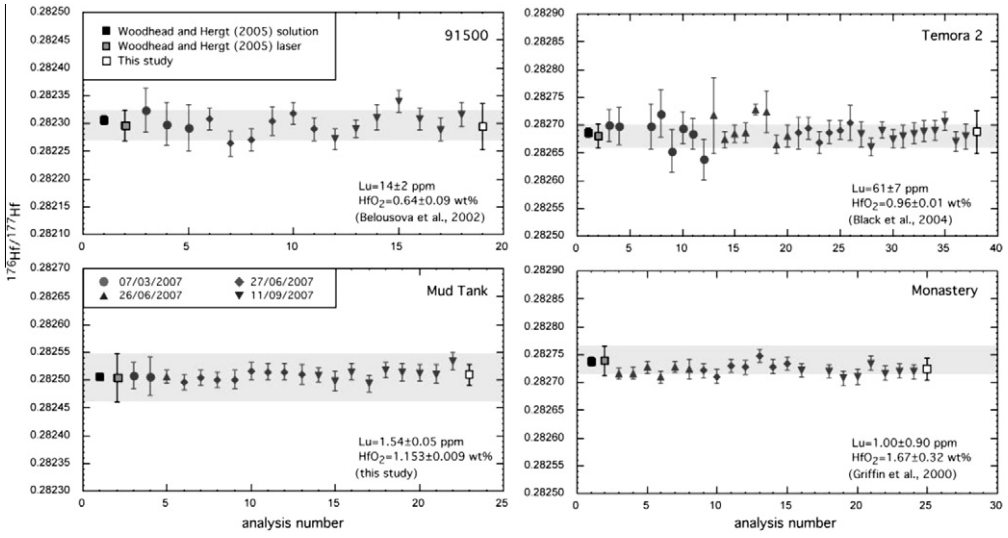

References:

Woodhead J. D. and Hergt J. M. (2005) A preliminary appraisal of severn natural zircon reference materials for in situ Hf isotope determination. *Geostand. Geoanaly. Res.* 183–195.

Chu N. C., Taylor R. N., Chavagnac V., Nesbitt R. W., Boella R. M., Milton J.A., German C. R., Bayon G. and Burton K. (2002) Hf isotope ratio analysis using multi-collector inductively coupled plasma mass spectrometry: an evaluation of isobaric interference corrections. *J. Anal. Atomic Spec.* **17**, 1567–1574.

APPENDIX B. SUPPLEMENTARY DATA

Supplementary data associated with this article can be found, in the online version, at doi:10.1016/j.gca.2010.12.010.

REFERENCES

Akinin V. V., Prokopiev A. V., Toro J., Miller E. L., Wooden J., Goryachev N. A., Alshevsky A. V., Bakharev A. G. and Trunilina V. A. (2009) U–Pb SHRIMP ages of granitoides from the main batholith belt (North East Asia). *Doklady Earth Sci.* **426**, 605–610.

Aplonov S. (1995) The tectonic evolution of west Siberia-an attempt at a geophysical analysis. *Tectonophysics* **245**, 61–84.

Armstrong R. L. (1981) Radiogenic isotopes: the case for crustal recycling on a near-steady-state no-continental-growth Earth. *Phil. Trans. R. Soc. Lond.* **A310**, 443–472.

Armstrong R. L. (1991) The persistent myth of crustal growth. *Aust. J. Earth Sci.* **38**, 613–630.

Bazhenov M. L., Zharov A. E., Levashova N. M., Kodama K., Bragin N. Y., Fedorov P. I., Bragina L. G. and Lyapunov S. M. (2001) Paleomagnetism of a Late Cretaceous Island arc complex from South Sakhalin, East Asia: convergent boundaries far away from the Asian continental margin? *J. Geophys. Res.* **106**(B9), 19193–19205.

Bibikova E., Kirnozova T., Kozakov I., Kotov A., Neymark L., Gorkhovskiy B. and Shuleshko I. (1992) U–Pb ages for polymetamorphic complexes on the southern flank of the Mongolian and Gobi Altai. *Geotectonics* **26**, 166–172.

Bibikova E. V., Bogdanova S. V., Larionov A. N., Fedotova A. A., Postnikov A. V., Popova L. P., Kirnozova T. I. and Fugzan M. M. (2008) New data on the early Archean age of granitoids in the Volga-Ural segment of the East European Craton. *Doklady Earth Sci.* **419**, 243–247.

Blichert-Toft J. and Albarede F. (1997) The Lu–Hf geochemistry of chondrites and the evolution of the mantle-crust system. *Earth Planet. Sci. Lett.* 148, 243–258 (Erratum. *Earth Planet. Sci. Lett.* **154**, 349 (1998)).

Bogdanova S. and Bibikova E. (1993) The Saamian of the Belomorian mobile belt-new geochronological constraints. *Precamb. Res.* **64**, 131–152.

Bogdanova S., De Waele B., Bibikova E., Postnikov A. and Popova L. (2005) Volgo-Uralia: SHRIMP evidence of strong Paleoproterozoic reworking of the Archean crust. In *Supercontinents and Earth Evolution Symposium 2005, Geol. Soc. Aus. Inc. Abst. 81, pp 118* (eds. M. Wingate and S. Pisarevsky). Fremantle, Western Australia.

Bogdanova S. V., Bingen B., Gorbatschev R., Kheraskova T. N., Kozlov V. I., Puchkov V. N. and Volozh Y. A. (2008) The East European Craton (Baltica) before and during the assembly of Rodinia. *Precamb. Res.* **160**, 23–45.

Bowring S. A. and Williams I. S. (1999) Priscoan (4.00–4.03 Ga) orthogneisses from northwestern Canada. *Contrib. Mineral Petrol* **147**, 3–16.

Buzlukova L., Shatsky V. and Sobolev N. (2004) Specific structure of the lowermost Earth's crust in the Zagadochnaya kimberlite pipe (Yakutia). *Geologiya I Geofizika* **45**, 992–1007.

Campbell I. H. and Allen C. M. (2008) Formation of supercontinents linked to increases in atmospheric oxygen. *Nat. Geosci.* **1**, 554–557.

Campbell I. H. and Hill R. I. (1988) A two-stage model for the formation of the granite-greenstone terrains of the Kalgoorlie-Norseman area, western Australia. *Earth Planet. Sci. Lett.* **90**, 11–25.

Campbell I. H., Reiners W., Allen C. M., Nicolescu S. and Upadhyay R. (2005) He–Pb double dating of detrital zircons from the Ganges and Indus Rivers: implication for quantifying sediment recycling and provenance studies. *Earth Planet. Sci. Lett.* **237**, 402–432.

Chauvel C., Lewin E., Carpentier M., Arndt N. T. and Marini J. C. (2008) Role of recycled oceanic basalt and sediment in generating the Hf–Nd mantle array. *Naturegeoscience* **1**, 64–67.

Condie K. C. (2005) *Earth as an evolving planetary system*. Elsevier, Amsterdam, Netherlands.

Condie K. C., O'Neill C. and Aster R. C. (2009) Evidence and implications for a widespread magmatic shutdown for 250 My on Earth. *Earth Planet. Sci. Lett.* **282**, 294–298.

Dobretsov N. L., Buslov M. M., Zhimulev F. I., Travin A. V. and Zayachkovsky A. A. (2006) Vendian-Early Ordovician geodynamic evolution and model for exhumation of ultrahighand high-pressure rocks from the Kokchetav subduction-collision zone (northern Kazakhstan). *Russ. Geol. Geophys.* **47**, 424–440.

Donskaya T. V., Windley B. F., Mazukabzov A. M., Kroener A., Sklyarov E. V., Gladkochub D. P., Ponomarchuk V. A., Badarch G., Reichow M. K. and Hegner E. (2008) Age and evolution of late Mesozoic metamorphic core complexes in southern Siberia and northern Mongolia. *J. Geol. Soc.* **165**, 405–421.

Donskaya T. V., Gladkochub D. P., Pisarevsky S. A., Poller U., Mazukabzov A. M. and Bayanova T. B. (2009) Discovery of Archaean crust within the Akitkan orogenic belt of the Siberian craton: new insight into its architecture and history. *Precamb. Res.* **170**, 61–72.

Eggins S. M., Grun R., McCulloch M. T., Pike A. W. G., Chappell J., Kinsley L., Mortimer G., Shelley M., Murray-Wallace C. V., Spotle C. and Taylor L. (2005) In situ U-series dating by laser-ablation multi-collector ICPMS: new prospects for Quaternary geochronology. *Quaternary Sci. Rev.* **24**, 2523–2538.

Egorova V. V., Volkova N. I., Shelepaev R. A. and Izokh A. E. (2006) The lithosphere beneath the Sangilen Plateau, Siberia: evidence from peridotite, pyroxenite and gabbro xenoliths from alkaline basalts. *Mineral. Petrol.* **88**, 419–441.

Faure M., Natal'in B. A., Monié P., Vrublevsky A. A., Borukaiev Ch. and Prikhodko V. (1995) Tectonic evolution of the Anuy metamorphic rocks (Sikhote Alin, Russia) and their place in the Mesozoic geodynamic framework of East Asia. *Tectonophysics* **241**, 279–301.

Fershtater G. B., Krasnobaev A. A., Bea F., Montero P. and Borodina N. S. (2007) Geodynamic settings and history of the Paleozoic intrusive magmatism of the central and southern Urals: results of zircon dating. *Geotectonics* **41**, 465–486.

Gladkochub D. P., Donskaya T. V., Wingate M. T. D., Poller U., Kroener A., Fedorovsky V. S., Mazukabzov A. M., Todt W. and Pisarevsky S. A. (2008) Petrology, geochronology, and tectonic implications of c. 500 Ma metamorphic and igneous rocks along the northern margin of the Central Asian Orogen

(Olkhon terrane, Lake Baikal, Siberia). *J. Geol. Soc.* **165**, 235–246.

Glukhan I. S. (1996) *Granite-related Ore deposits of Central Kazakhstan and Adjacent Areas, chapter Geology and tectonic evolution of Central Kazakhstan*. Glagol Publ. House, St Petersburg (pp. 11–24).

Gorbatschev R. and Bogdanova S. (1993) Frontiers in the Baltic shield. *Precamb. Res.* **64**, 3–21.

Gordienko I. V. (2001) Geodynamic evolution of the Central-Asian and Mongol-Okhotsk fold belts and formation of the endogenic deposits. *Geosci. J.* **5**, 233–241.

Griffin W. L., Wang X., Jackson S. E., Pearson N. J., O'Reilly S. Y., Xu X. S. and Zhou X. M. (2002) Zircon chemistry and magma mixing, SE China: in-situ analysis of Hf isotopes, Tonglu and Pingtan igneous complexes. *Lithos* **61**, 237–269.

Hawkesworth C. J. and Kemp A. I. S. (2006a) Using hafnium and oxygen isotopes in zircons to unravel the record of crustal evolution. *Chem. Geol.* **226**, 144–162.

Hawkesworth C. J. and Kemp A. I. S. (2006b) Evolution of the continental crust. *Nature* **443**, 811–817.

Hawkesworth C. J., Cawood P. A., Kemp A. I. S., Storey C. D. and Dhuime B. (2009) A matter of preservation. *Science* **323**, 49–50.

Hawkesworth C. J., Dhuime B., Pietranik A. B., Cawood P. A., Kemp A. I. S. and Storey C. D. (2010) The generation and evolution of the continental crust. *J. Geol. Soc. Lond.* **167**, 229–248.

Heinhorst J., Lehmann B., Ermolov P., Serykh V. and Zhurutin S. (2000) Paleozoic crustal growth and metallogeny of Central Asia: evidence from magmatic-hydrothermal ore systems of Central Kazakhstan. *Tectonophysics* **328**, 69–87.

Ickert R. B., Hiess J., Williams I. S., Holden P., Ireland T. R., Chappell B. W., Lanc P., Schram N., Foster J. J. and Clement S. W. (2008) Determining high precision, in situ, oxygen isotope ratios with a SHRIMP II: analyses of MPI-DING silicate glass reference materials and zircon from contrasting granites. *Chem. Geol.* **257**, 114–128.

Jacobsen S. B. and Dymek R. F. (1987) Nd and Sr isotopic systematics of clastic metasediments from Isua, West Greenland: identification of pre-3.8 Ga differentiated crustal components. *J. Geophys. Res.* **93**, 338–354.

Jahn B.-M. (2004) The central Asian orogenic belt and growth of the continental crust in the Phanerozoic. In *Aspects of the tectonic evolution of China. Geol Soc. Lond.* (eds. J. Malpas, C. J. N. Fletcher, J. R. Ali, J.C. Aitchison) Spec. Publ. **226**, 73–100.

Kemp A. I. S., Hawkesworth C. J., Paterson B. A. and Kinny P. D. (2006) Episodic growth of the Gondwana supercontinent from hafnium and oxygen isotopes in zircon. *Nature* **439**, 580–583.

Khain E., Bibikova E., Salnikova E., Kroner A., Gibsher A., Didenko A., Degtyarev K. and Fedotova A. (2003) The Palaeo-Asian Ocean in the Neoproterozoic and early Palaeozoic: new geochronologic data and palaeotectonic reconstructions. *Precamb. Res.* **122**, 329–358.

Koreshkova M. Y., Downes H., Nikitina L. P., Vladykin N. V., Larionov A. N. and Sergeev S. A. (2009) Trace element and age characteristics of zircons in granulite xenoliths from the Udachnaya kimberlite pipe, Siberia. *Precamb. Res.* **168**, 197–212.

Kostitsyn Y. (1996) *Granite-related Ore deposits of Central Kazakhstan and adjacent areas, chapter K–Ar Dates for the Kazahstan Granites: an overview. pp 287–299*. Glagol Pablishing House, St Petersburg.

Kovach V. P., Kotov A. B., Smelov A. P., Starosel'tsev K. V., Sal'nikova E. B., Zagornaya N. Yu., Safronov A. F. and Pavlushin A. D. (2000) Evolutionary stages of the continental crust in the buried Basement of the Eastern Siberian Platform: Sm–Nd isotopic data. *Petrology* **8**, 353–365.

Kovalenko V., Kostitsyn Y., Yarmolyuk V., Budnikov S., Kovach V., Kotov A., Sal'nikova E. and Antipin V. (1999) Magma sources and the isotopic (Sr and Nd) evolution of Li–F rare-metal granites. *Petrology* **7**, 383–409.

Kuzmichev A., Bibikova E. and Zhuravlev D. (2001) Neoproterozoic (similar to 800 Ma) orogeny in the Tuva-Mongolia Massif (Siberia): island arc-continent collision at the northeast Rodinia margin. *Precamb. Res.* **110**, 109–126.

Kuznetsov N. B., Soboleva A. A., Udoratina O. V., Hertseva M. V. and Andrelchev V. L. (2007) Pre-Ordovician tectonic evolution and volcano-plutonic associations of the Timanides and northern Pre-Uralides, northeast part of the East European Craton. *Gondwana Res.* **12**, 305–323.

Land L. S. and Lynch F. L. (1996) $\delta^{18}O$ values of mudrocks: more evidence for an $\delta^{18}O$-buffered ocean. *Geochim. Cosmochim. Acta* **60**, 3347–3352.

Lee J. K. W., Williams I. S. and Ellis D. J. (1997) Pb, U and Th diffusion in natural zircon source. *Nature* **390**, 159–162.

Letnikov F. A., Kotov A. B., Degtyarev K. E., Sal'nikova E. B., Levchenlov O. A., Shershakova M. M., Shershakov A. V., Rizvanova N. G., Makeev A. F. and Tolkachev M. D. (2009) Silurian granites of Northern Kazakhstan: U–Pb age and tectonic position. *Stratigraph. Geol. Correlation* **17**, 275–282.

Li Q. L., Chen F., Guo J. H., Li X. H., Yang Y. H. and Siebel W. (2007) Zircon ages and nd–hf isotopic composition of the Zhaertai Group (Inner Mongolia): evidence for early Proterozoic evolution of the northern North China Craton. *J. Asian Earth Sci.* **30**, 573–590.

Litvinovsky B. A., Posokhov V. E. and Zanvilevich A. N. (1999) New Rb–Sr data on the age of Late Paleozoic granitoids in Western Transbaikalia. *Geologiya I Geofizika* **40**, 694–702.

McLaren S. and Sandiford M. (2001) Long-term thermal consequences of tectonic activity at Mount Isa, Australia: implications for polyphase tectonism in the Proterozoic. In *Continental reactivation and reworking. Geol. Soc. Lond.* (eds. J.A. Miller, R.E. Holdsworth, I.S. Buick and M. Hand) Spec. Publ. **184**, 219–236.

McLennan S. M. and Taylor S. R. (1982) Geochemical constraints on the growth of the continental crust. *J. Geol.* **90**, 347–361.

Metelkin D. and Vernikovsky V. (2005) *Regional geology of Russia (Short lectures course)*. Novosibirsk State University. pp. 96 (in Russian).

Nozhkin A., Turkina O., Bibikova E., Terleev A. and Khomentovsky V. (1999) Riphean granite-gneiss domes of the Yenisei range: geological structure and U–Pb isotopic age. *Geologiya I Geofizika* **40**, 1305–1313.

Nutman A. P. (2001) On the scarcity of >3900 Ma detrital zircons in 3500 Ma metasediments. *Precamb. Res.* **105**, 93–114.

Nutman A. P., Chernyshev I., Baadsgaard H. and Smelov A. (1992) The Aldan shield of Siberia, USSR – the age of its Archean components and evidence for widespread reworking in the Midproterozoic. *Precamb. Res.* **54**, 195–210.

Pease V. and Scott R. A. (2009) Crustal affinities in the Arctic Uralides, northern Russia: significance of detrital zircon ages from Neoproterozoic and Palaeozoic sediments in Novaya Zemlya and Taimyr. *J. Geol. Soc.* **166**, 517–527.

Perry E. C. and Lefticariu L. (2003) Formation and geochemistry of Precambrian cherts. *Treat. Geochem.* **7**, 99–113.

Pietranik A. B., Hawkesworth C. J., Storey C. D., Kemp A. I. S., Sircombe K. N., Whitehouse M. J. and Bleeker W. (2008) Episodic, mafi c crust formation from 4.5 to 2.8 Ga: New evidence from detrital zircons, Slave craton, Canada. *Geology* **36**, 875–878.

Pushcharovskiy Y. M., Zinkevich V. P., Mazarovich A. O., Peyve A. A., Raznitsin Y. N., Rikhter A. V. and Tsukanov N. V. (1983) Overthrusts and imbricate structures of the northwestern pacific margin. *Geotectonics* **17**(6), 466–477.

Rainbird R., Stern R., Khudoley A., Kropachev A., Heaman L. and Sukhorukov V. (1998) U–Pb geochronology of Riphean sandstone and gabbro from southeast Siberia and its bearing on the Laurentia-Siberia connection. *Earth Planet. Sci. Lett.* **164**, 409–420.

Rosen O. and Turkina O. (2007) *Earth's Oldest Rocks, chapter The oldest rock assemblages of the Siberian Craton*. Elsevier. pp.793–838.s

Rudnick R. L. and Gao S. (2003) Composition of the continental crust. In *The crust, treatise on geochemistry*, vol. 3 (ed. R. L. Rudnick). Elsevier, pp. 1–64.

Safonova I., Maruyama S., Hirata T., Kon Y. and Rino S. (2010) LA-ICP-MS U–Pb ages of detrital zircons from Russia largest rivers: Implications for major granitoid events in Eurasia and global episodes of supercontinent formation. *J. Geodynamic* **50**, 134–153.

Sengör A. M. C. and Natal'in B. A. (1996) Turkic-type orogeny and its role in the making of the continental crust. *Annu. Rev. Earth Planet. Sci.* **24**, 263–337.

Sengör A. M. C., Natal'in B. A. and Burtman V. S. (1993) Evolution of the Altaid tectonic collage and Palaeozoic crustal growth in Eurasia. *Nature* **364**, 299–307.

Shatsky V., Buzlukova L., Jagoutz E., Koz'menko O. and Mityukhin S. (2005) Structure and evolution of the lower crust of the Daldyn-Alakit district in the Yakutian Diamond Province (from data on xenoliths). *Russ. Geol. Geophys.* **46**, 1252–1270.

Shchipansky A. and Bogdanova S. (1996) The Sarmatian crustal segment: Precambrian correlation between the Voronezh Massif and the Ukrainian Shield across the Dniepr-Donets Aulacogen. *Tectonophysics* **268**, 109–125.

Shields G. and Veizer J. (2002) Precambrian marine carbonate isotope database: Version 1.1. *Geochem. Geophys. Geosyst.* **3**, doi: 10.1029/2001GC000266.

Simonov V. A., Mikolaichuk A. V., Rasskazov S. V. and Kovyazin S. V. (2008) Cretaceous-Paleogene within-plate magmatism in Central Asia: data from the Tien Shan basalts. *Russ. Geol. Geophys.* **49**, 520–533.

Smelov A. P. and Timofeev V. F. (2007) The age of the North Asian Cratonic basement: an overview. *Gondwana Res.* **12**, 279–288.

Söderlund U., Patchett P. J., Vervoort J. D. and Isachsen C. E. (2004) The ^{176}Lu decay constant determined by Lu–Hf and U–Pb isotope systematics of Precambrian mafic intrusions. *Earth Planet. Sci. Lett.* **219**, 311–324.

Squire R. J., Allen C. M., Cas R. A. F., Campbell I. H., Blewett R. S. and Nemchin A.A. (2010) Two cycles of voluminous pyroclastic volcanism and sedimentation related to episodic granite emplacement during the late Archean: Eastern Yilgarn Craton, Western Australia. *Precamb. Res.* doi: 10.1016/j.precamres.2010.08.009.

Stampfli G. and Borel G. (2002) A plate tectonic model for the Paleozoic and Mesozoic constrained by dynamic plate boundaries and restored synthetic oceanic isochrons. *Earth Planet. Sci. Lett.* **196**, 17–33.

Taylor S. R. (1967) The origin and growth of continents. *Tectonophysics* **4**, 17–34.

Tsygankov A. A., Matukov D. I., Berezhnaya N. G., Larionov A. N., Posokhov V. F., Tsyrenov B. T., Khromov A. A. and Sergeev S. A. (2007) Late Paleozoic granitoids of western Transbaikalia: magma sources and stages of formation. *Russ. Geol. Geophys.* **48**, 120–140.

Turkina O. M. (2010) Formation stages of the Early Precambrian crust in the Sharyzhalgai basement uplift, southwestern Siberian craton: synthesis of Sm–Nd and U–Pb data. *Petrology* **18**, 158–176.

Turkina O. M., Nozhkin A. D., Bayanova T. B. and Dmitrieva N. V. (2007) Precambrian terranes in the southwestern framing of the Siberian craton: isotopic provinces, stages of crustal evolution and accretion-collision events. *Russ. Geol. Geophys.* **48**, 61–70.

Turkina O. M., Berezhnaya N. G., Larionov A. N., Lepekhina E. N., Presnyakov S. L. and Saltykova T. E. (2009) Paleoarchean tonalite-trondhjemite complex in the northwestern part of the Sharyzhalgai uplift (southwestern Siberian craton): results of U–Pb and Sm–Nd study. *Russ. Geol. Geophys.* **50**, 15–28.

Valley J. W. (2003) Oxygen isotope in zircon. In (eds. J.M. Hanchar and P. W. O. Hoskin) *Zircon. Rev. Mineral. Geochem.* **53**, 343–385.

Valley J. W., Kinny P. D., Schulze D. J. and Spicuzza M. J. (1998) Zircon megacrysts from kimberlite: oxygen isotope variability among mantle melts. *Contrib. Mineral. Petrol.* **133**, 1–11.

Valley J. W., Lackey J. S., Cavosie A. J., Clechenko C. C., Spicuzza M. J., Basei M. A. S., Bindeman I. N., Ferreira V. P., Sial A. N., King E. M., Peck W. H., Sinha A. K. and Wei C. S. (2005) 4.4 billion years of crystal maturation: oxygen isotope ratios of magmatic zircon. *Contrib. Mineral. Petrol.* **150**, 561–580.

Vernikovsky V. A., Vernikovskaya A. E., Wingate M. T. D., Popov N. V. and Kovach V. P. (2007) The 880–864 Ma granites of the Yenisey Ridge, western Siberian margin: Geochemistry, SHRIMP geochronology, and tectonic implications. *Precamb. Res.* **154**, 175–191.

Vladimirov A. G., Ponomareva A. P., Shokalskii S. P., Khalilov V. A., Kostitsyn Y. A., Ponomarchuk V. A., Rudnev S. N., Vystavnoi S. A., Kruk N. N. and Titov A. V. (1997) Late Paleozoic-early Mesozoic granitoid magmatism in Altai. *Geologiya I Geofizika* **38**, 715–729.

Vladimirov A., Ponamareva A., Kargopolov S., Babin G., Plotnikov A., Gibsher A., Izokh A., Shokal'skii S., Bibikova E., Zhuravlev D., Ponomarchuk V., Khalilov V. and Travin A. (1999) Neoproterozoic age of oldest rocks from the Tom' inlier (Mountainous Shoriya): implication of U–Pb, Sm–Nd, Rb–Sr, and Ar–Ar dating. *Stratigraphy Geol. Correlation* **7**, 437–451.

Wang C. Y., Campbell I., Allen C., Williams I. and Heggins S. (2009) Rate of growth of the preserved North American continental crust: evidence from Hf and O isotopes in Mississippi detrital zircons. *Geochim. Cosmochim. Acta* **73**, 712–728.

Wilde S. A., Valley J. W., Peck W. H. and Graham C. M. (2001) Evidence from detrital zircons for the existence of continental crust and oceans on the Earth 4.4 Gyr ago. *Nature* **409**, 175–178.

Woodhead J. D. and Hergt J. M. (2005) A preliminary appraisal of severn natural zircon reference materials for in situ Hf isotope determination. *Geostand. Geoanaly. Res.* 183–195.

Yolkin E. A., Kontorovich A. E., Bakharev N. K., Belyaev S. Y., Varlamov A. I., Izokh N. G., Kanygin A. V., Kashtanov V. A., Kirda N. P., Klets A. G., Kontorovich V. A., Krasnov V. I., Krinin V. A., Moiseev S. A., Obut O. T., Saraev S. V., Sennikov N. V., Tishchenko V. M., Filippov Y. F., Khomenko A. V. and Khromykh V. G. (2007) Paleozoic facies megazones in the basement of the West Siberian geosyncline. *Russ. Geol. Geophys.* **48**, 491–504.

Zonenshain L., Kuzmin M., and Natapov L. (1990) Geology of the USSR. a plate tectonic synthesis. *Geodynamics Ser. AGU* **242**.

Zorin Y., Sklyarov E., Mazukabzov A. and Belichenko V. (1997) Metamorphic core complexes and early Cretaceous rifting in Transbaikalia. *Geologiya I Geofizika* **38**, 1574–1583.

Zorin Y. A., Turutanov E. K., Kozhevnikov V. M., Rasskazov S. V. and Ivanov A. I. (2006) The nature of Cenozoic upper mantle plumes in East Siberia (Russia) and Central Mongolia. *Russ. Geol. Geophys.* **47**, 1046–1059.

Zorin Y. A., Sklyarov E. V., Belichenko V. G. and Mazukabzov A. M. (2009) Island arc-back-arc basin evolution: implications for Late Riphean-Early Paleozoic geodynamic history of the Sayan-Baikal folded area. *Russ. Geol. Geophys.* **50**, 149–161.

Associate editor: Steve Shirey